Eur. Phys. J. C (2024) 84:315
https://doi.org/10.1140/epjc/s10052-024-12438-w

THE EUROPEAN PHYSICAL JOURNAL C

Regular Article - Experimental Physics

A precise measurement of the Z-boson double-differential transverse momentum and rapidity distributions in the full phase space of the decay leptons with the ATLAS experiment at $\sqrt{s} = 8$ TeV

ATLAS Collaboration[⋆]

CERN, 1211 Geneva 23, Switzerland

Received: 19 September 2023 / Accepted: 12 January 2024 / Published online: 25 March 2024

Abstract This paper presents for the first time a precise measurement of the production properties of the Z boson in the full phase space of the decay leptons. This is in contrast to the many previous precise unfolded measurements performed in the fiducial phase space of the decay leptons. The measurement is obtained from proton–proton collision data collected by the ATLAS experiment in 2012 at $\sqrt{s} = 8$ TeV at the LHC and corresponding to an integrated luminosity of 20.2 fb^{-1}. The results, based on a total of 15.3 million Z-boson decays to electron and muon pairs, extend and improve a previous measurement of the full set of angular coefficients describing Z-boson decay. The double-differential cross-section distributions in Z-boson transverse momentum p_{T} and rapidity y are measured in the pole region, defined as $80 < m^{\ell\ell} < 100$ GeV, over the range $|y| < 3.6$. The total uncertainty of the normalised cross-section measurements in the peak region of the p_{T} distribution is dominated by statistical uncertainties over the full range and increases as a function of rapidity from 0.5–1.0% for $|y| < 2.0$ to $2-7$% at higher rapidities. The results for the rapidity-dependent transverse momentum distributions are compared to state-of-the-art QCD predictions, which combine in the best cases approximate N^{4}LL resummation with N^{3}LO fixed-order perturbative calculations. The differential rapidity distributions integrated over p_{T} are even more precise, with accuracies from 0.2–0.3% for $|y| < 2.0$ to 0.4–0.9% at higher rapidities, and are compared to fixed-order QCD predictions using the most recent parton distribution functions. The agreement between data and predictions is quite good in most cases.

1 Introduction and motivation

The production of Z bosons and their decay to lepton pairs at the Large Hadron Collider (LHC) through the Drell–Yan mechanism [1] has been the topic of very fruitful and detailed studies in the LHC experiments [2–8]. The precision of the measurements has motivated over the past decade impressive theoretical developments, mostly in the area of higher-accuracy quantum chromodynamic (QCD) predictions, but also in the area of parton distribution functions (PDFs). The sub-percent precision achieved for the absolute and normalised fiducial cross-section measurements of the Z-boson transverse momentum, p_{T}, as a function of its rapidity, $|y|$, at the Z pole strongly constrains state-of-the-art theoretical calculations. In the best cases, these calculations combine approximate next-to-next-to-next-to-next-to-leading logarithm (N^{4}LL) perturbative resummation at low p_{T} with O(α_s^3) (N^{3}LO) fixed-order perturbative calculations at high p_{T}, where α_s denotes the strong coupling constant. Similarly, the precision obtained for the fiducial cross-section measurements of $|y|$ provides strong constraints on the parton distribution functions.

This paper presents for the first time a double-differential measurement in (p_{T},$|y|$) of absolute and normalised cross-sections at the Z pole within the full phase space of the decay leptons. The measurement uses the full coverage of the ATLAS detector to combine 6.2 million electron and 7.8 million muon pairs from Z-boson decays in the central region (ee_{CC} and $\mu\mu_{CC}$ channels), complemented by 1.3 million electron pairs with one electron in the forward region of the detector (ee_{CF} channel). Such a measurement is possible using the methodology already developed and published for the extraction of the Zboson polarisation [6]. It relies on the decomposition of the lepton angular $\cos\theta$ and ϕ distributions in the Collins–Soper frame [9] into nine spherical harmonic polynomials, P_i, multiplied by angular coefficients, A_i [10–13]. For pure Z-boson production, the full five-dimensional differential cross section describing the kinematics of the two Born-level leptons can be written as:

⋆ e-mail: atlas.publications@cern.ch

$$\frac{\mathrm{d}\sigma}{\mathrm{d}p_{\mathrm{T}}\,\mathrm{d}y\,\mathrm{d}m\,\mathrm{d}\cos\theta\,\mathrm{d}\phi} = \frac{3}{16\pi}\frac{\mathrm{d}\sigma^{U+L}}{\mathrm{d}p_{\mathrm{T}}\,\mathrm{d}y\,\mathrm{d}m} \times \Big\{(1+\cos^2\theta) + \frac{1}{2}A_0(1-3\cos^2\theta) + A_1\ \sin 2\theta\ \cos\phi + \frac{1}{2}A_2\ \sin^2\theta\ \cos 2\phi + A_3\ \sin\theta\ \cos\phi + A_4\ \cos\theta + A_5\ \sin^2\theta\ \sin 2\phi + A_6\ \sin 2\theta\ \sin\phi + A_7\ \sin\theta\ \sin\phi\Big\}. \quad (1)$$

The dependence of the differential cross section on $\cos\theta$ and ϕ is analytical and is fully contained in the harmonic polynomials. On the other hand, the dependence on p_{T}, $|y|$ and m is entirely contained in the unpolarised cross section, denoted by σ^{U+L}, and in the A_i angular coefficients. Therefore, all hadronic dynamics from the production mechanism are factorised from the decay kinematics in the Z-boson rest frame. This allows the measurement precision to be essentially insensitive to all uncertainties in QCD, quantum electrodynamics (QED), and electroweak (EW) effects related to Z-boson production and decay. In particular, EW corrections that couple the initial-state quarks to the final-state leptons have a negligible impact (below 0.05%) at the Z-boson pole. This has been shown for the LEP precision measurements [14,15], when calculating the interference between initial-state and final-state QED radiation and more recently for Z-boson measurements at the LHC [16]. The small fraction of γ^* production in the Z-boson pole region and its interference with the Z boson can also be described by Eq. (1), but with different coefficients, so the A_i coefficients discussed in this paper are effective coefficients, containing the small γ^* contribution at the Z pole.

The decomposition is based on a simple and model-independent ansatz: the spin-one nature of the intermediate gauge boson, and the spin one-half nature of the decay leptons, and on the assumption of angular momentum conservation and quantisation. It removes the need for predictions to model accurately the polarisation and decay of the Z-boson; only its production properties are of interest for comparison to the measurements. Therefore, any phenomenological interpretation of this measurement avoids the theoretical uncertainties and ambiguities related to spin correlations and to the resummation of fiducial power corrections [17–20].

One striking example of the advantage of exploiting measurements in the full phase space of the decay leptons is the rapidity dependence of the Z-boson transverse momentum spectrum: whereas the fiducial measurements of Ref. [2] are insensitive to this production property because the fiducial lepton selections essentially remove the rapidity dependence of the spectrum, the measurements reported here probe this dependence very precisely. The differential angular distributions also provide extra constraints on certain experimental systematic uncertainties since they are not used in the calibration procedures of the detectors. Finally, they have even less sensitivity to theoretical systematic uncertainties than the unfolded p_{T} fiducial measurements.

These measurements pave the way for unambiguous interpretations in terms of QCD. A precise determination of the Z-boson transverse momentum spectrum leads to excellent sensitivity to the strong coupling constant at the m_Z scale, while the even more precise rapidity-dependent cross-sections, obtained after integrating over p_{T}, can be compared directly to state-of-the-art fixed-order predictions with excellent sensitivity to the parton distribution functions.

This paper is structured as follows. Section 2 first presents an overview of the measurement methodology and of the likelihood fit performed to extract the observables of interest from the experimental distributions. Section 3 describes briefly the data analysis, and Sect. 4 discusses the systematic uncertainties in the measured differential cross-sections. Section 5 compares the $\frac{d^2\sigma}{dp_T dy}$ measurements to theoretical predictions combining perturbative resummation with fixed-order calculations, and then compares the $\frac{d\sigma}{dy}$ and the total cross-section measurements to the predictions from QCD N^{3}LO calculations using different PDF sets. Finally, Sect. 6 summarises and concludes the paper.

2 Measurement methodology

The angular coefficients are extracted from the data by fitting templates of the P_i polynomial terms, defined in Eq. (1), to the reconstructed angular distributions using 8×8 bins in $(\cos\theta, \phi)$ space (see Ref. [6] for a detailed description). Each template is normalised by a free parameter for its corresponding polynomial coefficient A_i and a common parameter representing the unpolarised cross section. The polynomial $P_8 = 1 + \cos^2\theta$ in Eq. (1) is only normalised by the parameter for the unpolarised cross-section. All the angular coefficients together with the corresponding unpolarised cross section parameters are measured in each of the analysis bins in $(p_{\mathrm{T}}, |y|)$ space.

In the absence of selections for the final state leptons, the angular distributions in the gauge boson rest frame are defined by its polarisation. In the presence of selection criteria applied to the leptons, the distributions are sculpted by kinematic effects, and can no longer be described by the sum of the nine P_i polynomials as in Eq. (1). Templates of the P_i terms are therefore constructed to account for this, which requires fully simulated signal Monte-Carlo (MC) samples to model the acceptance, efficiency, and migration of events. Reference A_i coefficients are extracted in a simple

way from the predicted shapes of the angular distributions in the full phase space of the decay leptons, using the orthogonality of the P_i polynomials (see Ref. [11] describing the underlying moment method used to extract the coefficients). Together with the reference unpolarised cross-section, they are used in a folding procedure based on the signal MC simulation. The folded polynomial templates (or simply templates) are built in $(\cos\theta, \phi)$ space for each of the nine original polynomials and for each of the measurement bins in $(p_{\mathrm{T}}^{\ell\ell}, y^{\ell\ell})$ space. They are then used to extract the angular coefficients and the unpolarised cross section in the full phase space of the leptons from Z-boson decay. The observables $m^{\ell\ell}$, $p_{\mathrm{T}}^{\ell\ell}$, and $y^{\ell\ell}$, which are defined using reconstructed lepton pairs, as described in Sect. 3.3, are to be distinguished from m, p_{T} and $|y|$, which are defined at generator level using lepton pairs at the Born level.

A likelihood is built from the nominal templates and the varied templates reflecting the systematic uncertainties, which are represented by two categories of nuisance parameters (NP), β and γ. The first category, β, represents experimental and theoretical uncertainties. Each β^m in the set $\beta = \{\beta^1, \ldots, \beta^M\}$ is constrained by a unit Gaussian probability density function, $G(0|\beta^m, 1)$, and linearly interpolates between the nominal and varied templates. The second category, γ^n, represents systematic uncertainties from the limited size of the MC signal and background samples, which are constrained by Poisson probability density functions, $P(N_{\mathrm{eff}}^{\mathrm{n}}|\gamma^n N_{\mathrm{eff}}^{\mathrm{n}})$ where $N_{\mathrm{eff}}^{\mathrm{n}}$ is the effective number of MC events in bin n, in each of the $N_{\mathrm{bins}} = 22528$ bins of the measurement. After including these auxiliary parameters, and after all signal and background templates (see Sect. 3 for details of the samples) are summed over (with their respective normalisations), the expected number of events N_{exp}^n in bin n of the measurement can be written as:

$$N_{\mathrm{exp}}^n(A, \sigma^{U+L}, \beta, \gamma) = \left\{ \sum_j \sigma_j^{U+L} \times L \times \left[t_{8j}^n(\beta) + \sum_{i=0}^{7} A_{ij} \times t_{ij}^n(\beta) \right] \right\} \times \gamma^n + \sum_B^{\mathrm{bkgs}} T_B^n(\beta), \quad (2)$$

where:

- index i runs over the eight angular coefficients and the corresponding P_i polynomials, while index j runs over all 352 bins in $(p_{\mathrm{T}},|y|)$ space.
- A is the set of all angular coefficients, A_{ij}.
- σ^{U+L} is the set of all unpolarised cross sections, σ_j^{U+L}.
- β is the set of all Gaussian-constrained nuisance parameters representing the systematic uncertainties.
- γ is the set of all Poisson-constrained nuisance parameters representing the statistical uncertainties in the simulated samples and in the background estimates.
- t is the set of all signal P_i polynomial templates, t_{ij}.
- T_B is the set of background templates, where the sum runs over all background sources.
- L is the total integrated luminosity.

The summation over index j accounts for the contributions from all analysis bins at generator level that migrate into other analysis bins at the reconstruction level. The likelihood is then constructed as a product of Poisson probabilities across all N_{bins} and of auxiliary constraints for each nuisance parameter β^m:

$$\mathcal{L}(A, \sigma^{U+L}, \theta|N_{\mathrm{obs}}) = \prod_n^{N_{\mathrm{bins}}} \left\{ P(N_{\mathrm{obs}}^n|N_{\mathrm{exp}}^n(A, \sigma^{U+L}, \theta)) \times P(N_{\mathrm{eff}}^n|\gamma^n N_{\mathrm{eff}}^{\mathrm{n}}) \right\} \times \prod_m^M G(0|\beta^m, 1). \quad (3)$$

A profile likelihood ratio method is used to extract the best fit values of the parameters of interest (POIs) and their uncertainties. The POIs include the angular coefficients A_{ij} and the cross sections ${\sigma_j}^{U+L}$ in each measurement bin. This procedure extends that presented in Ref. [6], in which only the angular coefficients were extracted as a function of p_{T} and $|y|$ without any fit constraints based on the ${\sigma_j}^{U+L}$ POIs. The results from the full fit focus on the differential cross-section results in each channel and each measurement bin. The results of the fit for the angular coefficients involving only central leptons are compatible with those of Ref. [6] within the uncertainties resulting from the slightly different selections and calibrations applied here. As explained in Sect. 3.3, the analysis of the forward electrons is significantly improved here with respect to that documented in Ref. [21]. As a result, the measurements of the ee_{CF} angular coefficients reported in this paper are published in HEPDATA and supersede those of Ref. [6].

3 Analysis

3.1 ATLAS detector

The ATLAS experiment [22] at the LHC is a multipurpose particle detector with a forward–backward symmetric cylindrical geometry and a near 4π coverage in solid angle.[1] It

[1] ATLAS uses a right-handed coordinate system with its origin at the nominal interaction point (IP) in the centre of the detector and the z-axis along the beam pipe. The x-axis points from the IP to the centre of

Table 1 MC samples used to estimate the signal and backgrounds in the analysis

Process	Generator	PDF
$Z/\gamma^* \to \ell\ell$	POWHEG BOX [24–26] + PYTHIA 8 [27]	CT10 NLO [28]
$Z/\gamma^* \to \tau\tau$	SHERPA [29–32]	CT10 NLO
$t\bar{t}$	POWHEG BOX + PYTHIA 6 [33]	CT10 NLO
Single top quark (Wt channel)	POWHEG BOX + PYTHIA 8	CT10 NLO
Dibosons	HERWIG [34]	CTEQ6L1
$\gamma\gamma \to \ell\ell$	PYTHIA 8	MRST2004QED NLO [35]

consists of an inner tracking detector, electromagnetic (EM) and hadronic calorimeters, and a muon spectrometer. The inner detector provides precision tracking of charged particles in the pseudorapidity range $|\eta| < 2.5$. This region is matched to a high-granularity EM sampling calorimeter covering the pseudorapidity range $|\eta| < 3.2$ and a coarser granularity calorimeter up to $|\eta| = 4.9$. A hadronic calorimeter system covers the entire pseudorapidity range up to $|\eta| = 4.9$. The muon spectrometer provides triggering and tracking capabilities in the range $|\eta| < 2.4$ and $|\eta| < 2.7$, respectively.

A first-level trigger is implemented in hardware, followed by two software-based trigger levels that together reduce the accepted event rate to 400 Hz on average. An extensive software suite [23] is used in the reconstruction and analysis of real and simulated data, in detector operations, and in the trigger and data acquisition systems of the experiment.

3.2 Data and Monte Carlo samples

The data were collected by the ATLAS detector in 2012 at a centre-of-mass energy of $\sqrt{s} = 8$ TeV, and correspond to an integrated luminosity of 20.2 fb^{-1}. The mean number of additional pp interactions per bunch crossing (pile-up events) in the data set is approximately 20.

The event generators used to produce the $Z/\gamma^* \to \ell\ell$ signal events and the backgrounds estimated from simulation are listed in Table 1. The baseline POWHEG BOX (v1/r2129) signal sample [24–26], using the CT10 NLO set of PDFs [28], is interfaced to PYTHIA 8 (v.8.170) [27] with the AU2 set of tuned parameters [36] to simulate the parton shower, hadronisation and underlying event, and to Photos (v2.154) [37] to simulate QED final-state radiation (FSR) in the Z-boson decay. The simulated line-shape of the Z-boson is reweighted to account for the running width and for mass-dependent NNLO QCD [38] effects, following the recipe described in Ref. [8]. This is a percent-level effect within the mass range used by the measurement, and provides the best possible leading-order EW prediction of the line-shape of the Z boson. The number of events available in the baseline POWHEG BOX + PYTHIA 8 signal sample corresponds to approximately four times that in the data.

Backgrounds from EW (diboson, $Z/\gamma^* \to \tau\tau$, and $\gamma\gamma \to \ell\ell$ production) and top-quark (production of top-quark pairs and of single top quarks) processes are evaluated from the MC samples listed in Table 1. All MC samples are processed through a full ATLAS detector simulation [39], based on GEANT4 [40], and reconstructed with the same software as that used for the data. Pile-up events, occurring in the same and neighbouring bunch crossings are simulated and overlaid at the detector hit level on top of the hard-scattering process from the MC simulation.

3.3 Analysis overview and event selection

For this paper, a central lepton (electron or muon) is one found in the region $|\eta| < 2.4$ (excluding, for electrons, the electromagnetic calorimeter barrel/end-cap transition region $1.37 < |\eta| < 1.52$), while a forward electron is one found in the region $2.5 < |\eta| < 4.9$ (excluding a transition region $3.00 < |\eta| < 3.35$ between the end-cap and forward calorimeters). The analysis is split into three orthogonal channels that are analysed independently, and then combined for the last stages of the analysis, after verifying their compatibility.

The ee_{CC} channel consists of candidate events with two central electrons, obtained using a logical OR of a dielectron trigger, requiring two electron candidates, each having $p_{\mathrm{T}} > 12$ GeV, with two high-p_{T} single-electron triggers, the main one corresponding to a p_{T} threshold of 24 GeV. Electron candidates are required offline to have $p_{\mathrm{T}} > 20$ GeV and $|\eta| < 2.4$, and are reconstructed from clusters of energy in the electromagnetic calorimeter matched to inner detector tracks. The electron candidates must satisfy a set of "medium" selection criteria [21], which have been optimised for the level of pile-up present in the 2012 data.

The $\mu\mu_{CC}$ channel consists of candidate events with two central muons, obtained using a logical OR of a dimuon trigger requiring two muon candidates with $p_{\mathrm{T}} > 18$ GeV and 8

the LHC ring, and the y-axis points upwards. Cylindrical coordinates (r, ϕ) are used in the transverse plane, ϕ being the azimuthal angle around the z-axis. The pseudorapidity is defined in terms of the polar angle θ as $\eta = -\ln\tan(\theta/2)$. Angular distance is measured in units of $\Delta R \equiv \sqrt{(\Delta\eta)^2 + (\Delta\phi)^2}$.

GeV, respectively, and of two high-p_{T} single-muon triggers, the main one corresponding to a p_{T} threshold of 24 GeV. Muon candidates are required offline to have $p_{\mathrm{T}} > 20$ GeV and $|\eta| < 2.4$, and are identified as tracks in the inner detector, which are matched and combined with track segments in the muon spectrometer [41]. Track-quality, and longitudinal and transverse impact-parameter requirements are imposed to suppress backgrounds, and to ensure that the muon candidates originate from a common primary pp interaction vertex.

The ee_{CF} channel consists of candidate events with one central and one forward electron, obtained using the logical OR of the two high-p_{T} single-electron triggers used for the ee_{CC} events, as described above. The central electron candidate is required to have $p_{\mathrm{T}} > 25$ GeV and $|\eta| < 2.4$. Because the expected background from multijet events is larger in this channel than in the ee_{CC} channel, the central electron candidate is required in addition to satisfy a set of "tight" selection criteria [21], including an explicit isolation requirement, which are optimised for the level of pile-up observed in the 2012 data. The forward electron candidate is required to have $p_{\mathrm{T}} > 20$ GeV and to satisfy a set of "medium" selection criteria, based only on the shower shapes in the calorimeters, since this region is outside the acceptance of the inner detector [42].

In the case of the ee_{CF} channel, the analysis of the forward electron candidates, in terms of the data quality, alignment, identification criteria, and calibration of the electromagnetic compartments of the calorimeters outside the acceptance of the inner detector, was improved significantly from those documented in Ref. [21]. A few examples illustrating these improvements are:

- misalignments of a few mm between the inner wheels of the electromagnetic end-cap calorimeters and the inner detector and a rotation of a few mrad between one of the forward calorimeters and the inner detector were found and corrected for when studying the azimuthal angle difference between the central and forward electrons. As a result, the two angular coefficients (A_1, A_6), for which the fully two-dimensional ($\cos\theta$, ϕ) measurement is necessary, can now be measured for the ee_{CF} channel, and are found to be in agreement with the SM predictions.
- an azimuthal inter-calibration of the forward electrons was performed to improve the baseline calibration. This corrected for large inhomogeneities of up to 10–15% in the energy response due to material from inner-detector services in front of the calorimeters not accounted for correctly in the simulation, and for high-voltage problems in some cells, which were inadequately corrected for online during data-taking.
- the largest improvement was obtained by adjusting the simulated lateral shower shapes in the calorimeters to data and then calibrating carefully each region of the calorimeters. This resulted in both improved efficiencies for the forward electrons in certain regions of phase space and improved energy calibration.

As a result, the p-value for the agreement between the combined ee_{CC} and $\mu\mu_{CC}$ channels and the ee_{CF} channel in the $|y|$ range where they overlap, $1.6 < |y| < 2.4$, was improved from $< 10^{-4}$ to 3% (see Fig. 6 in Sect. 5.1).

In each channel, the events are required to contain exactly two lepton candidates satisfying the criteria described above. For the central-central channels, where the charges of both leptons are measured, the two lepton candidates are required to be of opposite charge.

As described in Sect. 1, this analysis is focused on the Z-boson pole region, and the lepton pair is required to have an invariant mass, $m^{\ell\ell}$, within a window around the Z-boson mass, $80 < m^{\ell\ell} < 100$ GeV. The simulated events are required to satisfy the same selection criteria as the data, after applying small corrections to account for the differences between data and simulation in terms of reconstruction, identification and trigger efficiencies and of energy scale and resolution for electrons and muons [41–43]. All simulated events are reweighted to match the distributions observed in data for the level of pile-up and for the primary vertex longitudinal position.

The measurements are binned in p_{T} and $|y|$, with fine bins in p_{T} and coarse bins in $|y|$, as follows:

1. ee_{CC} and $\mu\mu_{CC}$ channels:
   - 23 bins in p_{T} with bin boundaries {0, 2.5, 5.0, 8.0, 11.4, 14.9, 18.5, 22.0, 25.5, 29.0, 32.6, 36.4, 40.4, 44.9, 50.2, 56.4, 63.9, 73.4, 85.4, 105.0, 132.0, 173.0, 253.0, 4000} GeV,
   - 6 bins in $|y|$ with bin boundaries {0, 0.4, 0.8, 1.2, 1.6, 2.0, 2.4};
2. ee_{CF} channel:
   - 19 bins in p_{T} with bin boundaries {0, 2.5, 5.0, 8.0, 11.4, 14.9, 18.5, 22.0, 25.5, 29.0, 32.6, 36.4, 40.4, 44.9, 50.2, 56.4, 63.9, 73.4, 85.4, 105.0} GeV,
   - 4 bins in $|y|$ with bin boundaries {1.6, 2.0, 2.4, 2.8, 3.6}.

The choice of bin boundaries in p_{T} is the result of an optimisation with respect to the limited resolution of the measurements at low p_{T} and the limited statistics at high p_{T}.

The angular coefficients and unpolarised cross-section results are extracted taking into account the correlations and migrations between the measurement bins. Figure 1 shows the expected products of the acceptance and the selection efficiency, defined as the ratio of the number of selected events

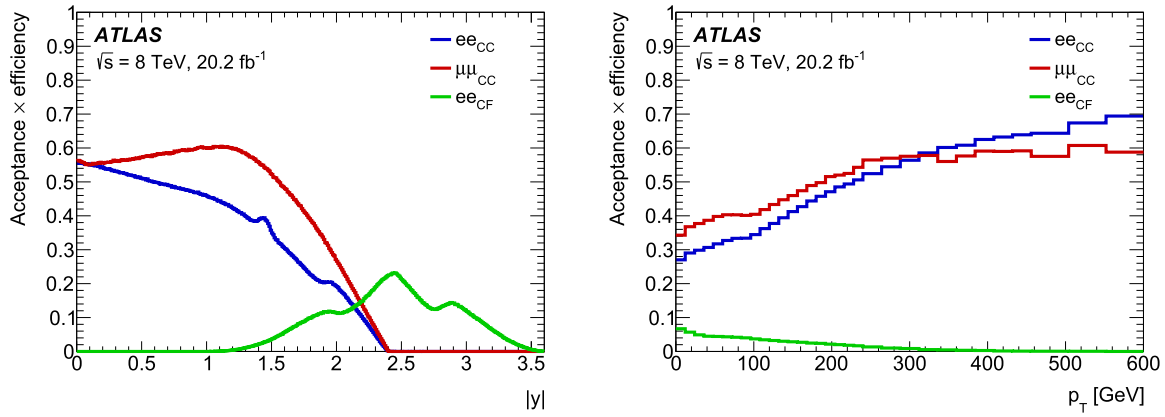

Fig. 1 Expected Z-boson acceptance times selection efficiencies as a function of $|y|$ (left) and p_{T} (right) for the ee_{CC}, $\mu\mu_{CC}$ and ee_{CF} analysis channels

to the number of events in the full decay lepton phase space, as functions of both $|y|$ and p_{T}. The shape of this product of acceptance and efficiency in $|y|$ results in part from the differences in reconstruction and identification efficiencies between central electrons and muons. The ee_{CF} channel covers a higher range in $|y|$ and overlaps with the central-central channels for $1.6 < |y| < 2.4$. In each of the analysis measurement bins, two-dimensional $(\cos\theta, \phi)$ angular distributions are computed (eight equal-sized bins in each observable) and they serve as the basis for the simultaneous extraction of all the angular coefficients and of the unpolarised cross-sections, following the methodology described in Sect. 2.

3.4 Background estimates and signal yields

Table 2 shows the event yields and breakdowns of the fraction of events originating from background sources, for the

Table 2 Data yields integrated over $p_{\mathrm{T}}^{\ell\ell}$ in each $|y^{\ell\ell}|$ analysis bin along with estimated background fractions in % for the ee_{CC}, $\mu\mu_{CC}$, and ee_{CF} channels

$\lvert y^{\ell\ell}\rvert$ range	Data (yield)	Top+EW (%)	Multijets (%)	Non-fiducial Z (%)
ee_{CC} channel				
0 – 0.4	1 573 411	0.2	0.1	0.8
0.4 – 0.8	1 441 923	0.2	0.1	0.9
0.8 – 1.2	1 285 026	0.2	0.2	0.9
1.2 – 1.6	1 025 043	0.2	0.1	0.9
1.6 – 2.0	621 017	0.1	0.2	1.0
2.0 – 2.4	248 261	0.1	0.3	0.9
$\lvert y^{\ell\ell}\rvert < 2.4$	6 194 681	0.2	0.1	0.9
$\mu\mu_{CC}$ channel				
0 – 0.4	1 617 521	0.3	< 0.1	0.7
0.4 – 0.8	1 657 881	0.2	< 0.1	0.7
0.8 – 1.2	1 680 981	0.2	< 0.1	0.8
1.2 – 1.6	1 503 977	0.2	< 0.1	0.8
1.6 – 2.0	1 010 432	0.2	< 0.1	0.9
2.0 – 2.4	335 788	0.2	< 0.1	0.9
$\lvert y^{\ell\ell}\rvert < 2.4$	7 806 580	0.2	< 0.1	0.8
ee_{CF} channel				
1.6 – 2.0	245 869	0.2	1.3	1.0
2.0 – 2.4	388 183	0.1	0.9	1.1
2.4 – 2.8	391 405	0.1	0.7	1.1
2.8 – 3.6	228 867	< 0.1	1.1	1.2
$1.6 < \lvert y^{\ell\ell}\rvert < 3.6$	1 254 324	0.1	1.0	1.1

ee_{CC}, $\mu\mu_{CC}$, and ee_{CF} channels, respectively. The numbers are shown in each $|y|$ analysis bin integrated over p_{T}. The backgrounds are divided into three major groups:

- the backgrounds containing a prompt isolated lepton, from top ($t\bar{t}$ and Wt), diboson, $Z \to \tau\tau$, and $\gamma\gamma \to ll$ processes, estimated from simulation samples (see Sect. 3.2),
- the multijet and W+jet backgrounds, estimated from data using a method very similar to that described in Ref. [6], and
- the non-fiducial Z background, which is estimated from simulation and consists almost entirely of events outside the full mass range considered for the analysis at generator level, but passing the selection cuts at reconstruction level owing to migrations.

The background contamination from other processes for the ee_{CC} and $\mu\mu_{CC}$ channels is very small and amounts to about 0.3%. The multijet background in the ee_{CF} channel is larger, amounting to about 1.0%. The non-fiducial Z background amounts to about 1% in all channels. Templates of the angular distributions of the sum of all these backgrounds are used in the fit to extract the angular coefficients, as described in Sect. 2.

3.5 Angular distributions

The criteria described above are applied to the data, leading to totals of 6.2 (ee_{CC}), 7.8 ($\mu\mu_{CC}$), and 1.3 (ee_{CF}) million selected events (see Table 2 for a more detailed breakdown as a function of $y^{\ell\ell}$). The reconstructed differential angular distributions, integrated over $p_{\mathrm{T}}^{\ell\ell}$ and $y^{\ell\ell}$, are shown in Fig. 2 for the three channels. Small normalisation differences between the data and the MC distributions are observed at the level of a few percent, compatible with the combination of uncertainties in integrated luminosity and signal cross section. The measurement of the angular coefficients is, however, independent of the normalisation between data and simulation in each measurement bin. Overall, the agreement in shape between the observed and predicted distributions of $\cos\theta$ and ϕ is good.

4 Systematic uncertainties

This section describes the systematic uncertainties in the measurements of the absolute and normalised differential cross-sections, $\frac{d^2\sigma}{dp_T dy}$ and $\frac{d\sigma}{dy}$, as extracted from the angular observables presented in Fig. 2. These systematic uncertainties are grouped according to their source, and their typical relative values over most of the kinematic range of the measured observables are listed in Table 3 in the case of the absolute cross-section measurements, $\frac{d^2\sigma}{dp_T dy}$. The overall uncertainty of 1.8% in the integrated luminosity is not shown in this table nor in the figures below, but affects of course all the absolute cross-section measurements presented in this paper. The variations of the uncertainties as a function of p_{T} and $|y|$ are shown in Figs. 3 (absolute cross-sections) and 4 (normalised cross-sections). The statistical uncertainty in the data is the dominant uncertainty over most of the measurement bins, followed by the statistical uncertainty in the MC samples. The variations are shown after combining the different channels together, so the uncertainties are correlated through the fit procedure. This explains for example why the forward electron systematic uncertainties do not vanish for $|y| < 1.6$ and why the muon systematic uncertainties do not vanish for $|y| > 2.4$. The breakdown between the different groups of uncertainties is obtained after freezing all the nuisance parameters of each group to their best-fit values, and then subtracting in quadrature the total uncertainty obtained by performing the fit in these conditions from the total uncertainty obtained by the full fit. Because of the correlations between the nuisance parameters, each of the resulting contributions is rescaled such that their sum in quadrature remains equal to the total uncertainty from the full fit.

Once these cross-sections are integrated over p_{T}, the statistical uncertainties obtained for $\frac{d\sigma}{dy}$ are significantly reduced and the experimental systematic uncertainties in the lepton measurements [21,41] become dominant, especially in the central region, as shown in Fig. 5. In all cases, theoretical uncertainties, arising essentially only from PDFs, are negligible (see Ref. [6] for a more detailed discussion). In particular, as mentioned in Sect. 1, higher-order QED/EW effects, such as initial-final state interference diagrammes, which break the factorisation assumption underlying the expression of the differential cross-section in Eq. (1), have a negligible impact in the Z-boson pole region studied here [16].

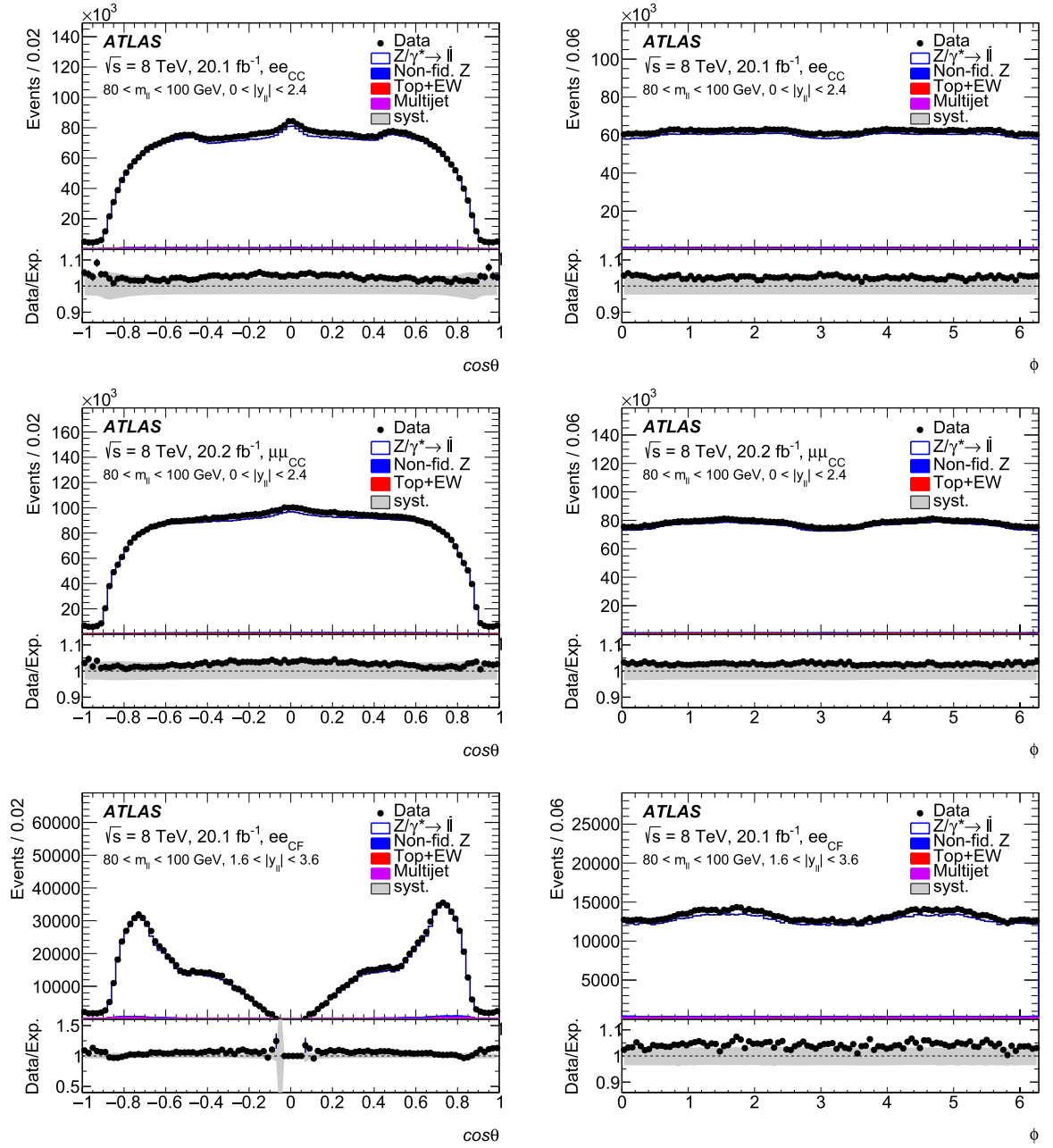

Fig. 2 The cosθ (left) and ϕ (right) angular distributions, integrated over $p_{\mathrm{T}}^{\ell\ell}$ and $y^{\ell\ell}$, for the ee_{CC} (top), $\mu\mu_{CC}$ (middle) and ee_{CF} (bottom) channels. The pre-fit expected distributions are shown separately for the signal and the different small background sources contributing to each channel. The grey band represents the experimental systematic uncertainties in the total expected yields from signal plus background. The small normalisation differences between the data and the MC distributions observed at the level of a few percent are compatible with the combination of uncertainties in integrated luminosity and signal cross section

5 Results and comparisons to predictions

5.1 Compatibility between measurements

Before considering the measurement results themselves, an important step is to evaluate the compatibility between the different channels. This is first done for $\frac{d^2\sigma}{dp_T dy}$ for the ee_{CC} versus $\mu\mu_{CC}$ channels, which are found to be compatible within their dominant statistical uncertainties in all cases, and are then combined into overall central-central (CC) measurements. In the results presented in this paper, there are two rapidity bins where the central-central and central-forward measurements overlap, namely in the range $1.6 < |y| < 2.4$. The $\frac{d^2\sigma}{dp_T dy}$ measurements from

Table 3 Examples of breakdown of relative uncertainties in the measured absolute differential cross-sections, as obtained from the full fit. The values are given in % for the region near the peak of the p_{T} distribution and are shown for two y bins in the case of the ee_{CC} and $\mu\mu_{CC}$ channels and for one y bin in the case of the ee_{CF} channel. Also shown are the total uncertainties. The uncertainty of 1.8% in the integrated luminosity is not included

Uncertainty source	ee_{CC} channel (%)	$\mu\mu_{CC}$ channel (%)	ee_{CC} channel (%)	$\mu\mu_{CC}$ channel (%)	ee_{CF} channel (%)
Rapidity range	$0 < \lvert y\rvert < 0.4$	$0 < \lvert y\rvert < 0.4$	$1.2 < \lvert y\rvert < 1.6$	$1.2 < \lvert y\rvert < 1.6$	$2.4 < \lvert y\rvert < 2.8$
Data stat.	0.5	0.5	0.8	0.6	2.7
MC stat.	0.3	0.3	0.4	0.3	1.5
Leptons	0.2	0.3	0.2	0.4	0.6
Background	< 0.1	< 0.1	< 0.1	< 0.1	< 0.1
PDF	< 0.1	< 0.1	< 0.1	< 0.1	< 0.1
Total	0.6	0.6	1.0	0.8	3.0

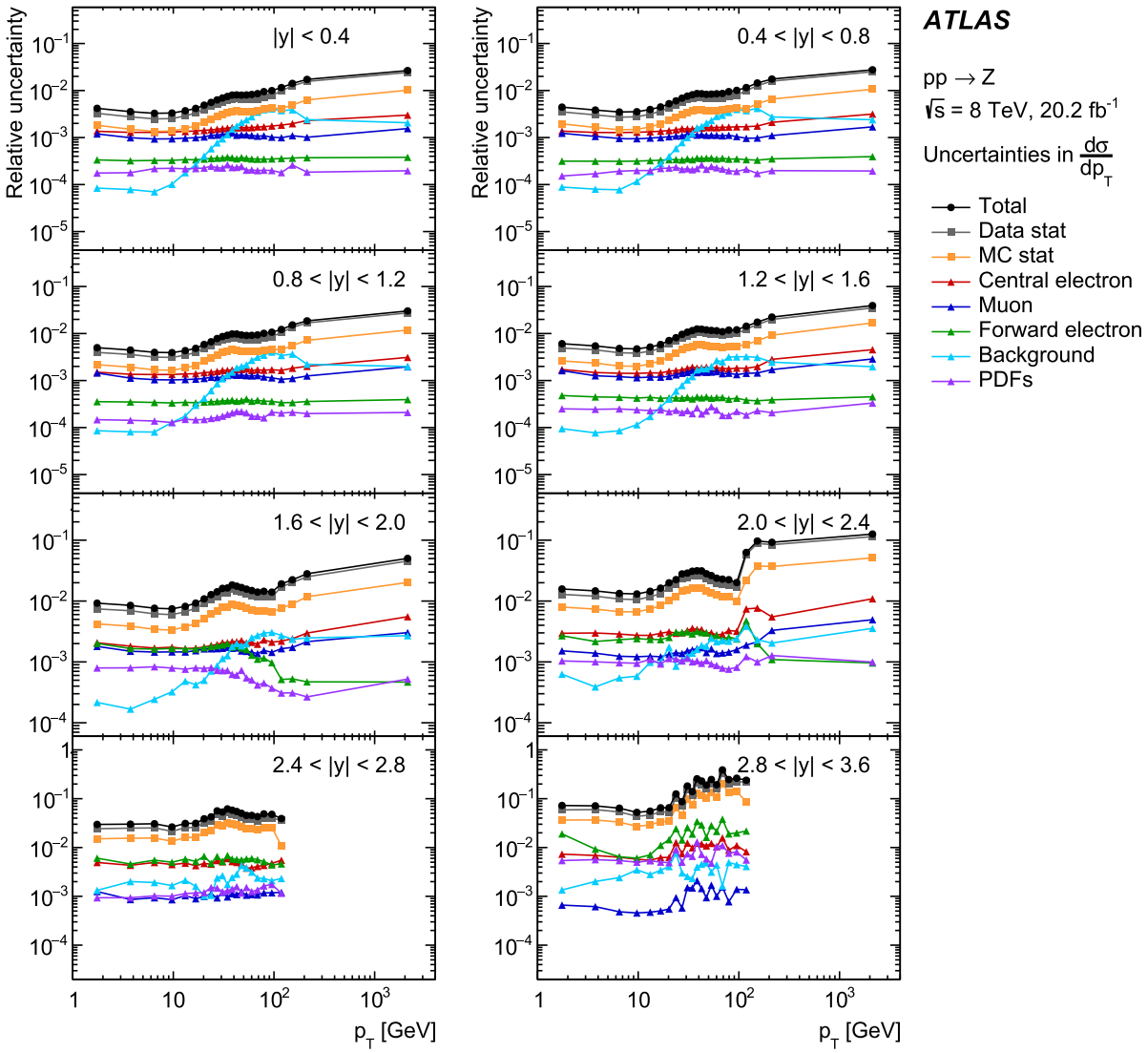

Fig. 3 Breakdown of relative uncertainties in the measured absolute differential cross-sections, $\frac{d^2\sigma}{dp_{\mathrm{T}}dy}$, as a function of p_{T}. The values are shown, as obtained from the full fit and for each $|y|$ bin, for the combination of the ee_{CC} and $\mu\mu_{CC}$ channels for $|y| < 1.6$, for the combination of all three channels for $1.6 < |y| < 2.4$, and for the ee_{CF} channel alone for $2.4 < |y| < 3.6$. The uncertainty of 1.8% in the integrated luminosity is not included

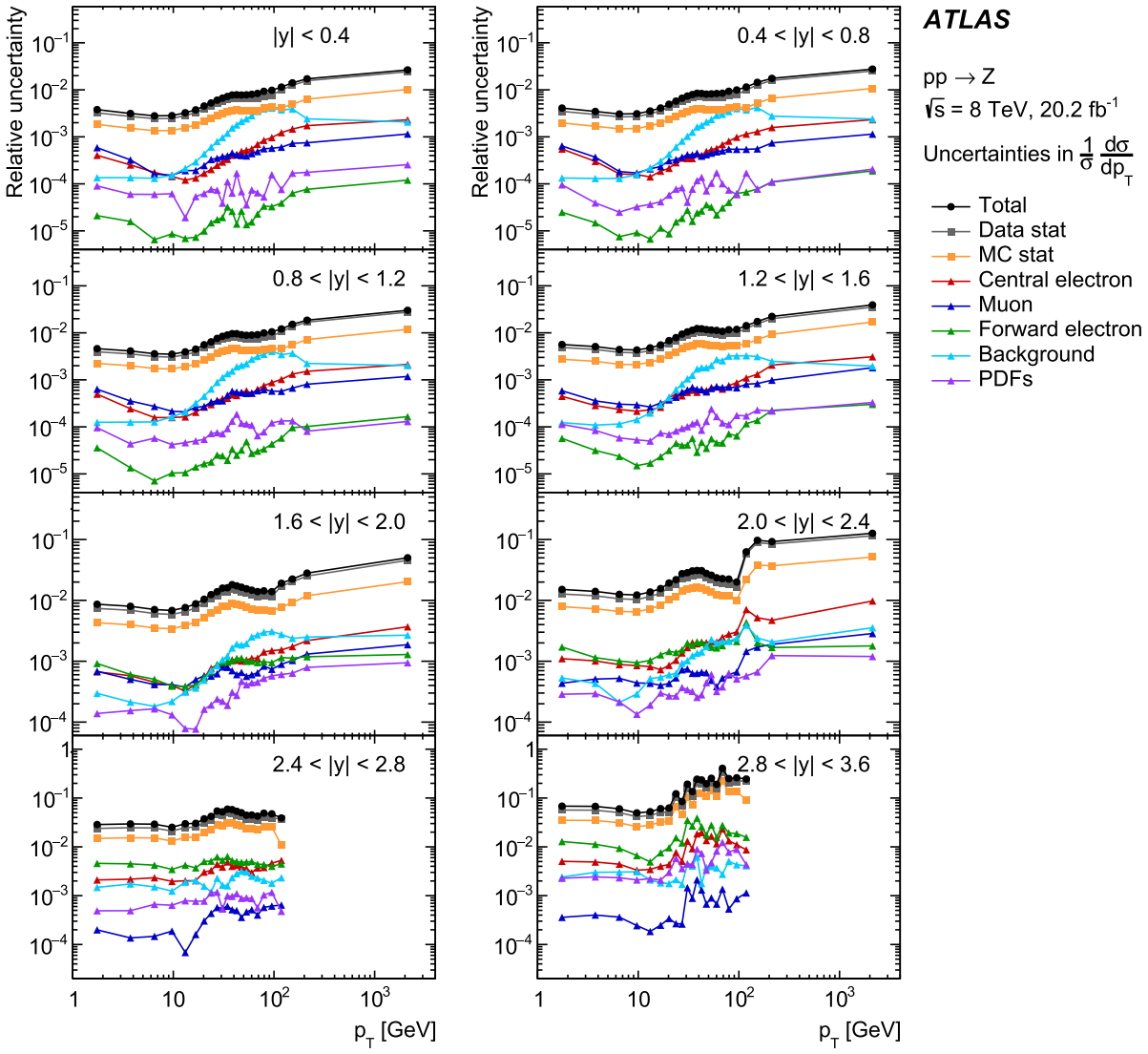

Fig. 4 Breakdown of relative uncertainties in the measured normalised differential cross-sections, $\frac{1}{\sigma}\frac{d^2\sigma}{dp_T dy}$, as a function of p_T. The values are shown, as obtained from the full fit and for each $|y|$ bin, for the combination of the ee_{CC} and $\mu\mu_{CC}$ channels for $|y| < 1.6$, for the combination of all three channels for $1.6 < |y| < 2.4$, and for the ee_{CF} channel alone for $2.4 < |y| < 3.6$

the ee_{CF} channel are compared in this overlap region with those from the CC channel. The distributions are found to be compatible within their dominant statistical uncertainties, and all three channels are then finally combined. The overall p-value of the combined fit is 4%, while the overall p-values of fits performed separately for each channel are found to be 11% for the ee_{CC} channel, 90% for the $\mu\mu_{CC}$ channel and 2% for the ee_{CF} channel.

A stringent test of the compatibility between channels can be performed for the $\frac{d\sigma}{dy}$ measurements after integration over p_T, since the statistical uncertainties are strongly reduced as shown in Fig. 5. The results of this test are shown as a function of $|y|$ in Fig. 6. The top panel of Fig. 6 shows comparisons between separate fits done to each of the three channels. The overall p-value for the compatibility between the ee_{CC} and $\mu\mu_{CC}$ channels is found to be 2%, while that between the ee_{CF} and CC channels is found to be 3%. The bottom panel of Fig. 6 shows the relative cross-section differences after performing the full combination of all channels between the ee_{CC} and $\mu\mu_{CC}$ channels for $|y| < 2.4$ and between the ee_{CF} and CC channels for $1.6 < |y| < 2.4$. The residual tensions between channels arise mostly from the highest $|y|$ bin.

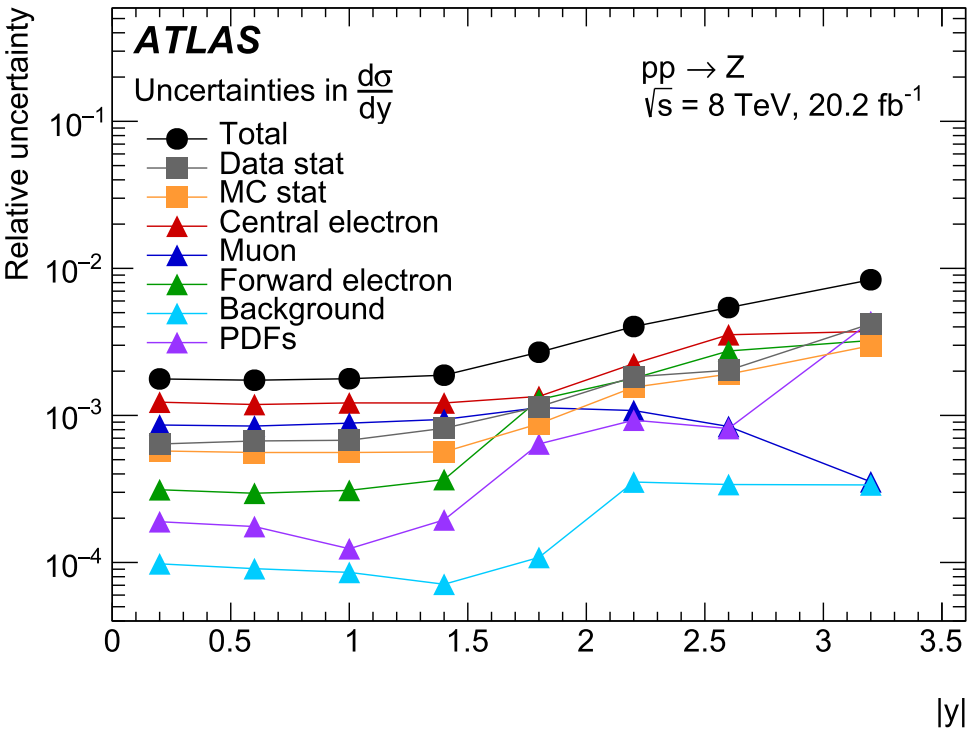

Fig. 5 Breakdown of relative uncertainties in the measured absolute differential cross-section, $\frac{d\sigma}{dy}$, as a function of $|y|$. The values are shown, as obtained from the full fit, for the combination of the ee_{CC} and $\mu\mu_{CC}$ channels for $|y| < 1.6$, for the combination of all three channels for $1.6 < |y| < 2.4$, and for the ee_{CF} channel alone for $2.4 < |y| < 3.6$. The uncertainty of 1.8% in the integrated luminosity is not included

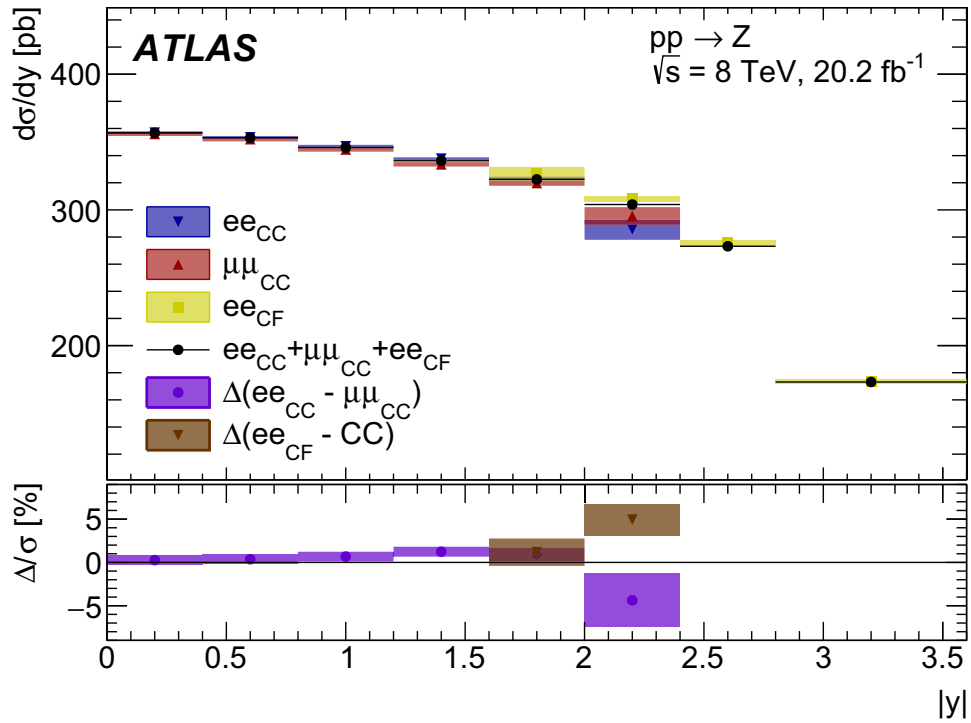

Fig. 6 Compatibility test between the different channels for the differential $\frac{d\sigma}{dy}$ cross-section measurements integrated over p_{T}. The top panel shows the measurements with their total uncertainties (except for the uncertainty of 1.8% in the integrated luminosity) for the three channels and their overall combination. The bottom panel shows, for the relevant $|y|$ bins, the relative $\frac{d\sigma}{dy}$ differences, Δ/σ, in % between the ee_{CC} and $\mu\mu_{CC}$ channels, $\Delta(ee_{CC} - \mu\mu_{CC})$, and between the ee_{CF} channel and the combination of the ee_{CC} and $\mu\mu_{CC}$ channels, $\Delta(ee_{CF} - CC)$

5.2 Comparison between $\frac{d^2\sigma}{dp_{\mathrm{T}}dy}$ measurements and predictions

For the double-differential $\frac{d^2\sigma}{dp_{\mathrm{T}}dy}$ measurements, the predictions are obtained by different state-of-the-art QCD perturbative calculations based on q_{T} resummation [44] at approximate approximate N^{4}LL accuracy. All these calculations, DYTurbo [45–47], CuTe-MCFM [48], Artemide [49], NangaParbat [50], RadISH [51–53], and SCETlib [54], are currently being benchmarked in the LHC Standard Model working group. Except for Artemide, they are matched at high values of p_{T} to a common state-of-the-art $\mathrm{O}(\alpha_s^3)$ fixed-order perturbative calculation from MCFM [48,55]. Each one of these perturbative resummation calculations has its own recipe for defining a total uncertainty in the prediction based on varia-

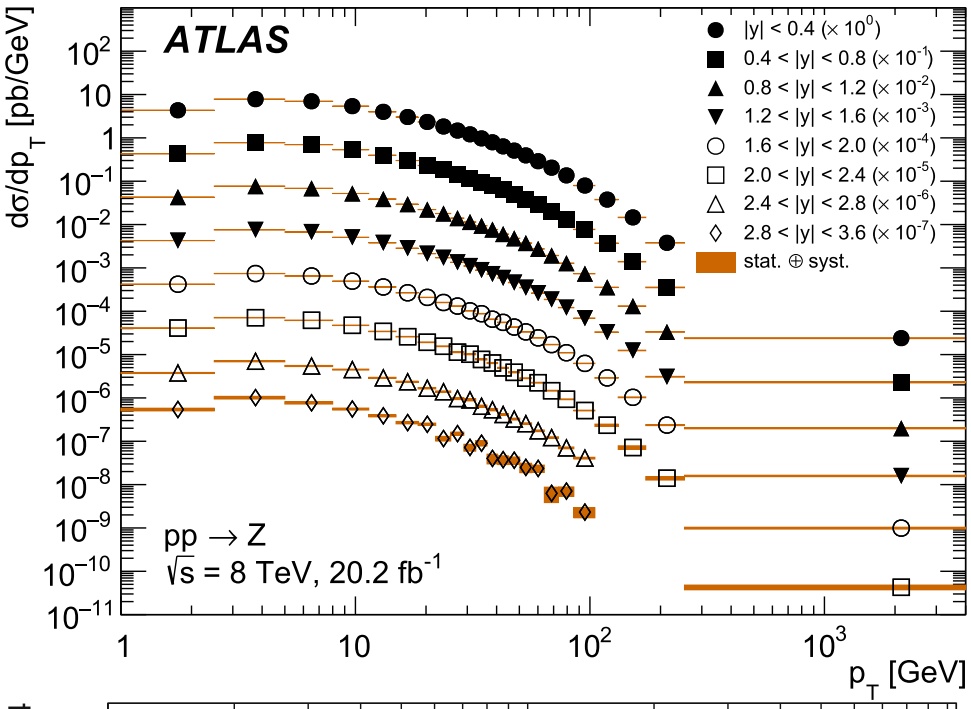

Fig. 7 Measured absolute differential $\frac{d\sigma}{dp_T}$ cross-sections with their total uncertainties shown as a function of p_T for each $|y|$ bin. The uncertainty of 1.8% in the integrated luminosity is not included. For each successive $|y|$ bin, the differential cross section is divided by a factor of ten for plotting purposes

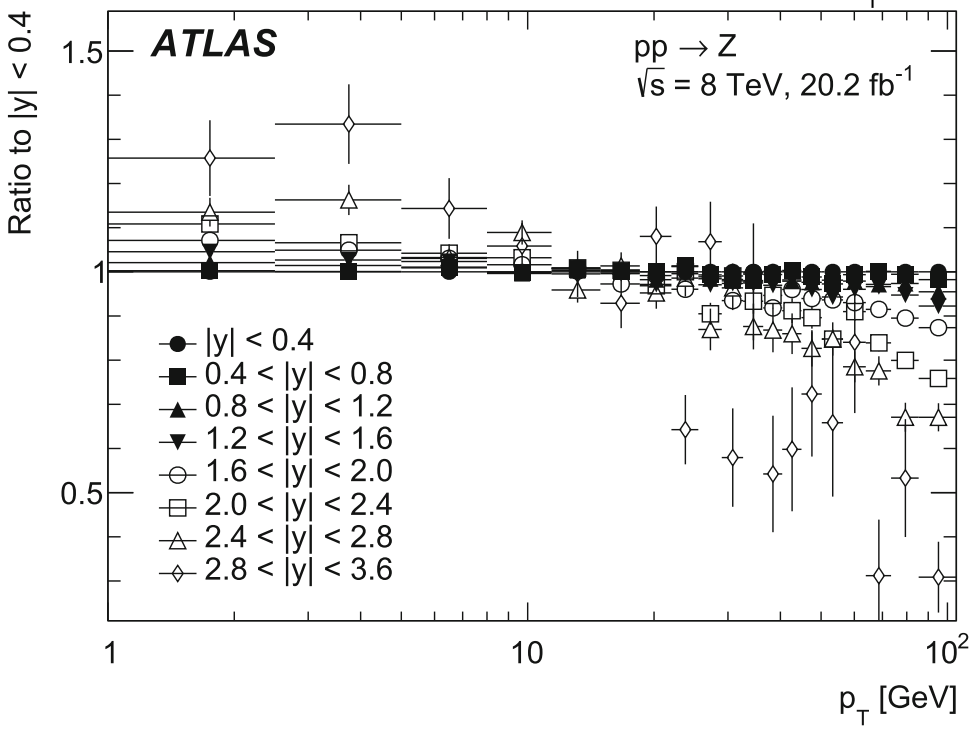

Fig. 8 Illustration of the softening of the p_T spectrum at large rapidities. Shown are the ratios of the measured differential $\frac{d\sigma}{dp_T}$ cross-sections in each $|y|$ bin to a reference one taken to be the most central one, $0 < |y| < 0.4$. The ratios shown do not include any correlated treatment of the uncertainties between different y bins

tions of several QCD scales related to the resummation and fixed-order contributions and the procedure used to match them such that the summed prediction is well behaved. It is beyond the scope of this paper to explain the differences between the various approaches and the theory predictions are therefore shown below with total uncertainty envelopes provided by the authors.

Figure 7 shows all the absolute differential $\frac{d^2\sigma}{dp_T dy}$ cross-section measurements with their total uncertainties (except for the uniform uncertainty of 1.8% in the integrated luminosity). This complete set of cross-section numbers with the full covariance matrix are published in HEPDATA and contain all the information required for comparisons to theory and for interpretation in terms of PDF fits or of the strong coupling constant. As $|y|$ increases, the p_T spectrum becomes softer and this is illustrated in Fig. 8, which presents a normalised ratio of the measurements, for which the reference is taken to be the measurement in the most central $|y|$ bin,

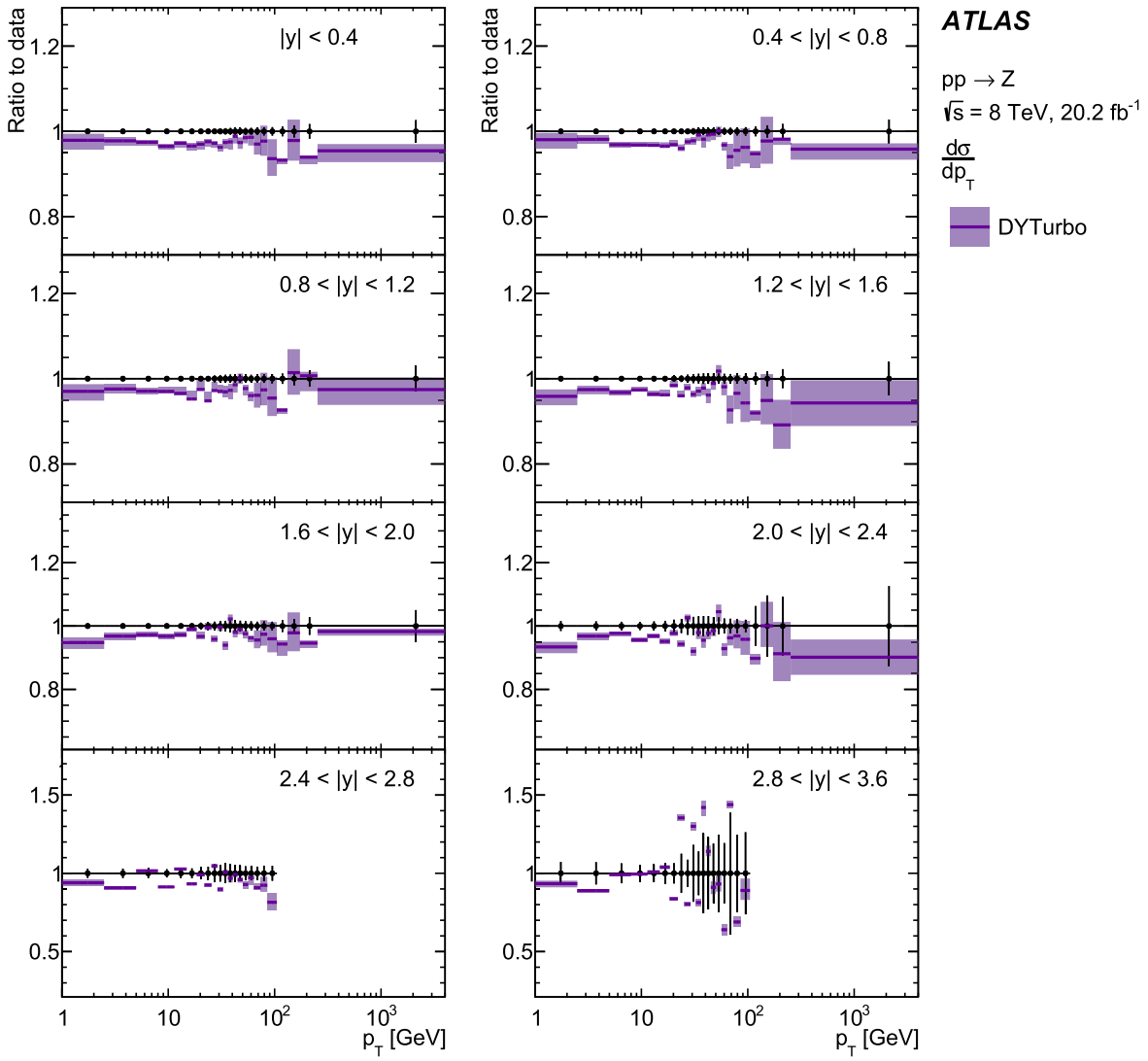

Fig. 9 Comparison between the measured absolute differential $\frac{d\sigma}{dp_T}$ cross-sections in each of the eight $|y|$ bins and the predictions from DYTurbo [45]. Shown are the ratios between the predictions with their uncertainties as obtained from renormalisation/factorisation/resummation scale variations and the data with their overall uncertainties (except for the uncertainty of 1.8% in the integrated luminosity). The predictions from DYTurbo are matched to the fixed-order O(α_s^3) contributions from MCFM [48,55]

namely $0 < |y| < 0.4$. Here the luminosity uncertainty cancels, and the softening of the p_{T} spectrum is clearly visible for the higher $|y|$ bins. This feature, measured for the first time, is expected and well reproduced by the predictions, as shown below. The standard fiducial measurements published for example using the same ATLAS data in Ref. [2] do not see this kinematic effect because the lepton fiducial selections in p_{T} and pseudorapidity largely compensate for it, resulting in a flat dependence of the differential fiducial measurement versus rapidity of the Z-boson.

Figure 9 shows the ratio of the absolute differential $\frac{d^2\sigma}{dp_T dy}$ cross-section measurements presented in Fig. 7 to the predictions from DYTurbo. In all $|y|$ bins, the predictions are a few percent lower than the measurements, a feature that is discussed more in detail in Sect. 5.3. In the region near the peak of the p_{T} distribution however, the shape of the predictions is in agreement with that of the measurements within the predominantly theoretical uncertainties. To illustrate this agreement in shape, Fig. 10 shows the ratios between the normalised differential measurements and predictions in the range $0 < p_{\mathrm{T}} < 100$ GeV. Over the full $|y|$ range measured, the data and predictions are found to be in agreement within better than 5%. There are rather strong anti-correlation terms between neighbouring bins, inducing for example the large fluctuations from bin to bin seen for the highest $|y|$ bin at high p_{T}, where the limited statistics induce terms as large as 40%.

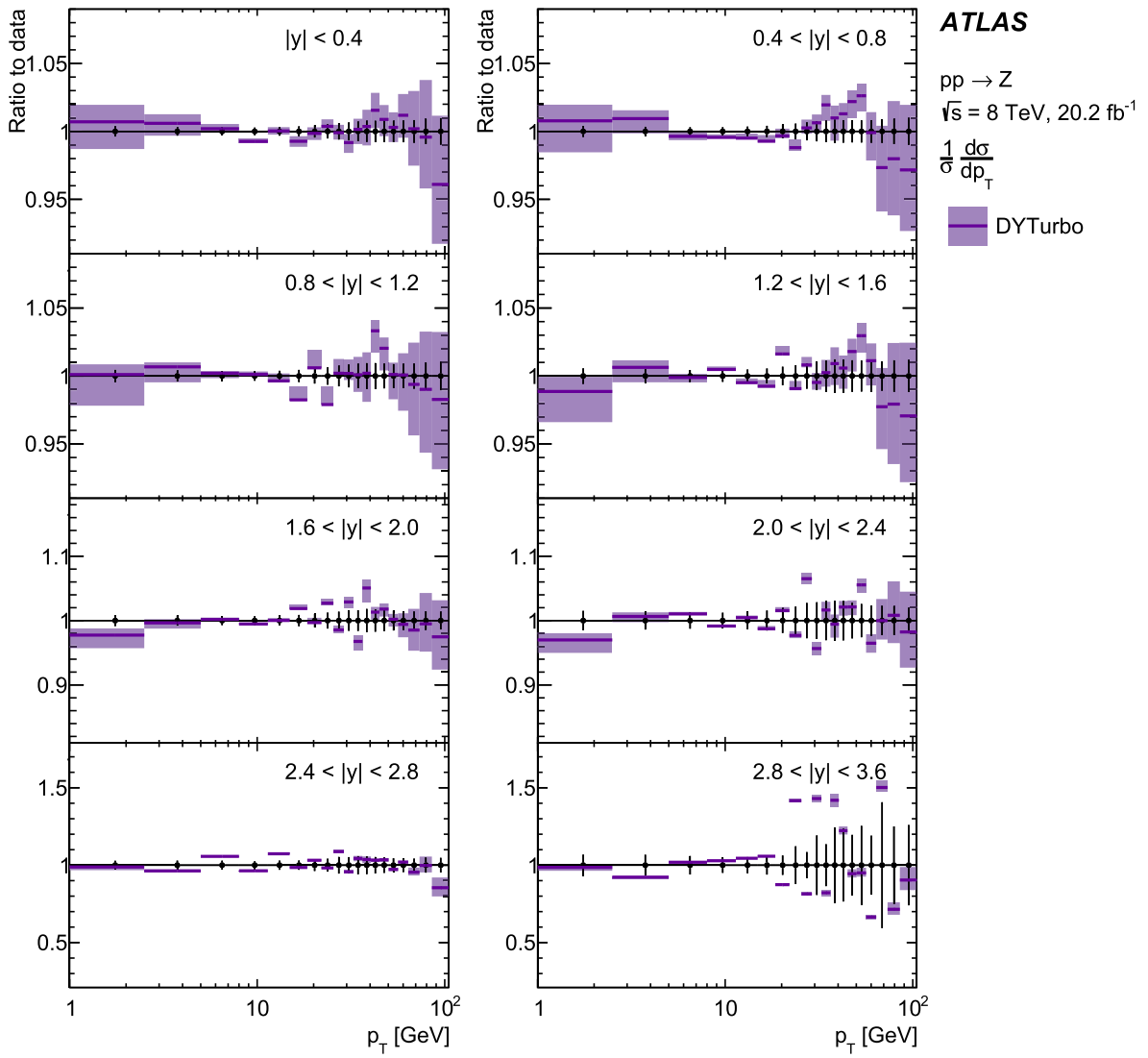

Fig. 10 Comparison between the measured normalised differential $\frac{1}{\sigma}\frac{d\sigma}{dp_T}$ cross-sections in each of the eight $|y|$ bins and the predictions from DYTurbo [45]. Shown are the ratios between the predictions with their uncertainties as obtained from renormalisation/factorisation/resummation scale variations and the data with their overall uncertainties. The predictions from DYTurbo are matched to the fixed-order O(α_s^3) contributions from MCFM [48,55]

Figures 11, 12, 13, 14, and 15 show the same ratios as in Fig. 9, successively for the CuTe-MCFM, Artemide, NangaParbat, RadISH, and SCETlib predictions. In all cases, the predictions agree with the measurements within their uncertainties, which range between 2 and 5% at the peak of the p_{T} distribution. The theory uncertainties in all the calculations are arguably incomplete at this stage, since variations between PDF sets are not included nor are uncertainties at low p_{T} related to heavy quark and non-perturbative effects.

To better assess the degree of accuracy with which the different resummation calculations agree with the data, the $\frac{d^2\sigma}{dp_T dy}$ cross-sections are integrated over $|y| < 1.6$. This improves considerably the statistical uncertainty in the measurements. Figure 16 shows these normalised $|y|$-integrated $\frac{d\sigma}{dp_T}$ spectra for the data and the predictions with their respective uncertainties, together with the ratios between each prediction and the data. The agreement of the predictions with the data is excellent, well within the scale variation uncertainties of 2–3% over most of the p_{T} range, except for two points in the lowest p_{T} bins from the RadISH predictions that are somewhat discrepant.

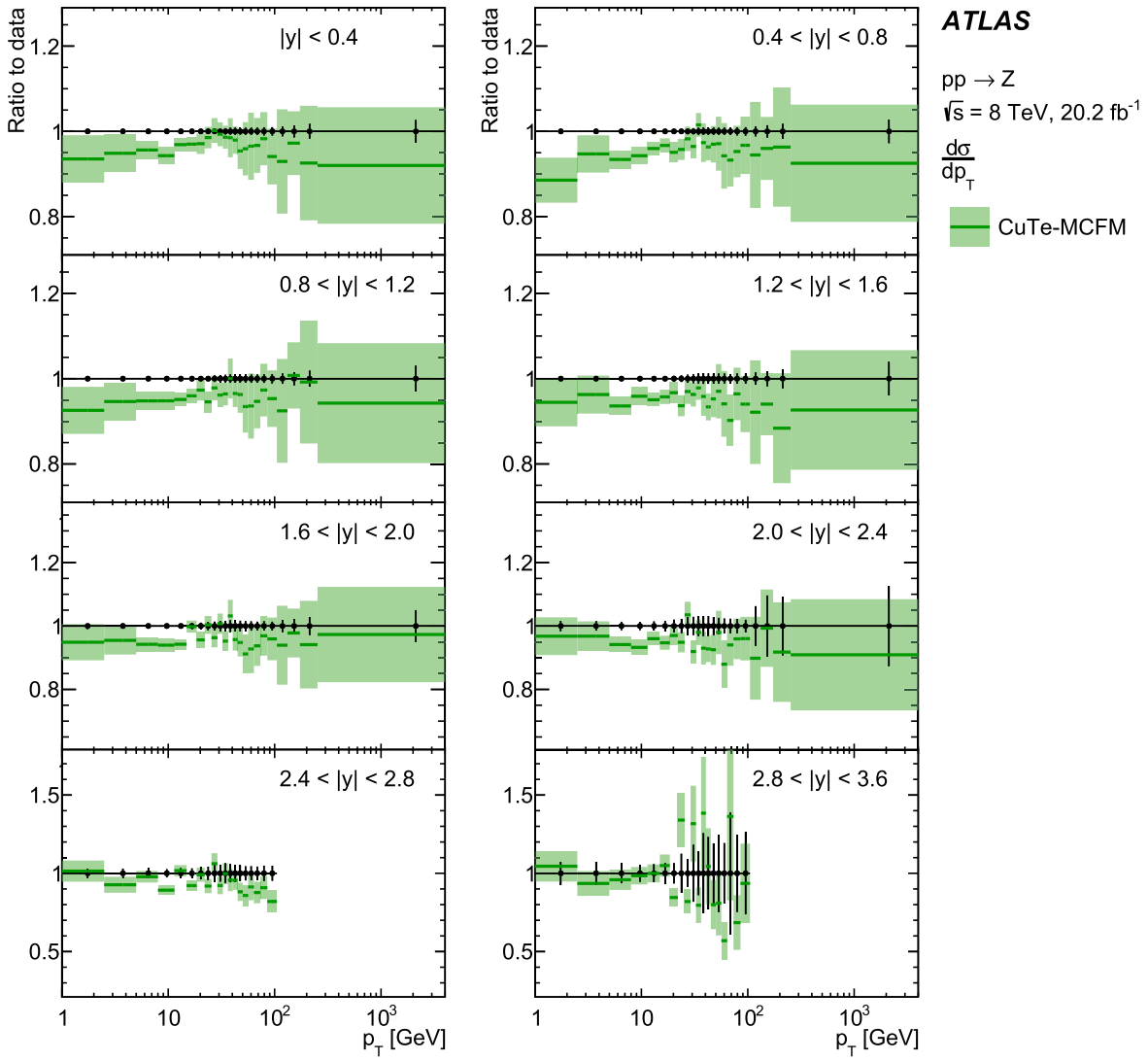

Fig. 11 Comparison between the measured absolute differential $\frac{d\sigma}{dp_T}$ cross-sections in each of the eight $|y|$ bins and the predictions from CuTe-MCFM [48]. Shown are the ratios between the predictions with their uncertainties as obtained from renormalisation/factorisation/resummation scale variations and the data with their overall uncertainties (except for the uncertainty of 1.8% in the integrated luminosity). The predictions from CuTe-MCFM are matched to the fixed-order $O(\alpha_s^3)$ contributions from MCFM [48,55]

Finally, Fig. 17 shows a comparison between the measured absolute $\frac{d\sigma}{dp_T}$ differential cross-section in each $|y|$ bin and two fixed-order $O(\alpha_s^3)$ predictions, that from MCFM, as used by the different calculations discussed above, and that from NNLOJET [56]. As expected, these fixed-order calculations are in agreement with the data at high p_T, and do not describe the data well at the lower values of p_T, where resummation is expected to play a major role, as shown for the case of the RadISH predictions matched to each of these fixed-order $O(\alpha_s^3)$ predictions in Fig. 18. The larger uncertainties seen in the case of MCFM are mostly due to limited statistics.

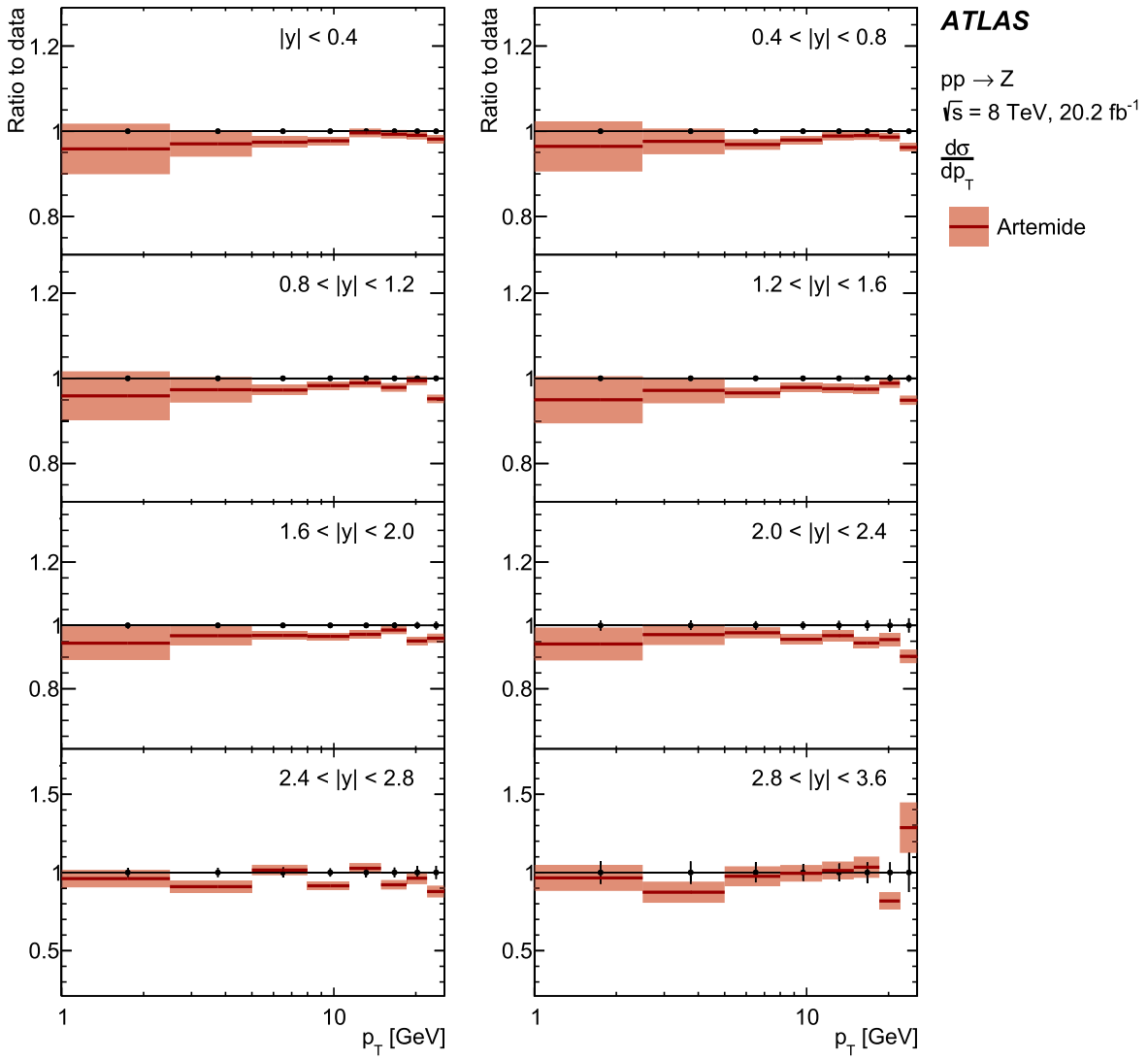

Fig. 12 Comparison between the measured absolute differential $\frac{d\sigma}{dp_T}$ cross-sections in each of the eight $|y|$ bins and the predictions from Artemide [49]. Shown are the ratios between the predictions with their uncertainties as obtained from renormalisation/factorisation/resummation scale variations and the data with their overall uncertainties (except for the uncertainty of 1.8% in the integrated luminosity). The predictions from Artemide are from pure resummation and are therefore shown only over the p_T range for which the contribution from fixed-order is below a few %

5.3 Comparison between $\frac{d\sigma}{dy}$ measurements and predictions

This section focuses on the $\frac{d\sigma}{dy}$ measurements obtained after integrating the $\frac{d^2\sigma}{dp_T dy}$ distributions shown above over p_T. As shown in Fig. 5, the experimental measurement is significantly more precise with a total uncertainty below 0.2% in the central rapidity region, owing to the large reduction of the uncertainties of a statistical nature. One also expects the theoretical uncertainties in the predictions to be significantly reduced compared to those shown for the $\frac{d^2\sigma}{dp_T dy}$ measurements. As a consequence, the focus of the comparisons between data and predictions in this section are on the PDFs, which are expected to provide the dominant uncertainty in the predictions.

Given the experimental accuracy achieved for the measurements presented in this section, higher-order effects from QED initial-state radiation (ISR) and from so-called genuine electroweak (EW) virtual corrections are considered at next-to-leading order and their sum is labelled NLO EW.

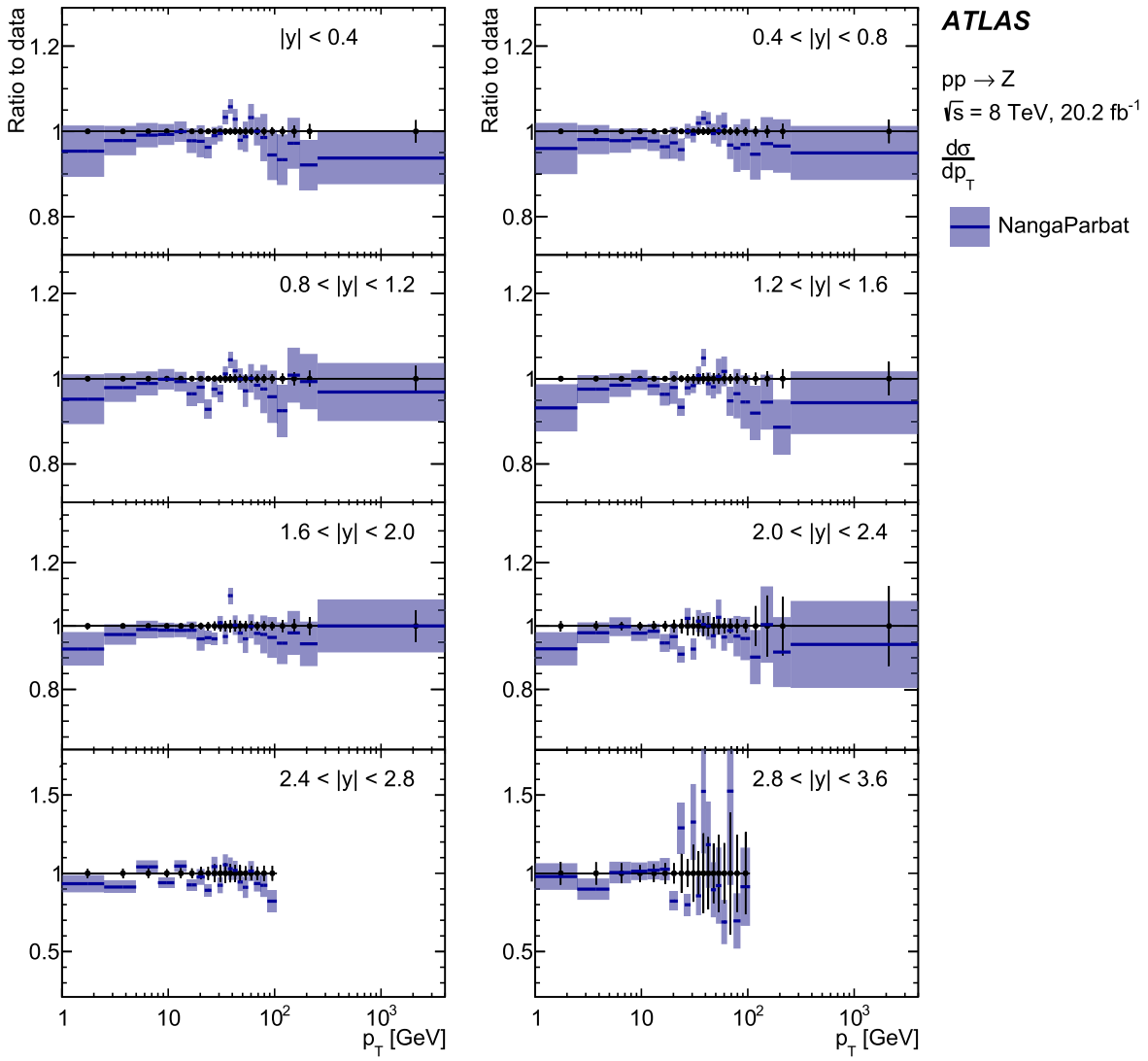

Fig. 13 Comparison between the measured absolute differential $\frac{d\sigma}{dp_T}$ cross-sections in each of the eight $|y|$ bins and the predictions from NangaParbat [50]. Shown are the ratios between the predictions with their uncertainties as obtained from renormalisation/factorisation/resummation scale variations and the data with their overall uncertainties (except for the uncertainty of 1.8% in the integrated luminosity). The predictions from NangaParbat are matched to the fixed-order $O(\alpha_s^3)$ contributions from MCFM [48,55]

These are directly computed using the code from Ref. [66], and are in agreement with earlier results from calculations benchmarked in the LHC EW working group [16,67–70]. At the Z pole, the virtual effects decrease the predicted cross-sections by 0.8%, while the QED ISR effects increase them by 0.4%. These corrections are found to be independent of rapidity. All QCD predictions shown below have therefore been decreased by a $|y|$-independent amount of 0.4% labelled as NLO EW corrections.

In this case, the comparisons to predictions do not depend on q_T resummation which, through unitarity constraints, does not affect the p_T-integrated differential cross-sections. The measurements are thus directly compared to the $O(\alpha_s^3)$ fixed-order perturbative predictions from DYTurbo, supplemented by MCFM [48,55] for the Z+jet contribution at $O(\alpha_s^3)$. These predictions are formally N^3LO in QCD and are obtained

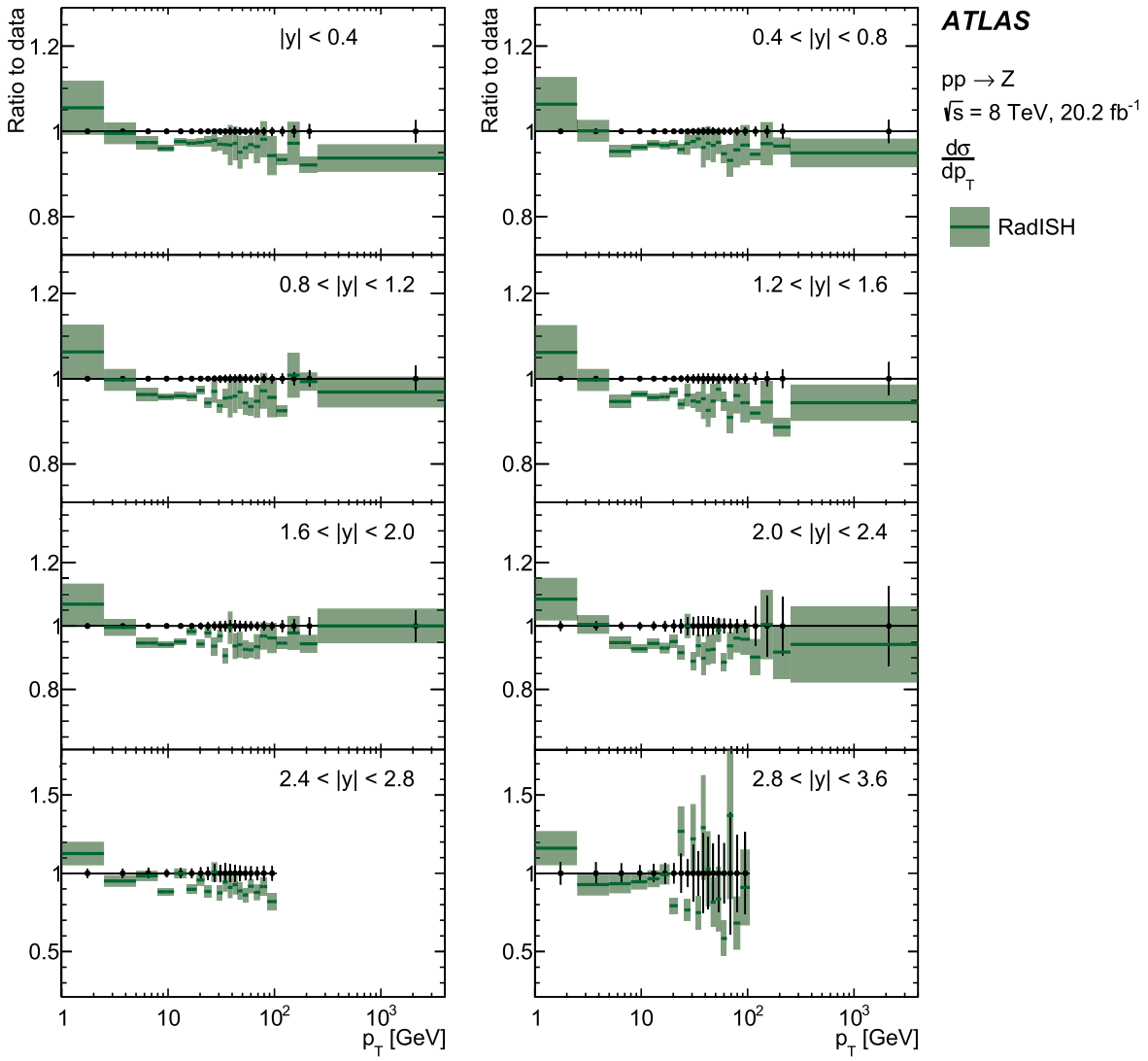

Fig. 14 Comparison between the measured absolute differential $\frac{d\sigma}{dp_T}$ cross-sections in each of the eight $|y|$ bins and the predictions from RadISH [53]. Shown are the ratios between the predictions with their uncertainties as obtained from renormalisation/factorisation/resummation scale variations and the data with their overall uncertainties (except for the uncertainty of 1.8% in the integrated luminosity). The predictions from RadISH are matched to the fixed-order O(α_s^3) contributions from MCFM [48,55]

using the very recent aN^{3}LO PDF set of Ref. [58]. For the first time, such a comparison between experimental measurements and predictions of this formal accuracy is possible and shown in Fig. 19. The theoretical uncertainty bands from QCD renormalisation/factorisation scale variations and from the aN^{3}LO PDF set are shown separately. The uncertainty arising from the scale variations rises slowly from 0.4 to 1.0% as $|y|$ increases, while the MSHT PDF uncertainty is constant at around 1.5%. As shown in the first line of Table 4, the compatibility of the theory with the data is reasonable, with a p value of 11% if one only includes the uncertainties in the PDFs for the predictions, a standard practice for many publications because most PDF sets do not usually provide scale variation uncertainties. If one combines the PDF uncertainties with a combined scale variation uncertainty from DYTurbo, assumed to be uncorrelated with that from the PDFs, the p value obtained is 12%.

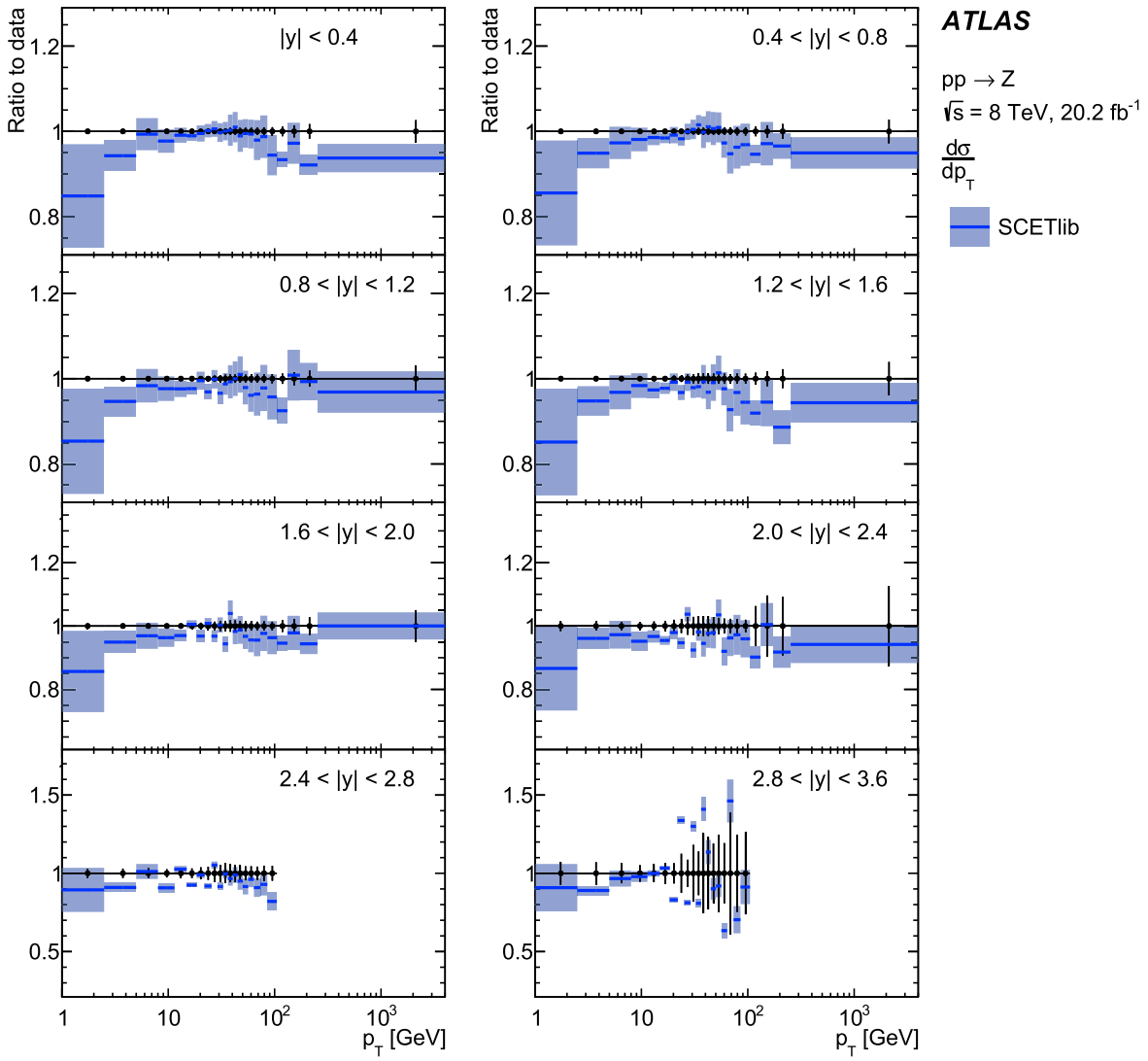

Fig. 15 Comparison between the measured absolute differential $\frac{d\sigma}{dp_T}$ cross-sections in each of the eight $|y|$ bins and the predictions from SCETlib [54]. Shown are the ratios between the predictions with their uncertainties as obtained from renormalisation/factorisation/resummation scale variations and the data with their overall uncertainties (except for the uncertainty of 1.8% in the integrated luminosity). The predictions from SCETlib are matched to the fixed-order O(α_s^3) contributions from MCFM [48,55]

To assess how the aN^{3}LO MSHT20-specific PDF uncertainty band compares to the presumably non-negligible spread between different PDF sets, the calculation has been performed one order lower, at NNLO in QCD using six of the most recent NNLO PDF sets. These comprise CT18A [59], MSHT20 [60], NNPDF4.0 [61], ABMP16 [62,63], HERAPDF2.0 [64], and ATLASpdf21 [65].

Figure 20 shows the results of these comparisons as ratios between the predictions and the data. The uncertainties in the theory predictions reflect here only the PDF specific uncertainties (the uncertainties from CT18A have been rescaled from 95 to 68% confidence level). Table 4 quantifies the quality of the agreement between the data and the predictions through the total χ^2 and its corresponding p value.

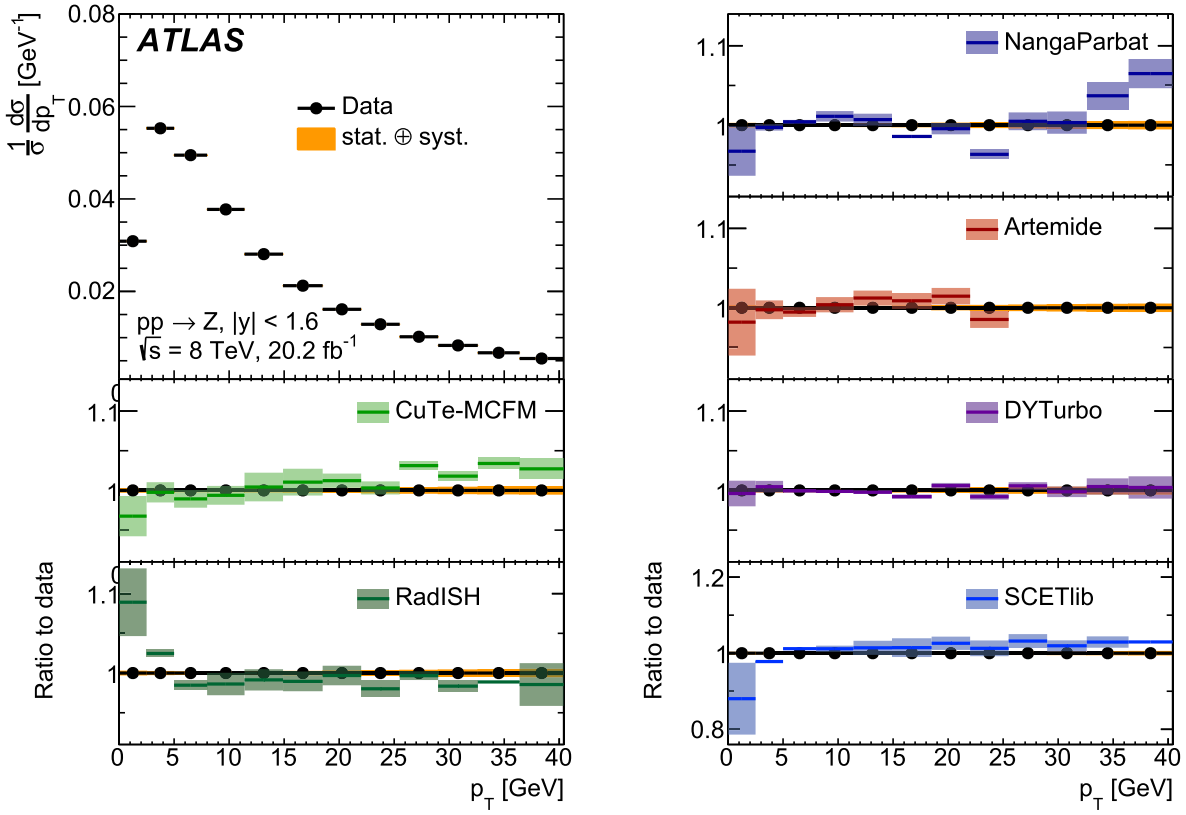

Fig. 16 Comparison between the measured normalised differential $\frac{1}{\sigma}\frac{d\sigma}{dp_T}$ cross-sections, integrated over $|y| < 1.6$, with their total uncertainties and the predictions from the various resummation calculations. The top left panel shows the data, while the next panels show one by one the ratios between each prediction with its uncertainties as obtained from renormalisation/factorisation/resummation scale variations and the data. Except for Artemide, the predictions are matched to the fixed-order $O(\alpha_s^3)$ contributions from MCFM [48,55]

Also shown is the pull on the integrated luminosity of the experiment for each PDF set. Only the aN^{3}LO MSHT, NNLO CT18A and NNLO MSHT PDF sets show reasonable agreement with the data, with a positive pull close to one standard deviation on the luminosity, corresponding to predictions approximately 1.6% lower than the data. The NNPDF4.0 PDF set with its much smaller uncertainties displays poor agreement with the data. This is due to the shape of the predicted distribution since the pull on the integrated luminosity is small. The ABMP16 PDF set is the one that most strongly pulls the integrated luminosity but its poor agreement with the data is also due to its significant difference in shape with respect to the data. The HERAPDF2.0 set and, to a lesser extent, the ATLASpdf21 set also display poor agreement because of a large discrepancy with the data in the highest $|y|$ bin due to the limited set of data used in these fits.

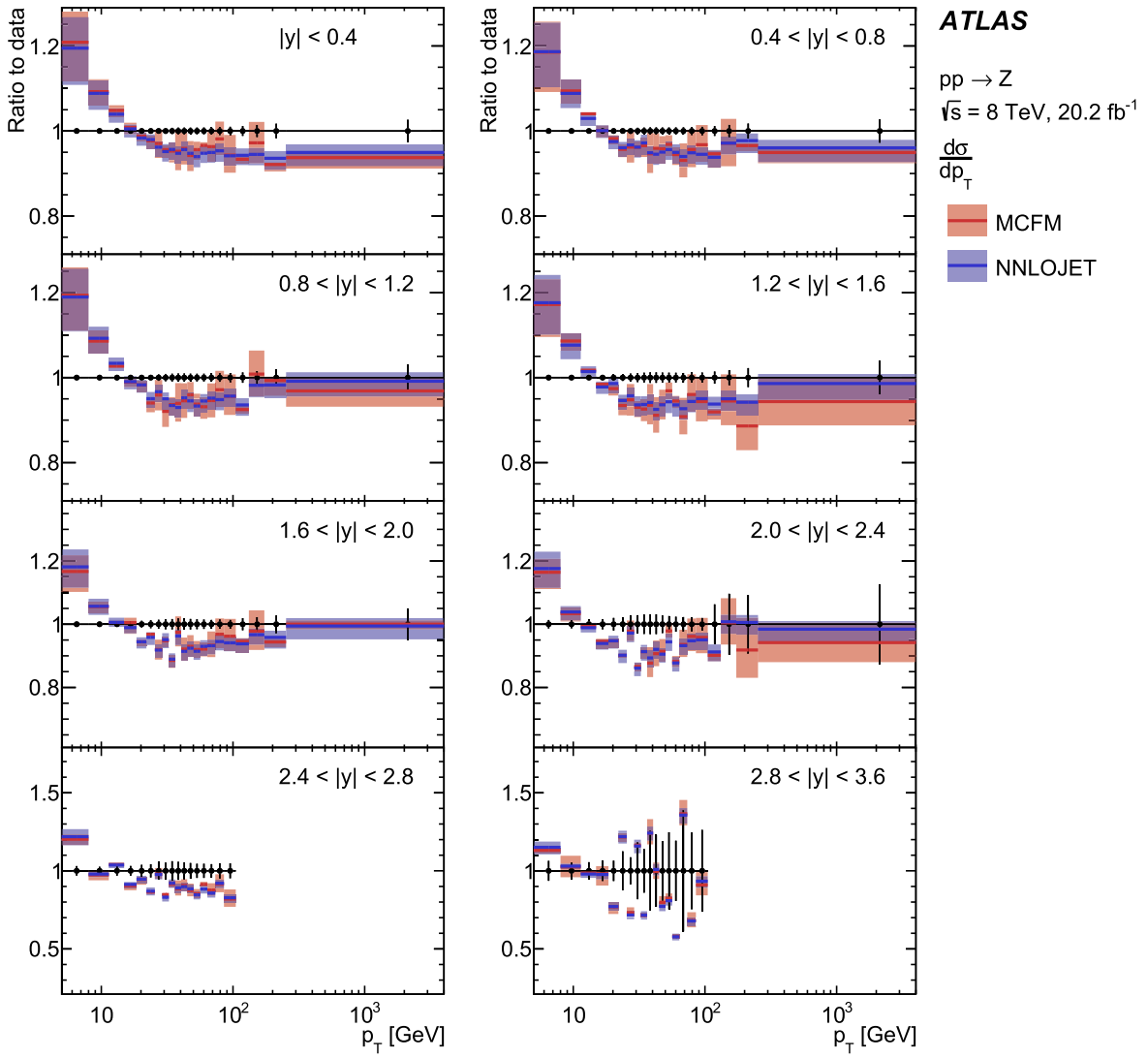

Fig. 17 Comparison between the absolute differential $\frac{d\sigma}{dp_T}$ cross-sections with their total uncertainties in each $|y|$ bin and the predictions from the two fixed-order O(α_s^3) calculations from MCFM [48,55] and NNLOJET [56]

Finally, the tot al cross-section times branching ratio of $Z \to \ell\ell$, σ_Z, for Z/γ^* production in the Z-boson pole region, $80 < m < 100$ GeV, and within $|y| < 3.6$ is extracted from the integration of the measured differential $\frac{d\sigma}{dy}$ cross-section:

$$\sigma_Z = 1055.3 \pm 0.7\,(\text{stat.}) \pm 2.2\,(\text{syst.}) \pm 19.0\,(\text{lumi.})\text{pb}.$$

Aside from the dominant uncertainty in the integrated luminosity, the overall systematic uncertainty of 0.2% in this measurement is dominated by experimental lepton efficiency systematic uncertainties and has a negligible contribution from theory uncertainties, which are below 0.1% and arise essentially from PDFs. Table 5 compares this measurement to the predictions obtained from DYTurbo with the same PDF sets as those shown in Table 4 for the rapidity-dependent cross-section $\frac{d\sigma}{dy}$.

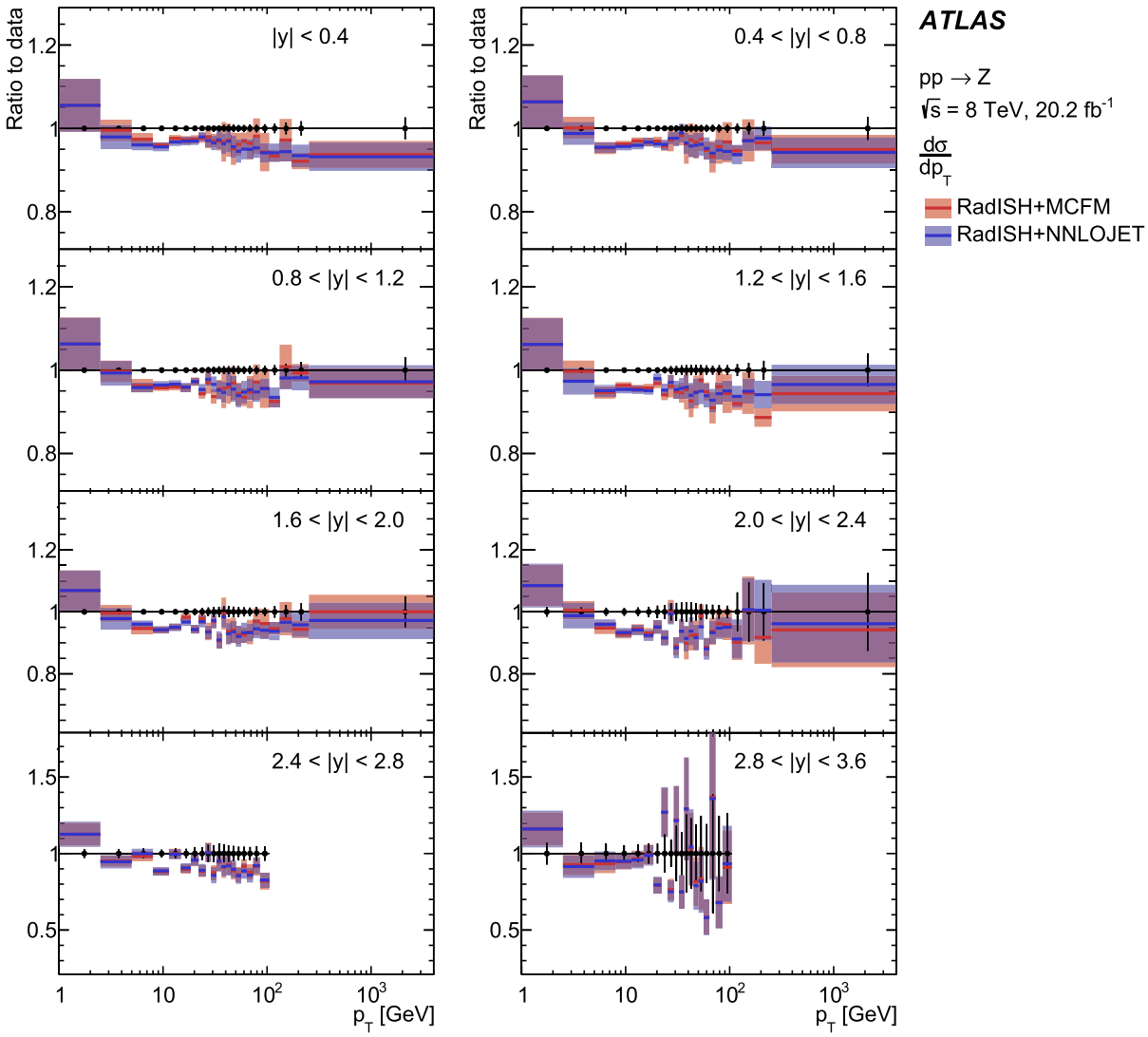

Fig. 18 Comparison between the absolute differential $\frac{d\sigma}{dp_T}$ cross-sections with their total uncertainties in each $|y|$ bin and the predictions from RadISH [53] matched to the two fixed-order O(α_s^3) calculations from MCFM [48,55] and NNLOJET [56,57]

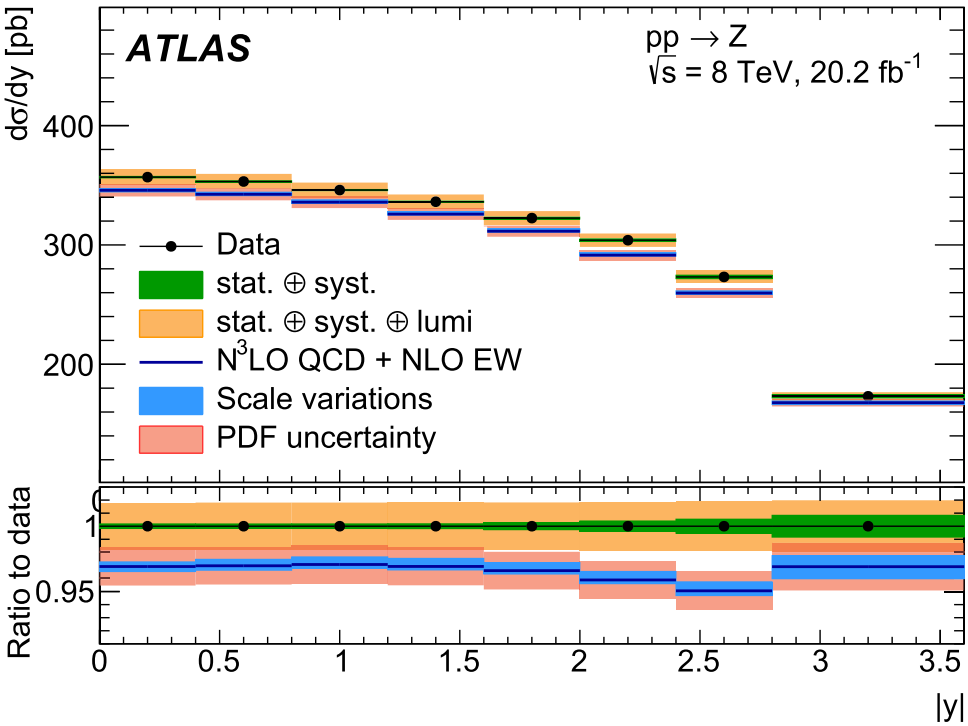

Fig. 19 Comparison between the $\frac{d\sigma}{dy}$ measurements and N^{3}LO QCD predictions obtained from DYTurbo using the recent aN^{3}LO MSHT PDF set. The N^{3}LO QCD theory prediction includes a negative correction of 0.4% from NLO EW effects and the theoretical uncertainty bands from QCD renormalisation/factorisation scale variations and from the aN^{3}LO PDF set are shown separately. The bottom panel shows the ratios between predictions and data, where the data uncertainty bands with and without inclusion of the dominant uncertainty of 1.8% in the integrated luminosity are shown separately

Table 4 Compatibility test between $\frac{d\sigma}{dy}$ measurements and predictions obtained from DYTurbo using different PDF sets. Based on the total uncertainties in the measurements and on the PDF uncertainties in the predictions shown in Figs. 19 and 20, the χ^2 per degree of freedom (d.o.f.) and corresponding p-values are shown for each PDF set (the uncertainties from CT18A have been rescaled from 95% to 68% confidence level). Also shown is the pull on the integrated luminosity in units of its total uncertainty of 1.8%

PDF set	Total χ^2/d.o.f.	χ^2 p value	Pull on luminosity
MSHT20aN^{3}LO [58]	13/8	0.11	1.2 ± 0.6
CT18A [59]	12/8	0.17	0.9 ± 0.7
MSHT20 [60]	10/8	0.26	0.9 ± 0.6
NNPDF4.0 [61]	30/8	0.0002	0.0 ± 0.2
ABMP16 [62,63]	30/8	0.0002	1.8 ± 0.4
HERAPDF2.0 [64]	22/8	0.005	-1.3 ± 0.8
ATLASpdf21 [65]	20/8	0.01	-1.1 ± 0.8

6 Conclusions

This paper presents for the first time a double-differential measurement in (p_{T}, $|y|$) of absolute and normalised cross-sections at the Z pole within the full phase space of the decay leptons. This is in contrast to the many previous precise unfolded measurements performed in the fiducial phase space of the decay leptons. The measurements in this paper are obtained through a four-dimensional measurement of the lepton angular distributions as a function of $p_{\mathrm{T}}^{\ell\ell}$ and $y^{\ell\ell}$ for a total sample of approximately 15 million Z-boson decays measured within the pole region, $80 < m^{\ell\ell} < 100$ GeV, and within the range $|y^{\ell\ell}| < 3.6$. Such a measurement is achieved by extending and improving the methodology already developed and published for the extraction of the Z-boson angular coefficients. A profile likelihood fit extracts at the same time these eight angular coefficients and the corresponding unpolarised cross-section as parameters of interest in each measurement bin in (p_{T}, $|y|$) space. The uncertainties in these measurements are mostly statistical in nature and the experimental and theoretical systematics are at the few per mille level over most of the range.

The $\frac{d^2\sigma}{dp_{\mathrm{T}}dy}$ measurements are compared to several state-of-the-art QCD perturbative predictions based on q_{T}-resummation at approximate N^{4}LL accuracy matched to fixed-order O(α_s^3) calculations at high p_{T}. The agreement between the data and the predictions is within 5% over the whole range of the measurements except in kinematic regions with limited statistics.

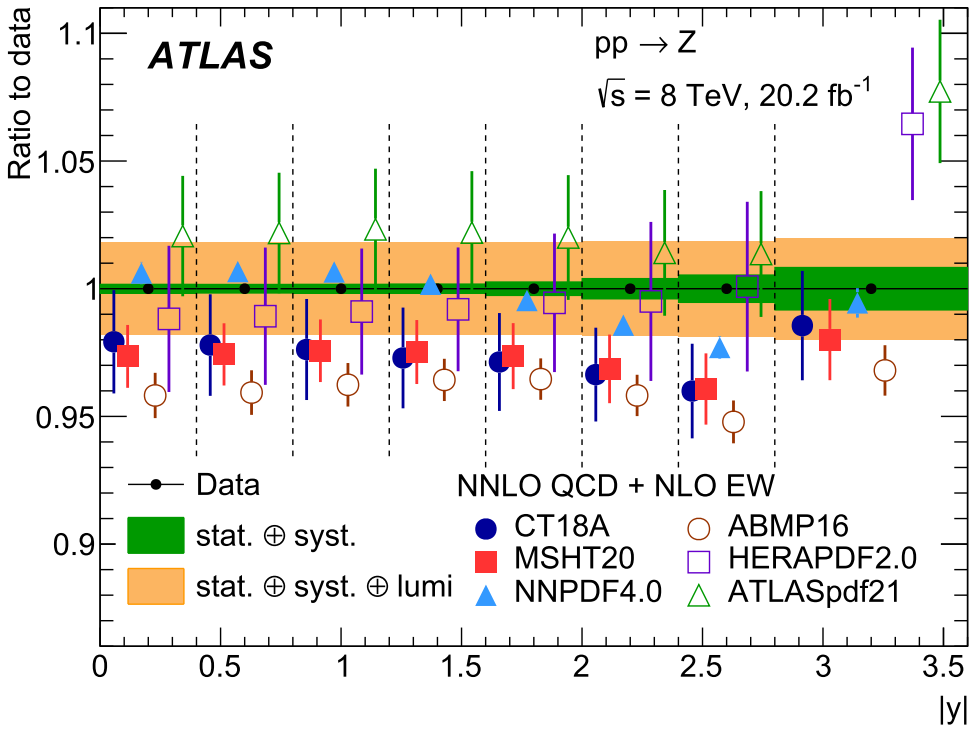

Fig. 20 Ratio comparison between the $\frac{d\sigma}{dy}$ measurements and NNLO QCD predictions obtained from DYTurbo using different NNLO PDF sets. The uncertainty bands in the predictions only show the uncertainties specific to each PDF set (the uncertainties from CT18A have been rescaled from 95% to 68% confidence level). In each $|y|$ bin, the ratios for each PDF set are gradually displaced to the right for plotting purposes

Table 5 Comparison between the measured total cross-section times branching ratio of $Z \to \ell\ell$, σ_Z, for Z/γ^* production with its uncertainty and predictions obtained from DYTurbo using different PDF sets. The prediction using the MSHTaN^{3}LO PDF from Ref. [58] shows separately the scale variation and PDF uncertainties. The uncertainties in the NNLO predictions include only the PDF uncertainties from each specific PDF set (the uncertainties from CT18A have been rescaled from 95% to 68% confidence level)

Data	σ_Z (pb) 1055 ± 19
MSHT20aN^{3}LO [58]	1023^{+6}_{-4} (scale) ± 15 (PDF)
CT18A [59]	1028 ± 19
MSHT20 [60]	1027 ± 13
NNPDF4.0 [61]	1054 ± 4
ABMP16 [62]	1014 ± 9
HERAPDF2.0 [64]	1058 ± 25
ATLASpdf21 [65]	1084 ± 25

Once integrated over p_{T}, the rapidity-dependent cross-sections are measured with an overall accuracy of 0.2–0.5% before accounting for the uncertainty in the integrated luminosity of 1.8%. They are compared to the predictions from different PDF sets, which display a varying degree of agreement with the data.

The total cross-section times branching ratio of $Z \to \ell\ell$, σ_Z, for Z/γ^* production in the Z-boson pole region, $80 < m < 100$ GeV, and within $|y| < 3.6$, is found to be: $\sigma_Z = 1055.3 \pm 0.7\,(\mathrm{stat.}) \pm 2.2\,(\mathrm{syst.}) \pm 19.0\,(\mathrm{lumi.})$ pb, in agreement with state-of-the-art predictions at N^{3}LO in QCD.

Acknowledgements We thank CERN for the very successful operation of the LHC, as well as the support staff from our institutions without whom ATLAS could not be operated efficiently. We acknowledge the support of ANPCyT, Argentina; YerPhI, Armenia; ARC, Australia; BMWFW and FWF, Austria; ANAS, Azerbaijan; CNPq and FAPESP, Brazil; NSERC, NRC and CFI, Canada; CERN; ANID, Chile; CAS, MOST and NSFC, China; Minciencias, Colombia; MEYS CR, Czech Republic; DNRF and DNSRC, Denmark; IN2P3-CNRS and CEA-DRF/IRFU, France; SRNSFG, Georgia; BMBF, HGF and MPG, Germany; GSRI, Greece; RGC and Hong Kong SAR, China; ISF and Benoziyo Center, Israel; INFN, Italy; MEXT and JSPS, Japan; CNRST, Morocco; NWO, Netherlands; RCN, Norway; MEiN, Poland; FCT, Portugal; MNE/IFA, Romania; MESTD, Serbia; MSSR, Slovakia; ARRS and MIZŠ, Slovenia; DSI/NRF, South Africa; MICINN, Spain; SRC and Wallenberg Foundation, Sweden; SERI, SNSF and Cantons of Bern and Geneva, Switzerland; MOST, Taiwan; TENMAK, Türkiye; STFC, United Kingdom; DOE and NSF, United States of America. In addition, individual groups and members have received support from BCKDF, CANARIE, Compute Canada and CRC, Canada; PRIMUS 21/SCI/017 and UNCE SCI/013, Czech Republic; COST, ERC, ERDF, Horizon 2020 and Marie Skłodowska-Curie Actions, European Union; Investissements d'Avenir Labex, Investissements d'Avenir Idex and ANR, France; DFG and AvH Foundation, Germany; Herakleitos, Thales and Aristeia programmes co-financed by EU-ESF and the Greek NSRF, Greece; BSF-NSF and MINERVA, Israel; Norwegian Financial Mechanism 2014-2021, Norway; NCN and NAWA, Poland; La Caixa Banking Foundation, CERCA Programme Generalitat de Catalunya and PROMETEO and GenT Programmes Generalitat Valenciana, Spain; Göran Gustafssons Stiftelse, Sweden; The Royal Society and Leverhulme Trust, United Kingdom. The crucial computing support from all WLCG partners is acknowledged gratefully, in particular from CERN, the ATLAS Tier-1 facilities at TRIUMF (Canada), NDGF (Denmark, Norway, Sweden), CC-IN2P3 (France), KIT/GridKA (Germany), INFN-CNAF (Italy), NL-T1 (Netherlands), PIC (Spain), ASGC (Taiwan), RAL (UK) and BNL (USA), the Tier-2 facilities worldwide and large non-WLCG resource providers. Major contributors of computing resources are listed in Ref. [71].

Data Availability This manuscript has no associated data or the data will not be deposited. [Authors' comment: "All ATLAS scientific output is published in journals, and preliminary results are made available in Conference Notes. All are openly available, without restriction on use by external parties beyond copyright law and the standard conditions agreed by CERN. Data associated with journal publications are also made available: tables and data from plots (e.g. cross section values, likelihood profiles, selection efficiencies, cross section limits, ...) are stored in appropriate repositories such as HEPDATA (http://hepdata.cedar.ac.uk/). ATLAS also strives to make additional material related to the paper available that allows a reinterpretation of the data in the context of new theoretical models. For example, an extended encapsulation of the analysis is often provided for measurements in the framework of RIVET (http://rivet.hepforge.org/)."

Funded by SCOAP[3].

References

1. S.D. Drell, T.M. Yan, Massive lepton-pair production in hadron-hadron collisions at high energies. Phys. Rev. Lett. **25**, 316 (1970)
2. ATLAS Collaboration, Measurement of the transverse momentum and ϕ^*_η distributions of Drell–Yan lepton pairs in proton–proton collisions at $\sqrt{s} = 8$ TeV with the ATLAS detector. Eur. Phys. J. C **76**, 291 (2016). https://doi.org/10.1140/epjc/s10052-016-4070-4. arXiv:1512.02192
3. ATLAS Collaboration, Measurement of the transverse momentum distribution of Drell–Yan lepton pairs in proton–proton collisions at $\sqrt{s} = 13$ TeV with the ATLAS detector. Eur. Phys. J. C **80**, 616 (2020). https://doi.org/10.1140/epjc/s10052-020-8001-z. arXiv:1912.02844 [hep-ex]
4. CMS Collaboration, Measurement of the Z boson differential cross section in transverse momentum and rapidity in proton-proton collisions at 8 TeV. Phys. Lett. B **749**, 187 (2015). https://doi.org/10.1016/j.physletb.2015.07.065. arXiv:1504.03511 [hep-ex]
5. CMS Collaboration, Measurements of differential Z boson production cross sections in proton-proton collisions at $\sqrt{s} = 13$ TeV. JHEP **12**, 061 (2019). https://doi.org/10.1007/JHEP12(2019)061. arXiv:1909.04133
6. ATLAS Collaboration, Measurement of the angular coefficients in Z-boson events using electron and muon pairs from data taken at $\sqrt{s} = 8$ TeV with the ATLAS detector. JHEP **08**, 159 (2016). https://doi.org/10.1007/JHEP08(2016)159. arXiv:1606.00689
7. CMS Collaboration, Angular coefficients of Z bosons produced in pp collisions at $\sqrt{s} = 8$ TeV and decaying to $\mu^+\mu^-$ as a function of transverse momentum and rapidity. Phys. Lett. B **750**, 154 (2015). https://doi.org/10.1016/j.physletb.2015.08.061. arXiv:1504.03512 [hep-ex]
8. ATLAS Collaboration, Measurement of the Drell–Yan triple-differential cross section in pp collisions at $\sqrt{s} = 8$ TeV. JHEP **12**, 059 (2017). https://doi.org/10.1007/JHEP12(2017)059. arXiv:1710.05167 [hep-ex]
9. J.C. Collins, D.E. Soper, Angular distribution of dileptons in high-energy hadron collisions. Phys. Rev. D **16**, 2219 (1977). https://doi.org/10.1103/PhysRevD.16.2219
10. E. Mirkes, Angular decay distribution of leptons from W-bosons at NLO in hadronic collisions. Nucl. Phys. B **387**, 3 (1992). https://doi.org/10.1016/0550-3213(92)90046-E
11. E. Mirkes, J. Ohnemus, W and Z polarization effects in hadronic collisions. Phys. Rev. D **50**, 5692 (1994). https://doi.org/10.1103/PhysRevD.50.5692. arXiv:hep-ph/9406381
12. E. Mirkes, J. Ohnemus, Angular distributions of Drell–Yan lepton pairs at the tevatron: order α_s^2 corrections and Monte Carlo studies. Phys. Rev. D **51**, 4891 (1995). https://doi.org/10.1103/PhysRevD.51.4891. arXiv:hep-ph/9412289
13. E. Mirkes, J. Ohnemus, Polarization effects in Drell–Yan type processes $h_1 + h_2 \to (W, Z, \gamma^*, J/psi) + X$ (1994). arXiv:hep-ph/9408402
14. S. Jadach, Z. Was, Suppression of QED interference contributions to the charge asymmetry at the Z^0 resonance. Phys. Lett. B **219**, 103 (1989). https://doi.org/10.1016/0370-2693(89)90847-2
15. S. Jadach et al., Initial-final-state interference in the Z line shape. Phys. Lett. B **465**, 254 (1999). https://doi.org/10.1016/S0370-2693(99)01047-3. arXiv:hep-ph/9907547
16. S. Jadach, B.F.L. Ward, Z.A. Was, S.A. Yost, KK MC-hh: systematic studies of exact $O(\alpha^2 L)$ CEEX EW corrections in a hadronic MC for precision Z/γ^* physics at LHC Energies. Phys. Rev. D **99**, 076016 (2019). https://doi.org/10.1103/PhysRevD.99.076016
17. M.A. Ebert, J.K.L. Michel, I.W. Stewart, F.J. Tackmann, Drell–Yan q_T resummation of fiducial power corrections at N^3LL. JHEP **04**, 102 (2021). https://doi.org/10.1007/JHEP04(2021)102. arXiv:2006.11382 [hep-ph]
18. A. Glazov, Defiducialization: providing experimental measurements for accurate fixed-order predictions. Eur. Phys. J. C **80**, 875 (2020). https://doi.org/10.1140/epjc/s10052-020-08435-4. arXiv:2001.02933 [hep-ex]
19. G.P. Salam, E. Slade, Cuts for two-body decays at colliders. JHEP **11**, 220 (2021). https://doi.org/10.1007/JHEP11(2021)220. arXiv:2106.08329 [hep-ph]
20. S. Alekhin, A. Kardos, S. Moch, Z. Trócsányi, Precision studies for Drell–Yan processes at NNLO. Eur. Phys. J. C **81**, 573 (2021). https://doi.org/10.1140/epjc/s10052-021-09361-9. arXiv:2104.02400 [hep-ph]
21. ATLAS Collaboration, Electron efficiency measurements with the ATLAS detector using 2012 LHC proton-proton collision data. Eur. Phys. J. C **77**, 195 (2017). https://doi.org/10.1140/epjc/s10052-017-4756-2. arXiv:1612.01456 [hep-ex]
22. ATLAS Collaboration, The ATLAS experiment at the CERN large hadron collider. JINST **3**, S08003 (2008). https://doi.org/10.1088/1748-0221/3/08/S08003
23. ATLAS Collaboration, The ATLAS Collaboration Software and Firmware, ATL-SOFT-PUB-2021-001 (2021). https://cds.cern.ch/record/2767187
24. P. Nason, A new method for combining NLO QCD with shower Monte Carlo algorithms. JHEP **11**, 040 (2004). https://doi.org/10.1088/1126-6708/2004/11/040
25. S. Frixione, P. Nason, C. Oleari, Matching NLO QCD computations with parton shower simulations: the POWHEG method. JHEP **11**, 070 (2007). https://doi.org/10.1088/1126-6708/2007/11/070. arXiv:0709.2092 [hep-ph]
26. S. Alioli, P. Nason, C. Oleari, E. Re, A general framework for implementing NLO calculations in shower Monte Carlo programs: the POWHEG BOX. JHEP **06**, 043 (2010). https://doi.org/10.1007/JHEP06(2010)043. arXiv:1002.2581 [hep-ph]

27. T. Sjöstrand, S. Mrenna, P. Skands, A brief introduction to PYTHIA 8.1. Comput. Phys. Commun. **178**, 852 (2008). https://doi.org/10.1016/j.cpc.2008.01.036
28. H.-L. Lai, M. Guzzi, J. Huston, Z. Li, P.M. Nadolsky et al., New parton distributions for collider physics. Phys. Rev. D **82**, 074024 (2010). https://doi.org/10.1103/PhysRevD.82.074024. arXiv:1007.2241 [hep-ph]
29. T. Gleisberg, S. Höche, F. Krauss et al., Event generation with SHERPA 1.1. JHEP **02**, 007 (2009). https://doi.org/10.1088/1126-6708/2009/02/007. arXiv:0811.4622 [hep-ph]
30. S. Höche, F. Krauss, S. Schumann, F. Siegert, QCD matrix elements and truncated showers. JHEP **05**, 053 (2009). https://doi.org/10.1088/1126-6708/2009/05/053. arXiv:0903.1219 [hep-ph]
31. T. Gleisberg, S. Höche, Comix, a new matrix element generator. JHEP **12**, 039 (2008). https://doi.org/10.1088/1126-6708/2008/12/039. arXiv:0808.3674 [hep-ph]
32. S. Schumann, F. Krauss, A parton shower algorithm based on Catani–Seymour dipole factorisation. JHEP **03**, 038 (2008). https://doi.org/10.1088/1126-6708/2008/03/038. arXiv:0709.1027 [hep-ph]
33. T. Sjöstrand, S. Mrenna, P.Z. Skands, PYTHIA 6.4 physics and manual. JHEP **05**, 026 (2006). https://doi.org/10.1088/1126-6708/2006/05/026. arXiv:hep-ph/0603175
34. G. Corcella et al., HERWIG 6: an event generator for hadron emission reactions with interfering gluons (including supersymmetric processes). JHEP **01**, 010 (2001). https://doi.org/10.1088/1126-6708/2001/01/010. arXiv:hep-ph/0011363
35. A.D. Martin et al., Parton distributions incorporating QED contributions. Eur. Phys. J. C **39**, 155 (2005). https://doi.org/10.1140/epjc/s2004-02088-7. arXiv:hep-ph/0411040
36. ATLAS Collaboration, Summary of ATLAS Pythia 8 tunes, ATL-PHYS-PUB-2012-003 (2012). https://cds.cern.ch/record/1474107
37. P. Golonka, Z. Was, PHOTOS Monte Carlo: a precision tool for QED corrections in Z and W decays. Eur. Phys. J. C **45**, 97 (2006). https://doi.org/10.1140/epjc/s2005-02396-4. arXiv:hep-ph/0506026
38. Y. Li, F. Petriello, Combining QCD and electroweak corrections to dilepton production in the framework of the FEWZ simulation code. Phys. Rev. D **86**, 094034 (2012). https://doi.org/10.1103/PhysRevD.86.094034. arXiv:1208.5967 [hep-ph]
39. ATLAS Collaboration, The ATLAS simulation infrastructure. Eur. Phys. J. C **70**, 823 (2010). https://doi.org/10.1140/epjc/s10052-010-1429-9. arXiv:1005.4568 [physics.ins-det]
40. S. Agostinelli et al., Geant4—a simulation toolkit. Nucl. Instrum. Methods A **506**, 250 (2003). https://doi.org/10.1016/S0168-9002(03)01368-8
41. ATLAS Collaboration, Measurement of the muon reconstruction performance of the ATLAS detector using 2011 and 2012 LHC proton-proton collision data. Eur. Phys. J. C **74**, 3130 (2014). https://doi.org/10.1140/epjc/s10052-014-3130-x. arXiv:1407.3935
42. ATLAS Collaboration, Electron reconstruction and identification efficiency measurements with the ATLAS detector using the 2011 LHC proton–proton collision data. Eur. Phys. J. C **74**, 2941 (2014). https://doi.org/10.1140/epjc/s10052-014-2941-0. arXiv:1404.2240 [hep-ex]
43. ATLAS Collaboration, Electron and photon energy calibration with the ATLAS detector using LHC Run 1 data. Eur. Phys. J. C **74**, 3071 (2014). https://doi.org/10.1140/epjc/s10052-014-3071-4. arXiv:1407.3935
44. G. Bozzi, S. Catani, D. de Florian, M. Grazzini, Transverse-momentum resummation and the spectrum of the Higgs boson at the LHC. Nucl. Phys. B **737**, 73 (2006). https://doi.org/10.1016/j.nuclphysb.2005.12.022. arXiv:hep-ph/0508068
45. S. Camarda et al., DYTurbo: fast predictions for Drell–Yan processes. Eur. Phys. J. C **80**, 251 (2020). [Erratum: Eur. Phys. J. C **80**, 440 (2020)]. https://doi.org/10.1140/epjc/s10052-020-7757-5. arXiv:1910.07049 [hep-ph]
46. S. Camarda, L. Cieri, G. Ferrera, Drell–Yan lepton-pair production: q_T resummation at N^3LL accuracy and fiducial cross sections at N^3LO. Phys. Rev. D **104**, L111503 (2021). https://doi.org/10.1103/PhysRevD.104.L111503. arXiv:2103.04974 [hep-ph]
47. S. Camarda, L. Cieri, G. Ferrera, Drell–Yan lepton-pair production: q_T resummation at approximate $N^4LL + N^4LO$ accuracy (2023). arXiv:2303.12781 [hep-ph]
48. T. Neumann, J. Campbell, Fiducial Drell–Yan production at the LHC improved by transverse-momentum resummation at $N^4LL_p + N^3LO$. Phys. Rev. D **107**, L011506 (2023). https://doi.org/10.1103/PhysRevD.107.L011506. arXiv:2207.07056 [hep-ph]
49. I. Scimemi, A. Vladimirov, Analysis of vector boson production within TMD factorization. Eur. Phys. J. C **78**, 89 (2018). https://doi.org/10.1140/epjc/s10052-018-5557-y. arXiv:1706.01473 [hep-ph]
50. A. Bacchetta et al., Transverse-momentum-dependent parton distributions up to N^3LL from Drell–Yan data. JHEP **07**, 117 (2020). https://doi.org/10.1007/JHEP07(2020)117. arXiv:1912.07550 [hep-ph]
51. P.F. Monni, E. Re, P. Torrielli, Higgs transverse-momentum resummation in direct space. Phys. Rev. Lett. **116**, 242001 (2016). https://doi.org/10.1103/PhysRevLett.116.242001. arXiv:1604.02191 [hep-ph]
52. W. Bizon, P.F. Monni, E. Re, L. Rottoli, P. Torrielli, Momentum-space resummation for transverse observables and the Higgs $p_\perp$ at $N^3LL + NNLO$. JHEP **02**, 108 (2018). https://doi.org/10.1007/JHEP02(2018)108. arXiv:1705.09127 [hep-ph]
53. E. Re, L. Rottoli, P. Torrielli, Fiducial Higgs and Drell–Yan distributions at $N^3LL' + NNLO$ with RadISH. JHEP **9**, 108 (2021). https://doi.org/10.1007/JHEP09(2021)108. arXiv:2104.07509 [hep-ph]
54. G. Billis, B. Dehnadi, M.A. Ebert, J.K.L. Michel, F.J. Tackmann, Higgs pT spectrum and total cross section with fiducial cuts at third resummed and fixed order in QCD. Phys. Rev. Lett. **127**, 072001 (2021). https://doi.org/10.1103/PhysRevLett.127.072001. arXiv:2102.08039 [hep-ph]
55. R. Boughezal et al., Z-boson production in association with a jet at next-to-next-to-leading order in perturbative QCD. Phys. Rev. Lett. **116**, 152001 (2016). https://doi.org/10.1103/PhysRevLett.116.152001. arXiv:1512.01291 [hep-ph]
56. A. G.-D. Ridder, T. Gehrmann, E. Glover, A. Huss, T. Morgan, Precise QCD predictions for the production of a Z boson in association with a hadronic jet. Phys. Rev. Lett. **117** (2016). https://doi.org/10.1103/physrevlett.117.022001. arXiv:1507.02850 [hep-ph]
57. X. Chen et al., Third-order fiducial predictions for Drell–Yan production at the LHC. Phys. Rev. Lett. **128**, 252001 (2022). https://doi.org/10.1103/PhysRevLett.128.252001. arXiv:2203.01565 [hep-ph]
58. J. McGowan, T. Cridge, L.A. Harland-Lang, R.S. Thorne, Approximate N^3LO parton distribution functions with theoretical uncertainties: $MSHT20aN^3LO$ PDFs. Eur. Phys. J. C **83** (2023). https://doi.org/10.1140/epjc/s10052-023-11236-0. arXiv:2207.04739 [hep-ph]
59. T.-J. Hou et al., New CTEQ global analysis of quantum chromodynamics with high-precision data from the LHC. Phys. Rev. D **103** (2021). https://doi.org/10.1103/physrevd.103.014013. arXiv:1912.10053
60. S. Bailey, T. Cridge, L.A. Harland-Lang, A.D. Martin, R.S. Thorne, Parton distributions from LHC, HERA, Tevatron and fixed target data: MSHT20 PDFs. Eur. Phys. J. C **81** (2021). https://doi.org/10.1140/epjc/s10052-021-09057-0

61. R.D. Ball et al., The path to proton structure at 1% accuracy. Eur. Phys. J. C **82** (2022). https://doi.org/10.1140/epjc/s10052-022-10328-7
62. S. Alekhin, J. Blümlein, S. Moch, R. Placakyte, Parton distribution functions, α_s, and heavy-quark masses for LHC Run II. Phys. Rev. D **96**, 014011 (2017). https://doi.org/10.1103/PhysRevD.96.014011. arXiv:1701.05838 [hep-ph]
63. S. Alekhin, J. Bluemlein, S. Moch, An update of the ABMP16 PDF fit (2019). arXiv:1909.03533 [hep-ph]
64. H1 and ZEUS Collaborations, Combination of Measurements of inclusive deep inelastic $e^{\pm}p$ scattering cross sections and QCD analysis of HERA data. Eur. Phys. J. C **75** (2015). https://doi.org/10.1140/epjc/s10052-015-3710-4
65. ATLAS Collaboration, Determination of the parton distribution functions of the proton using diverse ATLAS data from pp collisions at $\sqrt{s} = 7, 8$ and 13 TeV. Eur. Phys. J. C **82** (2022). https://doi.org/10.48550/arXiv.2112.11266
66. S. Bondarenko, Y. Dydyshka, L. Kalinovskaya, R. Sadykov, V. Yermolchyk, Hadron-hadron collision mode in ReneSANCe-v.1.3.0. Comput. Phys. Commun. **285**, 108646 (2023). https://doi.org/10.1016/j.cpc.2022.108646. arXiv:2207.04332 [hep-ph]
67. M. Chiesa, F. Piccinini, A. Vicini, Direct determination of $\sin^2\vartheta^{\ell}_{\rm eff}$ at hadron colliders. Phys. Rev. D **100**, 071302 (2019). https://doi.org/10.1103/PhysRevD.100.071302. arXiv:1906.11569 [hep-ph]
68. A. Arbuzov et al., Update of the MCSANC Monte Carlo integrator, v. 1.20. JETP Lett. **103**, 131 (2016). https://doi.org/10.1134/S0021364016020041. arXiv:1509.03052 [hep-ph]
69. S. Dittmaier, A. Huss, C. Schwinn, Mixed QCD-electroweak $O(\alpha_s\alpha)$ corrections to Drell–Yan processes in the resonance region: pole approximation and non-factorizable corrections. Nucl. Phys. B **885**, 318 (2014). https://doi.org/10.1016/j.nuclphysb.2014.05.027. arXiv:1403.3216 [hep-ph]
70. E. Richter-Was, Z. Was, Adequacy of effective Born for electroweak effects and TauSpinner algorithms for high energy physics simulated samples. Eur. Phys. J. C **137**, 95 (2022). https://doi.org/10.1140/epjp/s13360-021-02294-y. arXiv:2012.10997 [hep-ph]
71. ATLAS Collaboration, ATLAS Computing Acknowledgements, ATL-SOFT-PUB-2023-001 (2023). https://cds.cern.ch/record/2869272

ATLAS Collaboration*

G. Aad[102], B. Abbott[120], K. Abeling[55], N. J. Abicht[49], S. H. Abidi[29], A. Aboulhorma[35e], H. Abramowicz[151], H. Abreu[150], Y. Abulaiti[117], A. C. Abusleme Hoffman[137a], B. S. Acharya[69a,69b,n], C. Adam Bourdarios[4], L. Adamczyk[86a], L. Adamek[155], S. V. Addepalli[26], M. J. Addison[101], J. Adelman[115], A. Adiguzel[21c], T. Adye[134], A. A. Affolder[136], Y. Afik[36], M. N. Agaras[13], J. Agarwala[73a,73b], A. Aggarwal[100], C. Agheorghiesei[27c], A. Ahmad[36], F. Ahmadov[38,z], W. S. Ahmed[104], S. Ahuja[95], X. Ai[62a], G. Aielli[76a,76b], M. Ait Tamlihat[35e], B. Aitbenchikh[35a], I. Aizenberg[169], M. Akbiyik[100], T. P. A. Åkesson[98], A. V. Akimov[37], D. Akiyama[168], N. N. Akolkar[24], K. Al Khoury[41], G. L. Alberghi[23b], J. Albert[165], P. Albicocco[53], G. L. Albouy[60], S. Alderweireldt[52], M. Aleksa[36], I. N. Aleksandrov[38], C. Alexa[27b], T. Alexopoulos[10], A. Alfonsi[114], F. Alfonsi[23b], M. Algren[56], M. Alhroob[120], B. Ali[132], H. M. J. Ali[91], S. Ali[148], S. W. Alibocus[92], M. Aliev[37], G. Alimonti[71a], W. Alkakhi[55], C. Allaire[66], B. M. M. Allbrooke[146], J. F. Allen[52], C. A. Allendes Flores[137f], P. P. Allport[20], A. Aloisio[72a,72b], F. Alonso[90], C. Alpigiani[138], M. Alvarez Estevez[99], A. Alvarez Fernandez[100], M. G. Alviggi[72a,72b], M. Aly[101], Y. Amaral Coutinho[83b], A. Ambler[104], C. Amelung[36], M. Amerl[101], C. G. Ames[109], D. Amidei[106], S. P. Amor Dos Santos[130a], K. R. Amos[163], V. Ananiev[125], C. Anastopoulos[139], T. Andeen[11], J. K. Anders[36], S. Y. Andrean[47a,47b], A. Andreazza[71a,71b], S. Angelidakis[9], A. Angerami[41,ac], A. V. Anisenkov[37], A. Annovi[74a], C. Antel[56], M. T. Anthony[139], E. Antipov[145], M. Antonelli[53], D. J. A. Antrim[17a], F. Anulli[75a], M. Aoki[84], T. Aoki[153], J. A. Aparisi Pozo[163], M. A. Aparo[146], L. Aperio Bella[48], C. Appelt[18], A. Apyan[26], N. Aranzabal[36], C. Arcangeletti[53], A. T. H. Arce[51], E. Arena[92], J.-F. Arguin[108], S. Argyropoulos[54], J.-H. Arling[48], A. J. Armbruster[36], O. Arnaez[4], H. Arnold[114], Z. P. Arrubarrena Tame[109], G. Artoni[75a,75b], H. Asada[111], K. Asai[118], S. Asai[153], N. A. Asbah[61], K. Assamagan[29], R. Astalos[28a], S. Atashi[160], R. J. Atkin[33a], M. Atkinson[162], N. B. Atlay[18], H. Atmani[62b], P. A. Atmasiddha[106], K. Augsten[132], S. Auricchio[72a,72b], A. D. Auriol[20], V. A. Austrup[101], G. Avolio[36], K. Axiotis[56], G. Azuelos[108,ag], D. Babal[28b], H. Bachacou[135], K. Bachas[152,q], A. Bachiu[34], F. Backman[47a,47b], A. Badea[61], P. Bagnaia[75a,75b], M. Bahmani[18], A. J. Bailey[163], V. R. Bailey[162], J. T. Baines[134], L. Baines[94], C. Bakalis[10], O. K. Baker[172], E. Bakos[15], D. Bakshi Gupta[8], R. Balasubramanian[114], E. M. Baldin[37], P. Balek[86a], E. Ballabene[23a,23b], F. Balli[135], L. M. Baltes[63a], W. K. Balunas[32], J. Balz[100], E. Banas[87], M. Bandieramonte[129], A. Bandyopadhyay[24], S. Bansal[24], L. Barak[151], M. Barakat[48], E. L. Barberio[105], D. Barberis[57a,57b], M. Barbero[102], G. Barbour[96], K. N. Barends[33a], T. Barillari[110], M.-S. Barisits[36], T. Barklow[143], P. Baron[122], D. A. Baron Moreno[101], A. Baroncelli[62a], G. Barone[29], A. J. Barr[126], J. D. Barr[96], L. Barranco Navarro[47a,47b], F. Barreiro[99], J. Barreiro Guimarães da Costa[14a], U. Barron[151], M. G. Barros Teixeira[130a], S. Barsov[37], F. Bartels[63a], R. Bartoldus[143], A. E. Barton[91], P. Bartos[28a], A. Basan[100], M. Baselga[49], A. Bassalat[66,b], M. J. Basso[156a], C. R. Basson[101], R. L. Bates[59], S. Batlamous[35e], J. R. Batley[32], B. Batool[141], M. Battaglia[136], D. Battulga[18],

M. Bauce[75a,75b], M. Bauer[36], P. Bauer[24], L. T. Bazzano Hurrell[30], J. B. Beacham[51], T. Beau[127], P. H. Beauchemin[158], F. Becherer[54], P. Bechtle[24], H. P. Beck[19,p], K. Becker[167], A. J. Beddall[82], V. A. Bednyakov[38], C. P. Bee[145], L. J. Beemster[15], T. A. Beermann[36], M. Begalli[83d], M. Begel[29], A. Behera[145], J. K. Behr[48], J. F. Beirer[55], F. Beisiegel[24], M. Belfkir[159], G. Bella[151], L. Bellagamba[23b], A. Bellerive[34], P. Bellos[20], K. Beloborodov[37], N. L. Belyaev[37], D. Benchekroun[35a], F. Bendebba[35a], Y. Benhammou[151], M. Benoit[29], J. R. Bensinger[26], S. Bentvelsen[114], L. Beresford[48], M. Beretta[53], E. Bergeaas Kuutmann[161], N. Berger[4], B. Bergmann[132], J. Beringer[17a], G. Bernardi[5], C. Bernius[143], F. U. Bernlochner[24], F. Bernon[36,102], T. Berry[95], P. Berta[133], A. Berthold[50], I. A. Bertram[91], S. Bethke[110], A. Betti[75a,75b], A. J. Bevan[94], M. Bhamjee[33c], S. Bhatta[145], D. S. Bhattacharya[166], P. Bhattarai[26], V. S. Bhopatkar[121], R. Bi[29,ai], R. M. Bianchi[129], G. Bianco[23a,23b], O. Biebel[109], R. Bielski[123], M. Biglietti[77a], T. R. V. Billoud[132], M. Bindi[55], A. Bingul[21b], C. Bini[75a,75b], A. Biondini[92], C. J. Birch-sykes[101], G. A. Bird[20,134], M. Birman[169], M. Biros[133], T. Bisanz[49], E. Bisceglie[43a,43b], D. Biswas[141], A. Bitadze[101], K. Bjørke[125], I. Bloch[48], C. Blocker[26], A. Blue[59], U. Blumenschein[94], J. Blumenthal[100], G. J. Bobbink[114], V. S. Bobrovnikov[37], M. Boehler[54], B. Boehm[166], D. Bogavac[36], A. G. Bogdanchikov[37], C. Bohm[47a], V. Boisvert[95], P. Bokan[48], T. Bold[86a], M. Bomben[5], M. Bona[94], M. Boonekamp[135], C. D. Booth[95], A. G. Borbély[59], I. S. Bordulev[37], H. M. Borecka-Bielska[108], L. S. Borgna[96], G. Borissov[91], D. Bortoletto[126], D. Boscherini[23b], M. Bosman[13], J. D. Bossio Sola[36], K. Bouaouda[35a], N. Bouchhar[163], J. Boudreau[129], E. V. Bouhova-Thacker[91], D. Boumediene[40], R. Bouquet[5], A. Boveia[119], J. Boyd[36], D. Boye[29], I. R. Boyko[38], J. Bracinik[20], N. Brahimi[62d], G. Brandt[171], O. Brandt[32], F. Braren[48], B. Brau[103], J. E. Brau[123], R. Brener[169], L. Brenner[114], R. Brenner[161], S. Bressler[169], D. Britton[59], D. Britzger[110], I. Brock[24], G. Brooijmans[41], W. K. Brooks[137f], E. Brost[29], L. M. Brown[165], L. E. Bruce[61], T. L. Bruckler[126], P. A. Bruckman de Renstrom[87], B. Brüers[48], D. Bruncko[28b,*], A. Bruni[23b], G. Bruni[23b], M. Bruschi[23b], N. Bruscino[75a,75b], T. Buanes[16], Q. Buat[138], D. Buchin[110], A. G. Buckley[59], M. K. Bugge[125], O. Bulekov[37], B. A. Bullard[143], S. Burdin[92], C. D. Burgard[49], A. M. Burger[40], B. Burghgrave[8], O. Burlayenko[54], J. T. P. Burr[32], C. D. Burton[11], J. C. Burzynski[142], E. L. Busch[41], V. Büscher[100], P. J. Bussey[59], J. M. Butler[25], C. M. Buttar[59], J. M. Butterworth[96], W. Buttinger[134], C. J. Buxo Vazquez[107], A. R. Buzykaev[37], G. Cabras[23b], S. Cabrera Urbán[163], L. Cadamuro[66], D. Caforio[58], H. Cai[129], Y. Cai[14a,14e], V. M. M. Cairo[36], O. Cakir[3a], N. Calace[36], P. Calafiura[17a], G. Calderini[127], P. Calfayan[68], G. Callea[59], L. P. Caloba[83b], D. Calvet[40], S. Calvet[40], T. P. Calvet[102], M. Calvetti[74a,74b], R. Camacho Toro[127], S. Camarda[36], D. Camarero Munoz[26], P. Camarri[76a,76b], M. T. Camerlingo[72a,72b], D. Cameron[125], C. Camincher[165], M. Campanelli[96], A. Camplani[42], V. Canale[72a,72b], A. Canesse[104], M. Cano Bret[80], J. Cantero[163], Y. Cao[162], F. Capocasa[26], M. Capua[43a,43b], A. Carbone[71a,71b], R. Cardarelli[76a], J. C. J. Cardenas[8], F. Cardillo[163], T. Carli[36], G. Carlino[72a], J. I. Carlotto[13], B. T. Carlson[129,r], E. M. Carlson[156a,165], L. Carminati[71a,71b], A. Carnelli[135], M. Carnesale[75a,75b], S. Caron[113], E. Carquin[137f], S. Carrá[71a], G. Carratta[23a,23b], F. Carrio Argos[33g], J. W. S. Carter[155], T. M. Carter[52], M. P. Casado[13,i], M. Caspar[48], E. G. Castiglia[172], F. L. Castillo[4], L. Castillo Garcia[13], V. Castillo Gimenez[163], N. F. Castro[130a,130e], A. Catinaccio[36], J. R. Catmore[125], V. Cavaliere[29], N. Cavalli[23a,23b], V. Cavasinni[74a,74b], Y. C. Cekmecelioglu[48], E. Celebi[21a], F. Celli[126], M. S. Centonze[70a,70b], K. Cerny[122], A. S. Cerqueira[83a], A. Cerri[146], L. Cerrito[76a,76b], F. Cerutti[17a], B. Cervato[141], A. Cervelli[23b], G. Cesarini[53], S. A. Cetin[82], Z. Chadi[35a], D. Chakraborty[115], M. Chala[130f], J. Chan[170], W. Y. Chan[153], J. D. Chapman[32], E. Chapon[135], B. Chargeishvili[149b], D. G. Charlton[20], T. P. Charman[94], M. Chatterjee[19], C. Chauhan[133], S. Chekanov[6], S. V. Chekulaev[156a], G. A. Chelkov[38,a], A. Chen[106], B. Chen[151], B. Chen[165], H. Chen[14c], H. Chen[29], J. Chen[62c], J. Chen[142], M. Chen[126], S. Chen[153], S. J. Chen[14c], X. Chen[62c], X. Chen[14b,af], Y. Chen[62a], C. L. Cheng[170], H. C. Cheng[64a], S. Cheong[143], A. Cheplakov[38], E. Cheremushkina[48], E. Cherepanova[114], R. Cherkaoui El Moursli[35e], E. Cheu[7], K. Cheung[65], L. Chevalier[135], V. Chiarella[53], G. Chiarelli[74a], N. Chiedde[102], G. Chiodini[70a], A. S. Chisholm[20], A. Chitan[27b], M. Chitishvili[163], M. V. Chizhov[38], K. Choi[11], A. R. Chomont[75a,75b], Y. Chou[103], E. Y. S. Chow[114], T. Chowdhury[33g], K. L. Chu[169], M. C. Chu[64a], X. Chu[14a,14e], J. Chudoba[131], J. J. Chwastowski[87], D. Cieri[110], K. M. Ciesla[86a], V. Cindro[93], A. Ciocio[17a], F. Cirotto[72a,72b], Z. H. Citron[169,l], M. Citterio[71a], D. A. Ciubotaru[27b], B. M. Ciungu[155], A. Clark[56], P. J. Clark[52], J. M. Clavijo Columbie[48], S. E. Clawson[48], C. Clement[47a,47b], J. Clercx[48], L. Clissa[23a,23b], Y. Coadou[102], M. Cobal[69a,69c], A. Coccaro[57b], R. F. Coelho Barrue[130a], R. Coelho Lopes De Sa[103], S. Coelli[71a], H. Cohen[151], A. E. C. Coimbra[71a,71b], B. Cole[41], J. Collot[60], P. Conde Muiño[130a,130g], M. P. Connell[33c], S. H. Connell[33c], I. A. Connelly[59], E. I. Conroy[126],

F. Conventi[72a,ah], H. G. Cooke[20], A. M. Cooper-Sarkar[126], A. Cordeiro Oudot Choi[127], F. Cormier[164], L. D. Corpe[40], M. Corradi[75a,75b], F. Corriveau[104,x], A. Cortes-Gonzalez[18], M. J. Costa[163], F. Costanza[4], D. Costanzo[139], B. M. Cote[119], G. Cowan[95], K. Cranmer[170], D. Cremonini[23a,23b], S. Crépé-Renaudin[60], F. Crescioli[127], M. Cristinziani[141], M. Cristoforetti[78a,78b], V. Croft[114], J. E. Crosby[121], G. Crosetti[43a,43b], A. Cueto[99], T. Cuhadar Donszelmann[160], H. Cui[14a,14e], Z. Cui[7], W. R. Cunningham[59], F. Curcio[43a,43b], P. Czodrowski[36], M. M. Czurylo[63b], M. J. Da Cunha Sargedas De Sousa[62a], J. V. Da Fonseca Pinto[83b], C. Da Via[101], W. Dabrowski[86a], T. Dado[49], S. Dahbi[33g], T. Dai[106], C. Dallapiccola[103], M. Dam[42], G. D'amen[29], V. D'Amico[109], J. Damp[100], J. R. Dandoy[128], M. F. Daneri[30], M. Danninger[142], V. Dao[36], G. Darbo[57b], S. Darmora[6], S. J. Das[29,ai], S. D'Auria[71a,71b], C. David[156b], T. Davidek[133], B. Davis-Purcell[34], I. Dawson[94], H. A. Day-hall[132], K. De[8], R. De Asmundis[72a], N. De Biase[48], S. De Castro[23a,23b], N. De Groot[113], P. de Jong[114], H. De la Torre[107], A. De Maria[14c], A. De Salvo[75a], U. De Sanctis[76a,76b], A. De Santo[146], J. B. De Vivie De Regie[60], D. V. Dedovich[38], J. Degens[114], A. M. Deiana[44], F. Del Corso[23a,23b], J. Del Peso[99], F. Del Rio[63a], F. Deliot[135], C. M. Delitzsch[49], M. Della Pietra[72a,72b], D. Della Volpe[56], A. Dell'Acqua[36], L. Dell'Asta[71a,71b], M. Delmastro[4], P. A. Delsart[60], S. Demers[172], M. Demichev[38], S. P. Denisov[37], L. D'Eramo[40], D. Derendarz[87], F. Derue[127], P. Dervan[92], K. Desch[24], C. Deutsch[24], F. A. Di Bello[57a,57b], A. Di Ciaccio[76a,76b], L. Di Ciaccio[4], A. Di Domenico[75a,75b], C. Di Donato[72a,72b], A. Di Girolamo[36], G. Di Gregorio[5], A. Di Luca[78a,78b], B. Di Micco[77a,77b], R. Di Nardo[77a,77b], C. Diaconu[102], F. A. Dias[114], T. Dias Do Vale[142], M. A. Diaz[137a,137b], F. G. Diaz Capriles[24], M. Didenko[163], E. B. Diehl[106], L. Diehl[54], S. Díez Cornell[48], C. Diez Pardos[141], C. Dimitriadi[24,161], A. Dimitrievska[17a], J. Dingfelder[24], I.-M. Dinu[27b], S. J. Dittmeier[63b], F. Dittus[36], F. Djama[102], T. Djobava[149b], J. I. Djuvsland[16], C. Doglioni[98,101], J. Dolejsi[133], Z. Dolezal[133], M. Donadelli[83c], B. Dong[107], J. Donini[40], A. D'Onofrio[77a,77b], M. D'Onofrio[92], J. Dopke[134], A. Doria[72a], N. Dos Santos Fernandes[130a], M. T. Dova[90], A. T. Doyle[59], M. A. Draguet[126], E. Dreyer[169], I. Drivas-koulouris[10], A. S. Drobac[158], M. Drozdova[56], D. Du[62a], T. A. du Pree[114], F. Dubinin[37], M. Dubovsky[28a], E. Duchovni[169], G. Duckeck[109], O. A. Ducu[27b], D. Duda[52], A. Dudarev[36], E. R. Duden[26], M. D'uffizi[101], L. Duflot[66], M. Dührssen[36], C. Dülsen[171], A. E. Dumitriu[27b], M. Dunford[63a], S. Dungs[49], K. Dunne[47a,47b], A. Duperrin[102], H. Duran Yildiz[3a], M. Düren[58], A. Durglishvili[149b], B. L. Dwyer[115], G. I. Dyckes[17a], M. Dyndal[86a], S. Dysch[101], B. S. Dziedzic[87], Z. O. Earnshaw[146], G. H. Eberwein[126], B. Eckerova[28a], S. Eggebrecht[55], M. G. Eggleston[51], E. Egidio Purcino De Souza[127], L. F. Ehrke[56], G. Eigen[16], K. Einsweiler[17a], T. Ekelof[161], P. A. Ekman[98], S. El Farkh[35b], Y. El Ghazali[35b], H. El Jarrari[35e,148], A. El Moussaouy[35a], V. Ellajosyula[161], M. Ellert[161], F. Ellinghaus[171], A. A. Elliot[94], N. Ellis[36], J. Elmsheuser[29], M. Elsing[36], D. Emeliyanov[134], Y. Enari[153], I. Ene[17a], S. Epari[13], J. Erdmann[49], P. A. Erland[87], M. Errenst[171], M. Escalier[66], C. Escobar[163], E. Etzion[151], G. Evans[130a], H. Evans[68], L. S. Evans[95], M. O. Evans[146], A. Ezhilov[37], S. Ezzarqtouni[35a], F. Fabbri[59], L. Fabbri[23a,23b], G. Facini[96], V. Fadeyev[136], R. M. Fakhrutdinov[37], S. Falciano[75a], L. F. Falda Ulhoa Coelho[36], P. J. Falke[24], J. Faltova[133], C. Fan[162], Y. Fan[14a], Y. Fang[14a,14e], M. Fanti[71a,71b], M. Faraj[69a,69b], Z. Farazpay[97], A. Farbin[8], A. Farilla[77a], T. Farooque[107], S. M. Farrington[52], F. Fassi[35e], D. Fassouliotis[9], M. Faucci Giannelli[76a,76b], W. J. Fawcett[32], L. Fayard[66], P. Federic[133], P. Federicova[131], O. L. Fedin[37,a], G. Fedotov[37], M. Feickert[170], L. Feligioni[102], D. E. Fellers[123], C. Feng[62b], M. Feng[14b], Z. Feng[114], M. J. Fenton[160], A. B. Fenyuk[37], L. Ferencz[48], R. A. M. Ferguson[91], S. I. Fern andez Luen go[137f], M. J. V. Fernoux[102], J. Ferrando[48], A. Ferrari[161], P. Ferrari[113,114], R. Ferrari[73a], D. Ferrere[56], C. Ferretti[106], F. Fiedler[100], A. Filipčič[93], E. K. Filmer[1], F. Filthaut[113], M. C. N. Fiolhais[130a,130c,c], L. Fiorini[163], W. C. Fisher[107], T. Fitschen[101], P. M. Fitzhugh[135], I. Fleck[141], P. Fleischmann[106], T. Flick[171], L. Flores[128], M. Flores[33d,ad], L. R. Flores Castillo[64a], L. Flores Sanz De Acedo[36], F. M. Follega[78a,78b], N. Fomin[16], J. H. Foo[155], B. C. Forland[68], A. Formica[135], A. C. Forti[101], E. Fortin[36], A. W. Fortman[61], M. G. Foti[17a], L. Fountas[9,j], D. Fournier[66], H. Fox[91], P. Francavilla[74a,74b], S. Francescato[61], S. Franchellucci[56], M. Franchini[23a,23b], S. Franchino[63a], D. Francis[36], L. Franco[113], L. Franconi[48], M. Franklin[61], G. Frattari[26], A. C. Freegard[94], W. S. Freund[83b], Y. Y. Frid[151], N. Fritzsche[50], A. Froch[54], D. Froidevaux[36], J. A. Frost[126], Y. Fu[62a], M. Fujimoto[118], E. Fullana Torregrosa[163,*], K. Y. Fung[64a], E. Furtado De Simas Filho[83b], M. Furukawa[153], J. Fuster[163], A. Gabrielli[23a,23b], A. Gabrielli[155], P. Gadow[48], G. Gagliardi[57a,57b], L. G. Gagnon[17a], E. J. Gallas[126], B. J. Gallop[134], K. K. Gan[119], S. Ganguly[153], J. Gao[62a], Y. Gao[52], F. M. Garay Walls[137a,137b], B. Garcia[29], C. García[163], A. Garcia Alonso[114], A. G. Garcia Caffaro[172], J. E. García Navarro[163], M. Garcia-Sciveres[17a], G. L. Gardner[128], R. W. Gardner[39], N. Garelli[158], D. Garg[80], R. B. Garg[143,o], J. M. Gargan[52], C. A. Garner[155],

S. J. Gasiorowski[138], P. Gaspar[83b], G. Gaudio[73a], V. Gautam[13], P. Gauzzi[75a,75b], I. L. Gavrilenko[37], A. Gavrilyuk[37], C. Gay[164], G. Gaycken[48], E. N. Gazis[10], A. A. Geanta[27b], C. M. Gee[136], C. Gemme[57b], M. H. Genest[60], S. Gentile[75a,75b], S. George[95], W. F. George[20], T. Geralis[46], P. Gessinger-Befurt[36], M. E. Geyik[171], M. Ghneimat[141], K. Ghorbanian[94], A. Ghosal[141], A. Ghosh[160], A. Ghosh[7], B. Giacobbe[23b], S. Giagu[75a,75b], P. Giannetti[74a], A. Giannini[62a], S. M. Gibson[95], M. Gignac[136], D. T. Gil[86b], A. K. Gilbert[86a], B. J. Gilbert[41], D. Gillberg[34], G. Gilles[114], N. E. K. Gillwald[48], L. Ginabat[127], D. M. Gingrich[2,ag], M. P. Giordani[69a,69c], P. F. Giraud[135], G. Giugliarelli[69a,69c], D. Giugni[71a], F. Giuli[36], I. Gkialas[9,j], L. K. Gladilin[37], C. Glasman[99], G. R. Gledhill[123], M. Glisic[123], I. Gnesi[43b,f], Y. Go[29,ai], M. Goblirsch-Kolb[36], B. Gocke[49], D. Godin[108], B. Gokturk[21a], S. Goldfarb[105], T. Golling[56], M. G. D. Gololo[33g], D. Golubkov[37], J. P. Gombas[107], A. Gomes[130a,130b], G. Gomes Da Silva[141], A. J. Gomez Delegido[163], R. Gonçalo[130a,130c], G. Gonella[123], L. Gonella[20], A. Gongadze[38], F. Gonnella[20], J. L. Gonski[41], R. Y. González Andana[52], S. González de la Hoz[163], S. Gonzalez Fernandez[13], R. Gonzalez Lopez[92], C. Gonzalez Renteria[17a], R. Gonzalez Suarez[161], S. Gonzalez-Sevilla[56], G. R. Gonzalvo Rodriguez[163], L. Goossens[36], P. A. Gorbounov[37], B. Gorini[36], E. Gorini[70a,70b], A. Gorišek[93], T. C. Gosart[128], A. T. Goshaw[51], M. I. Gostkin[38], S. Goswami[121], C. A. Gottardo[36], M. Gouighri[35b], V. Goumarre[48], A. G. Goussiou[138], N. Govender[33c], I. Grabowska-Bold[86a], K. Graham[34], E. Gramstad[125], S. Grancagnolo[70a,70b], M. Grandi[146], P. M. Gravila[27f], F. G. Gravili[70a,70b], H. M. Gray[17a], M. Greco[70a,70b], C. Grefe[24], I. M. Gregor[48], P. Grenier[143], C. Grieco[13], A. A. Grillo[136], K. Grimm[31], S. Grinstein[13,t], J.-F. Grivaz[66], E. Gross[169], J. Grosse-Knetter[55], C. Grud[106], J. C. Grundy[126], L. Guan[106], W. Guan[29], C. Gubbels[164], J. G. R. Guerrero Rojas[163], G. Guerrieri[69a,69b], F. Guescini[110], R. Gugel[100], J. A. M. Guhit[106], A. Guida[18], T. Guillemin[4], E. Guilloton[134,167], S. Guindon[36], F. Guo[14a,14e], J. Guo[62c], L. Guo[48], Y. Guo[106], R. Gupta[48], S. Gurbuz[24], S. S. Gurdasani[54], G. Gustavino[36], M. Guth[56], P. Gutierrez[120], L. F. Gutierrez Zagazeta[128], C. Gutschow[96], C. Gwenlan[126], C. B. Gwilliam[92], E. S. Haaland[125], A. Haas[117], M. Habedank[48], C. Haber[17a], H. K. Hadavand[8], A. Hadef[100], S. Hadzic[110], J. J. Hahn[141], E. H. Haines[96], M. Haleem[166], J. Haley[121], J. J. Hall[139], G. D. Hallewell[102], L. Halser[19], K. Hamano[165], H. Hamdaoui[35e], M. Hamer[24], G. N. Hamity[52], E. J. Hampshire[95], J. Han[62b], K. Han[62a], L. Han[14c], L. Han[62a], S. Han[17a], Y. F. Han[155], K. Hanagaki[84], M. Hance[136], D. A. Hangal[41,ac], H. Hanif[142], M. D. Hank[128], R. Hankache[101], J. B. Hansen[42], J. D. Hansen[42], P. H. Hansen[42], K. Hara[157], D. Harada[56], T. Harenberg[171], S. Harkusha[37], M. L. Harris[103], Y. T. Harris[126], J. Harrison[13], N. M. Harrison[119], P. F. Harrison[167], N. M. Hartman[110], N. M. Hartmann[109], Y. Hasegawa[140], A. Hasib[52], S. Haug[19], R. Hauser[107], C. M. Hawkes[20], R. J. Hawkings[36], Y. Hayashi[153], S. Hayashida[111], D. Hayden[107], C. Hayes[106], R. L. Hayes[114], C. P. Hays[126], J. M. Hays[94], H. S. Hayward[92], F. He[62a], M. He[14a,14e], Y. He[154], Y. He[127], N. B. Heatley[94], V. Hedberg[98], A. L. Heggelund[125], N. D. Hehir[94], C. Heidegger[54], K. K. Heidegger[54], W. D. Heidorn[81], J. Heilman[34], S. Heim[48], T. Heim[17a], J. G. Heinlein[128], J. J. Heinrich[123], L. Heinrich[110,ae], J. Hejbal[131], L. Helary[48], A. Held[170], S. Hellesund[16], C. M. Helling[164], S. Hellman[47a,47b], C. Helsens[36], R. C. W. Henderson[91], L. Henkelmann[32], A. M. Henriques Correia[36], H. Herde[98], Y. Hernández Jiménez[145], L. M. Herrmann[24], T. Herrmann[50], G. Herten[54], R. Hertenberger[109], L. Hervas[36], M. E. Hesping[100], N. P. Hessey[156a], H. Hibi[85], S. J. Hillier[20], J. R. Hinds[107], F. Hinterkeuser[24], M. Hirose[124], S. Hirose[157], D. Hirschbuehl[171], T. G. Hitchings[101], B. Hiti[93], J. Hobbs[145], R. Hobincu[27e], N. Hod[169], M. C. Hodgkinson[139], B. H. Hodkinson[32], A. Hoecker[36], J. Hofer[48], T. Holm[24], M. Holzbock[110], L. B. A. H. Hommels[32], B. P. Honan[101], J. Hong[62c], T. M. Hong[129], B. H. Hooberman[162], W. H. Hopkins[6], Y. Horii[111], S. Hou[148], A. S. Howard[93], J. Howarth[59], J. Hoya[6], M. Hrabovsky[122], A. Hrynevich[48], T. Hryn'ova[4], P. J. Hsu[65], S.-C. Hsu[138], Q. Hu[41], Y. F. Hu[14a,14e], S. Huang[64b], X. Huang[14c], Y. Huang[62a], Y. Huang[14a], Z. Huang[101], Z. Hubacek[132], M. Huebner[24], F. Huegging[24], T. B. Huffman[126], C. A. Hugli[48], M. Huhtinen[36], S. K. Huiberts[16], R. Hulsken[104], N. Huseynov[12,a], J. Huston[107], J. Huth[61], R. Hyneman[143], G. Iacobucci[56], G. Iakovidis[29], I. Ibragimov[141], L. Iconomidou-Fayard[66], P. Iengo[72a,72b], R. Iguchi[153], T. Iizawa[84], Y. Ikegami[84], N. Ilic[155], H. Imam[35a], M. Ince Lezki[56], T. Ingebretsen Carlson[47a,47b], G. Introzzi[73a,73b], M. Iodice[77a], V. Ippolito[75a,75b], R. K. Irwin[92], M. Ishino[153], W. Islam[170], C. Issever[18,48], S. Istin[21a,ak], H. Ito[168], J. M. Iturbe Ponce[64a], R. Iuppa[78a,78b], A. Ivina[169], J. M. Izen[45], V. Izzo[72a], P. Jacka[131,132], P. Jackson[1], R. M. Jacobs[48], B. P. Jaeger[142], C. S. Jagfeld[109], P. Jain[54], G. Jäkel[171], K. Jakobs[54], T. Jakoubek[169], J. Jamieson[59], K. W. Janas[86a], A. E. Jaspan[92], M. Javurkova[103], F. Jeanneau[135], L. Jeanty[123], J. Jejelava[149a,aa], P. Jenni[54,g], C. E. Jessiman[34], S. Jézéquel[4], C. Jia[62b], J. Jia[145], X. Jia[61], X. Jia[14a,14e], Z. Jia[14c], Y. Jiang[62a], S. Jiggins[48], J. Jimenez Pena[13], S. Jin[14c], A. Jinaru[27b], O. Jinnouchi[154], P. Johansson[139], K. A. Johns[7], J. W. Johnson[136], D. M. Jones[32], E. Jones[48], P. Jones[32], R. W. L. Jones[91],

T. J. Jones[92], R. Joshi[119], J. Jovicevic[15], X. Ju[17a], J. J. Junggeburth[36], T. Junkermann[63a], A. Juste Rozas[13,t], M. K. Juzek[87], S. Kabana[137e], A. Kaczmarska[87], M. Kado[110], H. Kagan[119], M. Kagan[143], A. Kahn[41], A. Kahn[128], C. Kahra[100], T. Kaji[168], E. Kajomovitz[150], N. Kakati[169], I. Kalaitzidou[54], C. W. Kalderon[29], A. Kamenshchikov[155], S. Kanayama[154], N. J. Kang[136], D. Kar[33g], K. Karava[126], M. J. Kareem[156b], E. Karentzos[54], I. Karkanias[152], O. Karkout[114], S. N. Karpov[38], Z. M. Karpova[38], V. Kartvelishvili[91], A. N. Karyukhin[37], E. Kasimi[152], J. Katzy[48], S. Kaur[34], K. Kawade[140], T. Kawamoto[135], E. F. Kay[36], F. I. Kaya[158], S. Kazakos[107], V. F. Kazanin[37], Y. Ke[145], J. M. Keaveney[33a], R. Keeler[165], G. V. Kehris[61], J. S. Keller[34], A. S. Kelly[96], J. J. Kempster[146], K. E. Kennedy[41], P. D. Kennedy[100], O. Kepka[131], B. P. Kerridge[167], S. Kersten[171], B. P. Kerševan[93], S. Keshri[66], L. Keszeghova[28a], S. Ketabchi Haghighat[155], M. Khandoga[127], A. Khanov[121], A. G. Kharlamov[37], T. Kharlamova[37], E. E. Khoda[138], T. J. Khoo[18], G. Khoriauli[166], J. Khubua[149b], Y. A. R. Khwaira[66], M. Kiehn[36], A. Kilgallon[123], D. W. Kim[47a,47b], Y. K. Kim[39], N. Kimura[96], A. Kirchhoff[55], C. Kirfel[24], F. Kirfel[24], J. Kirk[134], A. E. Kiryunin[110], C. Kitsaki[10], O. Kivernyk[24], M. Klassen[63a], C. Klein[34], L. Klein[166], M. H. Klein[106], M. Klein[92], S. B. Klein[56], U. Klein[92], P. Klimek[36], A. Klimentov[29], T. Klioutchnikova[36], P. Kluit[114], S. Kluth[110], E. Kneringer[79], T. M. Knight[155], A. Knue[54], R. Kobayashi[88], S. F. Koch[126], M. Kocian[143], P. Kodyš[133], D. M. Koeck[123], P. T. Koenig[24], T. Koffas[34], M. Kolb[135], I. Koletsou[4], T. Komarek[122], K. Köneke[54], A. X. Y. Kong[1], T. Kono[118], N. Konstantinidis[96], B. Konya[98], R. Kopeliansky[68], S. Koperny[86a], K. Korcyl[87], K. Kordas[152,e], G. Koren[151], A. Korn[96], S. Korn[55], I. Korolkov[13], N. Korotkova[37], B. Kortman[114], O. Kortner[110], S. Kortner[110], W. H. Kostecka[115], V. V. Kostyukhin[141], A. Kotsokechagia[135], A. Kotwal[51], A. Koulouris[36], A. Kourkoumeli-Charalampidi[73a,73b], C. Kourkoumelis[9], E. Kourlitis[6], O. Kovanda[146], R. Kowalewski[165], W. Kozanecki[135], A. S. Kozhin[37], V. A. Kramarenko[37], G. Kramberger[93], P. Kramer[100], M. W. Krasny[127], A. Krasznahorkay[36], J. W. Kraus[171], J. A. Kremer[100], T. Kresse[50], J. Kretzschmar[92], K. Kreul[18], P. Krieger[155], S. Krishnamurthy[103], M. Krivos[133], K. Krizka[20], K. Kroeninger[49], H. Kroha[110], J. Kroll[131], J. Kroll[128], K. S. Krowpman[107], U. Kruchonak[38], H. Krüger[24], N. Krumnack[81], M. C. Kruse[51], J. A. Krzysiak[87], O. Kuchinskaia[37], S. Kuday[3a], S. Kuehn[36], R. Kuesters[54], T. Kuhl[48], V. Kukhtin[38], Y. Kulchitsky[37,a], S. Kuleshov[137b,137d], M. Kumar[33g], N. Kumari[102], A. Kupco[131], T. Kupfer[49], A. Kupich[37], O. Kuprash[54], H. Kurashige[85], L. L. Kurchaninov[156a], O. Kurdysh[66], Y. A. Kurochkin[37], A. Kurova[37], M. Kuze[154], A. K. Kvam[103], J. Kvita[122], T. Kwan[104], N. G. Kyriacou[106], L. A. O. Laatu[102], C. Lacasta[163], F. Lacava[75a,75b], H. Lacker[18], D. Lacour[127], N. N. Lad[96], E. Ladygin[38], B. Laforge[127], T. Lagouri[137e], S. Lai[55], I. K. Lakomiec[86a], N. Lalloue[60], J. E. Lambert[165], S. Lammers[68], W. Lampl[7], C. Lampoudis[152,e], A. N. Lancaster[115], E. Lançon[29], U. Landgraf[54], M. P. J. Landon[94], V. S. Lang[54], R. J. Langenberg[103], O. K. B. Langrekken[125], A. J. Lankford[160], F. Lanni[36], K. Lantzsch[24], A. Lanza[73a], A. Lapertosa[57a,57b], J. F. Laporte[135], T. Lari[71a], F. Lasagni Manghi[23b], M. Lassnig[36], V. Latonova[131], A. Laudrain[100], A. Laurier[150], S. D. Lawlor[95], Z. Lawrence[101], M. Lazzaroni[71a,71b], B. Le[101], E. M. Le Boulicaut[51], B. Leban[93], A. Lebedev[81], M. LeBlanc[36], F. Ledroit-Guillon[60], A. C. A. Lee[96], S. C. Lee[148], S. Lee[47a,47b], T. F. Lee[92], L. L. Leeuw[33c], H. P. Lefebvre[95], M. Lefebvre[165], C. Leggett[17a], G. Lehmann Miotto[36], M. Leigh[56], W. A. Leight[103], W. Leinonen[113], A. Leisos[152,s], M. A. L. Leite[83c], C. E. Leitgeb[48], R. Leitner[133], K. J. C. Leney[44], T. Lenz[24], S. Leone[74a], C. Leonidopoulos[52], A. Leopold[144], C. Leroy[108], R. Les[107], C. G. Lester[32], M. Levchenko[37], J. Levêque[4], D. Levin[106], L. J. Levinson[169], M. P. Lewicki[87], D. J. Lewis[4], A. Li[5], B. Li[62b], C. Li[62a], C.-Q. Li[62c], H. Li[62a], H. Li[62b], H. Li[14c], H. Li[62b], K. Li[138], L. Li[62c], M. Li[14a,14e], Q. Y. Li[62a], S. Li[14a,14e], S. Li[62c,62d,d], T. Li[5], X. Li[104], Z. Li[126], Z. Li[104], Z. Li[92], Z. Li[14a,14e], Z. Liang[14a], M. Liberatore[48], B. Liberti[76a], K. Lie[64c], J. Lieber Marin[83b], H. Lien[68], K. Lin[107], R. E. Lindley[7], J. H. Lindon[2], A. Linss[48], E. Lipeles[128], A. Lipniacka[16], A. Lister[164], J. D. Little[4], B. Liu[14a], B. X. Liu[142], D. Liu[62c,62d], J. B. Liu[62a], J. K. K. Liu[32], K. Liu[62c,62d], M. Liu[62a], M. Y. Liu[62a], P. Liu[14a], Q. Liu[62c,62d,138], X. Liu[62a], Y. Liu[14d,14e], Y. L. Liu[106], Y. W. Liu[62a], J. Llorente Merino[142], S. L. Lloyd[94], E. M. Lobodzinska[48], P. Loch[7], S. Loffredo[76a,76b], T. Lohse[18], K. Lohwasser[139], E. Loiacono[48], M. Lokajicek[131,*], J. D. Lomas[20], J. D. Long[162], I. Longarini[160], L. Longo[70a,70b], R. Longo[162], I. Lopez Paz[67], A. Lopez Solis[48], J. Lorenz[109], N. Lorenzo Martinez[4], A. M. Lory[109], G. Löschcke Centeno[146], O. Loseva[37], X. Lou[47a,47b], X. Lou[14a,14e], A. Lounis[66], J. Love[6], P. A. Love[91], G. Lu[14a,14e], M. Lu[80], S. Lu[128], Y. J. Lu[65], H. J. Lubatti[138], C. Luci[75a,75b], F. L. Lucio Alves[14c], A. Lucotte[60], F. Luehring[68], I. Luise[145], O. Lukianchuk[66], O. Lundberg[144], B. Lund-Jensen[144], N. A. Luongo[123], M. S. Lutz[151], D. Lynn[29], H. Lyons[92], R. Lysak[131], E. Lytken[98], V. Lyubushkin[38], T. Lyubushkina[38], M. M. Lyukova[145], H. Ma[29], K. Ma[62a], L. L. Ma[62b], Y. Ma[121],

D. M. Mac Donell[165], G. Maccarrone[53], J. C. MacDonald[100], R. Madar[40], W. F. Mader[50], J. Maeda[85], T. Maeno[29], M. Maerker[50], H. Maguire[139], V. Maiboroda[135], A. Maio[130a,130b,130d], K. Maj[86a], O. Majersky[48], S. Majewski[123], N. Makovec[66], V. Maksimovic[15], B. Malaescu[127], Pa. Malecki[87], V. P. Maleev[37], F. Malek[60], M. Mali[93], D. Malito[95], U. Mallik[80], S. Maltezos[10], S. Malyukov[38], J. Mamuzic[13], G. Mancini[53], G. Manco[73a,73b], J. P. Mandalia[94], I. Mandić[93], L. Manhaes de Andrade Filho[83a], I. M. Maniatis[169], J. Manjarres Ramos[102,ab], D. C. Mankad[169], A. Mann[109], B. Mansoulie[135], S. Manzoni[36], A. Marantis[152,s], G. Marchiori[5], M. Marcisovsky[131], C. Marcon[71a], M. Marinescu[20], M. Marjanovic[120], E. J. Marshall[91], Z. Marshall[17a], S. Marti-Garcia[163], T. A. Martin[167], V. J. Martin[52], B. Martin dit Latour[16], L. Martinelli[75a,75b], M. Martinez[13,t], P. Martinez Agullo[163], V. I. Martinez Outschoorn[103], P. Martinez Suarez[13], S. Martin-Haugh[134], V. S. Martoiu[27b], A. C. Martyniuk[96], A. Marzin[36], D. Mascione[78a,78b], L. Masetti[100], T. Mashimo[153], J. Masik[101], A. L. Maslennikov[37], L. Massa[23b], P. Massarotti[72a,72b], P. Mastrandrea[74a,74b], A. Mastroberardino[43a,43b], T. Masubuchi[153], T. Mathisen[161], J. Matousek[133], N. Matsuzawa[153], J. Maurer[27b], B. Maček[93], D. A. Maximov[37], R. Mazini[148], I. Maznas[152], M. Mazza[107], S. M. Mazza[136], E. Mazzeo[71a,71b], C. Mc Ginn[29], J. P. Mc Gowan[104], S. P. Mc Kee[106], E. F. McDonald[105], A. E. McDougall[114], J. A. Mcfayden[146], R. P. McGovern[128], G. Mchedlidze[149b], R. P. Mckenzie[33g], T. C. Mclachlan[48], D. J. Mclaughlin[96], K. D. McLean[165], S. J. McMahon[134], P. C. McNamara[105], C. M. Mcpartland[92], R. A. McPherson[165,x], S. Mehlhase[109], A. Mehta[92], D. Melini[150], B. R. Mellado Garcia[33g], A. H. Melo[55], F. Meloni[48], A. M. Mendes Jacques Da Costa[101], H. Y. Meng[155], L. Meng[91], S. Menke[110], M. Mentink[36], E. Meoni[43a,43b], C. Merlassino[126], L. Merola[72a,72b], C. Meroni[71a,71b], G. Merz[106], O. Meshkov[37], J. Metcalfe[6], A. S. Mete[6], C. Meyer[68], J.-P. Meyer[135], R. P. Middleton[134], L. Mijović[52], G. Mikenberg[169], M. Mikestikova[131], M. Mikuž[93], H. Mildner[100], A. Milic[36], C. D. Milke[44], D. W. Miller[39], L. S. Miller[34], A. Milov[169], D. A. Milstead[47a,47b], T. Min[14c], A. A. Minaenko[37], I. A. Minashvili[149b], L. Mince[59], A. I. Mincer[117], B. Mindur[86a], M. Mineev[38], Y. Mino[88], L. M. Mir[13], M. Miralles Lopez[163], M. Mironova[17a], A. Mishima[153], M. C. Missio[113], T. Mitani[168], A. Mitra[167], V. A. Mitsou[163], O. Miu[155], P. S. Miyagawa[94], Y. Miyazaki[89], A. Mizukami[84], T. Mkrtchyan[63a], M. Mlinarevic[96], T. Mlinarevic[96], M. Mlynarikova[36], S. Mobius[19], K. Mochizuki[108], P. Moder[48], P. Mogg[109], A. F. Mohammed[14a,14e], S. Mohapatra[41], G. Mokgatitswane[33g], L. Moleri[169], B. Mondal[141], S. Mondal[132], K. Mönig[48], E. Monnier[102], L. Monsonis Romero[163], J. Montejo Berlingen[13,84], M. Montella[119], F. Montereali[77a,77b], F. Monticelli[90], S. Monzani[69a,69c], N. Morange[66], A. L. Moreira De Carvalho[130a], M. Moreno Llácer[163], C. Moreno Martinez[56], P. Morettini[57b], S. Morgenstern[36], M. Morii[61], M. Morinaga[153], A. K. Morley[36], F. Morodei[75a,75b], L. Morvaj[36], P. Moschovakos[36], B. Moser[36], M. Mosidze[149b], T. Moskalets[54], P. Moskvitina[113], J. Moss[31,m], E. J. W. Moyse[103], O. Mtintsilana[33g], S. Muanza[102], J. Mueller[129], D. Muenstermann[91], R. Müller[19], G. A. Mullier[161], A. J. Mullin[32], J. J. Mullin[128], D. P. Mungo[155], D. Munoz Perez[163], F. J. Munoz Sanchez[101], M. Murin[101], W. J. Murray[134,167], A. Murrone[71a,71b], J. M. Muse[120], M. Muškinja[17a], C. Mwewa[29], A. G. Myagkov[37,a], A. J. Myers[8], A. A. Myers[129], G. Myers[68], M. Myska[132], B. P. Nachman[17a], O. Nackenhorst[49], A. Nag[50], K. Nagai[126], K. Nagano[84], J. L. Nagle[29,ai], E. Nagy[102], A. M. Nairz[36], Y. Nakahama[84], K. Nakamura[84], K. Nakkalil[5], H. Nanjo[124], R. Narayan[44], E. A. Narayanan[112], I. Naryshkin[37], M. Naseri[34], S. Nasri[159], C. Nass[24], G. Navarro[22a], J. Navarro-Gonzalez[163], R. Nayak[151], A. Nayaz[18], P. Y. Nechaeva[37], F. Nechansky[48], L. Nedic[126], T. J. Neep[20], A. Negri[73a,73b], M. Negrini[23b], C. Nellist[114], C. Nelson[104], K. Nelson[106], S. Nemecek[131], M. Nessi[36,h], M. S. Neubauer[162], F. Neuhaus[100], J. Neundorf[48], R. Newhouse[164], P. R. Newman[20], C. W. Ng[129], Y. W. Y. Ng[48], B. Ngair[35e], H. D. N. Nguyen[108], R. B. Nickerson[126], R. Nicolaidou[135], J. Nielsen[136], M. Niemeyer[55], J. Niermann[36,55], N. Nikiforou[36], V. Nikolaenko[37,a], I. Nikolic-Audit[127], K. Nikolopoulos[20], P. Nilsson[29], I. Ninca[48], H. R. Nindhito[56], G. Ninio[151], A. Nisati[75a], N. Nishu[2], R. Nisius[110], J.-E. Nitschke[50], E. K. Nkadimeng[33g], S. J. Noacco Rosende[90], T. Nobe[153], D. L. Noel[32], T. Nommensen[147], M. B. Norfolk[139], R. R. B. Norisam[96], B. J. Norman[34], J. Novak[93], T. Novak[48], L. Novotny[132], R. Novotny[112], L. Nozka[122], K. Ntekas[160], N. M. J. Nunes De Moura Junior[83b], E. Nurse[96], J. Ocariz[127], A. Ochi[85], I. Ochoa[130a], S. Oerdek[161], J. T. Offermann[39], A. Ogrodnik[133], A. Oh[101], C. C. Ohm[144], H. Oide[84], R. Oishi[153], M. L. Ojeda[48], Y. Okazaki[88], M. W. O'Keefe[92], Y. Okumura[153], L. F. Oleiro Seabra[130a], S. A. Olivares Pino[137d], D. Oliveira Damazio[29], D. Oliveira Goncalves[83a], J. L. Oliver[160], A. Olszewski[87], Ö. O. Öncel[54], D. C. O'Neil[142], A. P. O'Neill[19], A. Onofre[130a,130e], P. U. E. Onyisi[11], M. J. Oreglia[39], G. E. Orellana[90], D. Orestano[77a,77b], N. Orlando[13], R. S. Orr[155], V. O'Shea[59], L. M. Osojnak[128], R. Ospanov[62a], G. Otero y Garzon[30], H. Otono[89], P. S. Ott[63a],

G. J. Ottino[17a], M. Ouchrif[35d], J. Ouellette[29], F. Ould-Saada[125], M. Owen[59], R. E. Owen[134], K. Y. Oyulmaz[21a], V. E. Ozcan[21a], N. Ozturk[8], S. Ozturk[82], H. A. Pacey[32], A. Pacheco Pages[13], C. Padilla Aranda[13], G. Padovano[75a,75b], S. Pagan Griso[17a], G. Palacino[68], A. Palazzo[70a,70b], S. Palestini[36], J. Pan[172], T. Pan[64a], D. K. Panchal[11], C. E. Pandini[114], J. G. Panduro Vazquez[95], H. Pang[14b], P. Pani[48], G. Panizzo[69a,69c], L. Paolozzi[56], C. Papadatos[108], S. Parajuli[44], A. Paramonov[6], C. Paraskevopoulos[10], D. Paredes Hernandez[64b], T. H. Park[155], M. A. Parker[32], F. Parodi[57a,57b], E. W. Parrish[115], V. A. Parrish[52], J. A. Parsons[41], U. Parzefall[54], B. Pascual Dias[108], L. Pascual Dominguez[151], F. Pasquali[114], E. Pasqualucci[75a], S. Passaggio[57b], F. Pastore[95], P. Pasuwan[47a,47b], P. Patel[87], U. M. Patel[51], J. R. Pater[101], T. Pauly[36], J. Pearkes[143], M. Pedersen[125], R. Pedro[130a], S. V. Peleganchuk[37], O. Penc[36], E. A. Pender[52], H. Peng[62a], K. E. Penski[109], M. Penzin[37], B. S. Peralva[83d], A. P. Pereira Peixoto[60], L. Pereira Sanchez[47a,47b], D. V. Perepelitsa[29,ai], E. Perez Codina[156a], M. Perganti[10], L. Perini[71a,71b,*], H. Pernegger[36], A. Perrevoort[113], O. Perrin[40], K. Peters[48], R. F. Y. Peters[101], B. A. Petersen[36], T. C. Petersen[42], E. Petit[102], V. Petousis[132], C. Petridou[152,e], A. Petrukhin[141], M. Pettee[17a], N. E. Pettersson[36], A. Petukhov[37], K. Petukhova[133], A. Peyaud[135], R. Pezoa[137f], L. Pezzotti[36], G. Pezzullo[172], T. M. Pham[170], T. Pham[105], P. W. Phillips[134], G. Piacquadio[145], E. Pianori[17a], F. Piazza[71a,71b], R. Piegaia[30], D. Pietreanu[27b], A. D. Pilkington[101], M. Pinamonti[69a,69c], J. L. Pinfold[2], B. C. Pinheiro Pereira[130a], A. E. Pinto Pinoargote[135], K. M. Piper[146], A. Pirttikoski[56], C. Pitman Donaldson[96], D. A. Pizzi[34], L. Pizzimento[76a,76b], A. Pizzini[114], M.-A. Pleier[29], V. Plesanovs[54], V. Pleskot[133], E. Plotnikova[38], G. Poddar[4], R. Poettgen[98], L. Poggioli[127], I. Pokharel[55], S. Polacek[133], G. Polesello[73a], A. Poley[142,156a], R. Polifka[132], A. Polini[23b], C. S. Pollard[167], Z. B. Pollock[119], V. Polychronakos[29], E. Pompa Pacchi[75a,75b], D. Ponomarenko[113], L. Pontecorvo[36], S. Popa[27a], G. A. Popeneciu[27d], A. Poreba[36], D. M. Portillo Quintero[156a], S. Pospisil[132], M. A. Postill[139], P. Postolache[27c], K. Potamianos[167], P. A. Potepa[86a], I. N. Potrap[38], C. J. Potter[32], H. Potti[1], T. Poulsen[48], J. Poveda[163], M. E. Pozo Astigarraga[36], A. Prades Ibanez[163], J. Pretel[54], D. Price[101], M. Primavera[70a], M. A. Principe Martin[99], R. Privara[122], T. Procter[59], M. L. Proffitt[138], N. Proklova[128], K. Prokofiev[64c], G. Proto[110], S. Protopopescu[29], J. Proudfoot[6], M. Przybycien[86a], W. W. Przygoda[86b], J. E. Puddefoot[139], D. Pudzha[37], D. Pyatiizbyantseva[37], J. Qian[106], D. Qichen[101], Y. Qin[101], T. Qiu[52], A. Quadt[55], M. Queitsch-Maitland[101], G. Quetant[56], G. Rabanal Bolanos[61], D. Rafanoharana[54], F. Ragusa[71a,71b], J. L. Rainbolt[39], J. A. Raine[56], S. Rajagopalan[29], E. Ramakoti[37], K. Ran[48,14e], N. P. Rapheeha[33g], H. Rasheed[27b], V. Raskina[127], D. F. Rassloff[63a], S. Rave[100], B. Ravina[55], I. Ravinovich[169], M. Raymond[36], A. L. Read[125], N. P. Readioff[139], D. M. Rebuzzi[73a,73b], G. Redlinger[29], A. S. Reed[110], K. Reeves[26], J. A. Reidelsturz[171], D. Reikher[151], A. Rej[141], C. Rembser[36], A. Renardi[48], M. Renda[27b], M. B. Rendel[110], F. Renner[48], A. G. Rennie[59], S. Resconi[71a], M. Ressegotti[57a,57b], S. Rettie[36], J. G. Reyes Rivera[107], B. Reynolds[119], E. Reynolds[17a], O. L. Rezanova[37], P. Reznicek[133], N. Ribaric[91], E. Ricci[78a,78b], R. Richter[110], S. Richter[47a,47b], E. Richter-Was[86b], M. Ridel[127], S. Ridouani[35d], P. Rieck[117], P. Riedler[36], M. Rijssenbeek[145], A. Rimoldi[73a,73b], M. Rimoldi[48], L. Rinaldi[23a,23b], T. T. Rinn[29], M. P. Rinnagel[109], G. Ripellino[161], I. Riu[13], P. Rivadeneira[48], J. C. Rivera Vergara[165], F. Rizatdinova[121], E. Rizvi[94], B. A. Roberts[167], B. R. Roberts[17a], S. H. Robertson[104,x], M. Robin[48], D. Robinson[32], C. M. Robles Gajardo[137f], M. Robles Manzano[100], A. Robson[59], A. Rocchi[76a,76b], C. Roda[74a,74b], S. Rodriguez Bosca[63a], Y. Rodriguez Garcia[22a], A. Rodriguez Rodriguez[54], A. M. Rodríguez Vera[156b], S. Roe[36], J. T. Roemer[160], A. R. Roepe-Gier[136], J. Roggel[171], O. Røhne[125], R. A. Rojas[103], C. P. A. Roland[68], J. Roloff[29], A. Romaniouk[37], E. Romano[73a,73b], M. Romano[23b], A. C. Romero Hernandez[162], N. Rompotis[92], L. Roos[127], S. Rosati[75a], B. J. Rosser[39], E. Rossi[126], E. Rossi[72a,72b], L. P. Rossi[57b], L. Rossini[48], R. Rosten[119], M. Rotaru[27b], B. Rottler[54], C. Rougier[102,ab], D. Rousseau[66], D. Rousso[32], A. Roy[162], S. Roy-Garand[155], A. Rozanov[102], Y. Rozen[150], X. Ruan[33g], A. Rubio Jimenez[163], A. J. Ruby[92], V. H. Ruelas Rivera[18], T. A. Ruggeri[1], A. Ruggiero[126], A. Ruiz-Martinez[163], A. Rummler[36], Z. Rurikova[54], N. A. Rusakovich[38], H. L. Russell[165], G. Russo[75a,75b], J. P. Rutherfoord[7], S. Rutherford Colmenares[32], K. Rybacki[91], M. Rybar[133], E. B. Rye[125], A. Ryzhov[44], J. A. Sabater Iglesias[56], P. Sabatini[163], L. Sabetta[75a,75b], H. F.-W. Sadrozinski[136], F. Safai Tehrani[75a], B. Safarzadeh Samani[146], M. Safdari[143], S. Saha[165], M. Sahinsoy[110], M. Saimpert[135], M. Saito[153], T. Saito[153], D. Salamani[36], A. Salnikov[143], J. Salt[163], A. Salvador Salas[13], D. Salvatore[43a,43b], F. Salvatore[146], A. Salzburger[36], D. Sammel[54], D. Sampsonidis[152,e], D. Sampsonidou[123], J. Sánchez[163], A. Sanchez Pineda[4], V. Sanchez Sebastian[163], H. Sandaker[125], C. O. Sander[48], J. A. Sandesara[103], M. Sandhoff[171], C. Sandoval[22b], D. P. C. Sankey[134], T. Sano[88], A. Sansoni[53], L. Santi[75a,75b], C. Santoni[40], H. Santos[130a,130b], S. N. Santpur[17a], A. Santra[169],

K. A. Saoucha[139], J. G. Saraiva[130a,130d], J. Sardain[7], O. Sasaki[84], K. Sato[157], C. Sauer[63b], F. Sauerburger[54], E. Sauvan[4], P. Savard[155,ag], R. Sawada[153], C. Sawyer[134], L. Sawyer[97], I. Sayago Galvan[163], C. Sbarra[23b], A. Sbrizzi[23a,23b], T. Scanlon[96], J. Schaarschmidt[138], P. Schacht[110], D. Schaefer[39], U. Schäfer[100], A. C. Schaffer[44,66], D. Schaile[109], R. D. Schamberger[145], C. Scharf[18], M. M. Schefer[19], V. A. Schegelsky[37], D. Scheirich[133], F. Schenck[18], M. Schernau[160], C. Scheulen[55], C. Schiavi[57a,57b], E. J. Schioppa[70a,70b], M. Schioppa[43a,43b], B. Schlag[143,o], K. E. Schleicher[54], S. Schlenker[36], J. Schmeing[171], M. A. Schmidt[171], K. Schmieden[100], C. Schmitt[100], S. Schmitt[48], L. Schoeffel[135], A. Schoening[63b], P. G. Scholer[54], E. Schopf[126], M. Schott[100], J. Schovancova[36], S. Schramm[56], F. Schroeder[171], T. Schroer[56], H.-C. Schultz-Coulon[63a], M. Schumacher[54], B. A. Schumm[136], Ph. Schune[135], A. J. Schuy[138], H. R. Schwartz[136], A. Schwartzman[143], T. A. Schwarz[106], Ph. Schwemling[135], R. Schwienhorst[107], A. Sciandra[136], G. Sciolla[26], F. Scuri[74a], C. D. Sebastiani[92], K. Sedlaczek[115], P. Seema[18], S. C. Seidel[112], A. Seiden[136], B. D. Seidlitz[41], C. Seitz[48], J. M. Seixas[83b], G. Sekhniaidze[72a], S. J. Sekula[44], L. Selem[60], N. Semprini-Cesari[23a,23b], D. Sengupta[56], V. Senthilkumar[163], L. Serin[66], L. Serkin[69a,69b], M. Sessa[76a,76b], H. Severini[120], F. Sforza[57a,57b], A. Sfyrla[56], E. Shabalina[55], R. Shaheen[144], J. D. Shahinian[128], D. Shaked Renous[169], L. Y. Shan[14a], M. Shapiro[17a], A. Sharma[36], A. S. Sharma[164], P. Sharma[80], S. Sharma[48], P. B. Shatalov[37], K. Shaw[146], S. M. Shaw[101], A. Shcherbakova[37], Q. Shen[5,62c], P. Sherwood[96], L. Shi[96], X. Shi[14a], C. O. Shimmin[172], Y. Shimogama[168], J. D. Shinner[95], I. P. J. Shipsey[126], S. Shirabe[56,h], M. Shiyakova[38,v], J. Shlomi[169], M. J. Shochet[39], J. Shojaii[105], D. R. Shope[125], B. Shrestha[120], S. Shrestha[119,aj], E. M. Shrif[33g], M. J. Shroff[165], P. Sicho[131], A. M. Sickles[162], E. Sideras Haddad[33g], A. Sidoti[23b], F. Siegert[50], Dj. Sijacki[15], R. Sikora[86a], F. Sili[90], J. M. Silva[20], M. V. Silva Oliveira[29], S. B. Silverstein[47a], S. Simion[66], R. Simoniello[36], E. L. Simpson[59], H. Simpson[146], L. R. Simpson[106], N. D. Simpson[98], S. Simsek[82], S. Sindhu[55], P. Sinervo[155], S. Singh[155], S. Sinha[48], S. Sinha[101], M. Sioli[23a,23b], I. Siral[36], E. Sitnikova[48], S.Yu. Sivoklokov[37,*], J. Sjölin[47a,47b], A. Skaf[55], E. Skorda[98], P. Skubic[120], M. Slawinska[87], V. Smakhtin[169], B. H. Smart[134], J. Smiesko[36], S.Yu. Smirnov[37], Y. Smirnov[37], L. N. Smirnova[37,a], O. Smirnova[98], A. C. Smith[41], E. A. Smith[39], H. A. Smith[126], J. L. Smith[92], R. Smith[143], M. Smizanska[91], K. Smolek[132], A. A. Snesarev[37], S. R. Snider[155], H. L. Snoek[114], S. Snyder[29], R. Sobie[165,x], A. Soffer[151], C. A. Solans Sanchez[36], E.Yu. Soldatov[37], U. Soldevila[163], A. A. Solodkov[37], S. Solomon[26], A. Soloshenko[38], K. Solovieva[54], O. V. Solovyanov[40], V. Solovyev[37], P. Sommer[36], A. Sonay[13], W. Y. Song[156b], J. M. Sonneveld[114], A. Sopczak[132], A. L. Sopio[96], F. Sopkova[28b], V. Sothilingam[63a], S. Sottocornola[68], R. Soualah[116b], Z. Soumaimi[35e], D. South[48], S. Spagnolo[70a,70b], M. Spalla[110], D. Sperlich[54], G. Spigo[36], M. Spina[146], S. Spinali[91], D. P. Spiteri[59], M. Spousta[133], E. J. Staats[34], A. Stabile[71a,71b], R. Stamen[63a], M. Stamenkovic[114], A. Stampekis[20], M. Standke[24], E. Stanecka[87], M. V. Stange[50], B. Stanislaus[17a], M. M. Stanitzki[48], B. Stapf[48], E. A. Starchenko[37], G. H. Stark[136], J. Stark[102,ab], D. M. Starko[156b], P. Staroba[131], P. Starovoitov[63a], S. Stärz[104], R. Staszewski[87], G. Stavropoulos[46], J. Steentoft[161], P. Steinberg[29], B. Stelzer[142,156a], H. J. Stelzer[129], O. Stelzer-Chilton[156a], H. Stenzel[58], T. J. Stevenson[146], G. A. Stewart[36], J. R. Stewart[121], M. C. Stockton[36], G. Stoicea[27b], M. Stolarski[130a], S. Stonjek[110], A. Straessner[50], J. Strandberg[144], S. Strandberg[47a,47b], M. Strauss[120], T. Strebler[102], P. Strizenec[28b], R. Ströhmer[166], D. M. Strom[123], L. R. Strom[48], R. Stroynowski[44], A. Strubig[47a,47b], S. A. Stucci[29], B. Stugu[16], J. Stupak[120], N. A. Styles[48], D. Su[143], S. Su[62a], W. Su[62d], X. Su[62a,66], K. Sugizaki[153], V. V. Sulin[37], M. J. Sullivan[92], D. M. S. Sultan[78a,78b], L. Sultanaliyeva[37], S. Sultansoy[3b], T. Sumida[88], S. Sun[106], S. Sun[170], O. Sunneborn Gudnadottir[161], N. Sur[102], M. R. Sutton[146], H. Suzuki[157], M. Svatos[131], M. Swiatlowski[156a], T. Swirski[166], I. Sykora[28a], M. Sykora[133], T. Sykora[133], D. Ta[100], K. Tackmann[48,u], A. Taffard[160], R. Tafirout[156a], J. S. Tafoya Vargas[66], E. P. Takeva[52], Y. Takubo[84], M. Talby[102], A. A. Talyshev[37], K. C. Tam[64b], N. M. Tamir[151], A. Tanaka[153], J. Tanaka[153], R. Tanaka[66], M. Tanasini[57a,57b], Z. Tao[164], S. Tapia Araya[137f], S. Tapprogge[100], A. Tarek Abouelfadl Mohamed[107], S. Tarem[150], K. Tariq[14a], G. Tarna[27b,102], G. F. Tartarelli[71a], P. Tas[133], M. Tasevsky[131], E. Tassi[43a,43b], A. C. Tate[162], G. Tateno[153], Y. Tayalati[35e,w], G. N. Taylor[105], W. Taylor[156b], H. Teagle[92], A. S. Tee[170], R. Teixeira De Lima[143], P. Teixeira-Dias[95], J. J. Teoh[155], K. Terashi[153], J. Terron[99], S. Terzo[13], M. Testa[53], R. J. Teuscher[155,x], A. Thaler[79], O. Theiner[56], N. Themistokleous[52], T. Theveneaux-Pelzer[102], O. Thielmann[171], D. W. Thomas[95], J. P. Thomas[20], E. A. Thompson[17a], P. D. Thompson[20], E. Thomson[128], Y. Tian[55], V. Tikhomirov[37,a], Yu.A. Tikhonov[37], S. Timoshenko[37], D. Timoshyn[133], E. X. L. Ting[1], P. Tipton[172], S. H. Tlou[33g], A. Tnourji[40], K. Todome[23a,23b], S. Todorova-Nova[133], S. Todt[50], M. Togawa[84], J. Tojo[89], S. Tokár[28a], K. Tokushuku[84], O. Toldaiev[68], R. Tombs[32], M. Tomoto[84,111], L. Tompkins[143,o],

K. W. Topolnicki[86b], E. Torrence[123], H. Torres[102,ab], E. Torró Pastor[163], M. Toscani[30], C. Tosciri[39], M. Tost[11], D. R. Tovey[139], A. Traeet[16], I. S. Trandafir[27b], T. Trefzger[166], A. Tricoli[29], I. M. Trigger[156a], S. Trincaz-Duvoid[127], D. A. Trischuk[26], B. Trocmé[60], C. Troncon[71a], L. Truong[33c], M. Trzebinski[87], A. Trzupek[87], F. Tsai[145], M. Tsai[106], A. Tsiamis[152,e], P. V. Tsiareshka[37], S. Tsigaridas[156a], A. Tsirigotis[152,s], V. Tsiskaridze[155], E. G. Tskhadadze[149a], M. Tsopoulou[152,e], Y. Tsujikawa[88], I. I. Tsukerman[37], V. Tsulaia[17a], S. Tsuno[84], O. Tsur[150], K. Tsuri[118], D. Tsybychev[145], Y. Tu[64b], A. Tudorache[27b], V. Tudorache[27b], A. N. Tuna[36], S. Turchikhin[38], I. Turk Cakir[3a], R. Turra[71a], T. Turtuvshin[38,y], P. M. Tuts[41], S. Tzamarias[152,e], P. Tzanis[10], E. Tzovara[100], K. Uchida[153], F. Ukegawa[157], P. A. Ulloa Poblete[137b,137c], E. N. Umaka[29], G. Unal[36], M. Unal[11], A. Undrus[29], G. Unel[160], J. Urban[28b], P. Urquijo[105], G. Usai[8], R. Ushioda[154], M. Usman[108], Z. Uysal[21b], L. Vacavant[102], V. Vacek[132], B. Vachon[104], K. O. H. Vadla[125], T. Vafeiadis[36], A. Vaitkus[96], C. Valderanis[109], E. Valdes Santurio[47a,47b], M. Valente[156a], S. Valentinetti[23a,23b], A. Valero[163], E. Valiente Moreno[163], A. Vallier[102,ab], J. A. Valls Ferrer[163], D. R. Van Arneman[114], T. R. Van Daalen[138], A. Van Der Graaf[49], P. Van Gemmeren[6], M. Van Rijnbach[36,125], S. Van Stroud[96], I. Van Vulpen[114], M. Vanadia[76a,76b], W. Vandelli[36], M. Vandenbroucke[135], E. R. Vandewall[121], D. Vannicola[151], L. Vannoli[57a,57b], R. Vari[75a], E. W. Varnes[7], C. Varni[17a], T. Varol[148], D. Varouchas[66], L. Varriale[163], K. E. Varvell[147], M. E. Vasile[27b], L. Vaslin[40], G. A. Vasquez[165], F. Vazeille[40], T. Vazquez Schroeder[36], J. Veatch[31], V. Vecchio[101], M. J. Veen[103], I. Veliscek[126], L. M. Veloce[155], F. Veloso[130a,130c], S. Veneziano[75a], A. Ventura[70a,70b], A. Verbytskyi[110], M. Verducci[74a,74b], C. Vergis[24], M. Verissimo De Araujo[83b], W. Verkerke[114], J. C. Vermeulen[114], C. Vernieri[143], P. J. Verschuuren[95], M. Vessella[103], M. C. Vetterli[142,ag], A. Vgenopoulos[152,e], N. Viaux Maira[137f], T. Vickey[139], O. E. Vickey Boeriu[139], G. H. A. Viehhauser[126], L. Vigani[63b], M. Villa[23a,23b], M. Villaplana Perez[163], E. M. Villhauer[52], E. Vilucchi[53], M. G. Vincter[34], G. S. Virdee[20], A. Vishwakarma[52], A. Visibile[114], C. Vittori[36], I. Vivarelli[146], V. Vladimirov[167], E. Voevodina[110], F. Vogel[109], P. Vokac[132], J. Von Ahnen[48], E. Von Toerne[24], B. Vormwald[36], V. Vorobel[133], K. Vorobev[37], M. Vos[163], K. Voss[141], J. H. Vossebeld[92], M. Vozak[114], L. Vozdecky[94], N. Vranjes[15], M. Vranjes Milosavljevic[15], M. Vreeswijk[114], R. Vuillermet[36], O. Vujinovic[100], I. Vukotic[39], S. Wada[157], C. Wagner[103], J. M. Wagner[17a], W. Wagner[171], S. Wahdan[171], H. Wahlberg[90], R. Wakasa[157], M. Wakida[111], J. Walder[134], R. Walker[109], W. Walkowiak[141], A. Wall[128], T. Wamorkar[6], A. Z. Wang[170], C. Wang[100], C. Wang[62c], H. Wang[17a], J. Wang[64a], R.-J. Wang[100], R. Wang[61], R. Wang[6], S. M. Wang[148], S. Wang[62b], T. Wang[62a], W. T. Wang[80], W. Wang[14a], X. Wang[14c], X. Wang[162], X. Wang[62c], Y. Wang[62d], Y. Wang[14c], Z. Wang[106], Z. Wang[51,62c,62d], Z. Wang[106], A. Warburton[104], R. J. Ward[20], N. Warrack[59], A. T. Watson[20], H. Watson[59], M. F. Watson[20], E. Watton[59,134], G. Watts[138], B. M. Waugh[96], C. Weber[29], H. A. Weber[18], M. S. Weber[19], S. M. Weber[63a], C. Wei[62a], Y. Wei[126], A. R. Weidberg[126], E. J. Weik[117], J. Weingarten[49], M. Weirich[100], C. Weiser[54], C. J. Wells[48], T. Wenaus[29], B. Wendland[49], T. Wengler[36], N. S. Wenke[110], N. Wermes[24], M. Wessels[63a], K. Whalen[123], A. M. Wharton[91], A. S. White[61], A. White[8], M. J. White[1], D. Whiteson[160], L. Wickremasinghe[124], W. Wiedenmann[170], C. Wiel[50], M. Wielers[134], C. Wiglesworth[42], D. J. Wilbern[120], H. G. Wilkens[36], D. M. Williams[41], H. H. Williams[128], S. Williams[32], S. Willocq[103], B. J. Wilson[101], P. J. Windischhofer[39], F. I. Winkel[30], F. Winklmeier[123], B. T. Winter[54], J. K. Winter[101], M. Wittgen[143], M. Wobisch[97], Z. Wolffs[114], R. Wölker[126], J. Wollrath[160], M. W. Wolter[87], H. Wolters[130a,130c], A. F. Wongel[48], S. D. Worm[48], B. K. Wosiek[87], K. W. Woźniak[87], S. Wozniewski[55], K. Wraight[59], C. Wu[20], J. Wu[14a,14e], M. Wu[64a], M. Wu[113], S. L. Wu[170], X. Wu[56], Y. Wu[62a], Z. Wu[135], J. Wuerzinger[110], T. R. Wyatt[101], B. M. Wynne[52], S. Xella[42], L. Xia[14c], M. Xia[14b], J. Xiang[64c], X. Xiao[106], M. Xie[62a], X. Xie[62a], S. Xin[14a,14e], J. Xiong[17a], D. Xu[14a], H. Xu[62a], L. Xu[62a], R. Xu[128], T. Xu[106], Y. Xu[14b], Z. Xu[52], Z. Xu[14a], B. Yabsley[147], S. Yacoob[33a], N. Yamaguchi[89], Y. Yamaguchi[154], E. Yamashita[153], H. Yamauchi[157], T. Yamazaki[17a], Y. Yamazaki[85], J. Yan[62c], S. Yan[126], Z. Yan[25], H. J. Yang[62c,62d], H. T. Yang[62a], S. Yang[62a], T. Yang[64c], X. Yang[62a], X. Yang[14a], Y. Yang[44], Y. Yang[62a], Z. Yang[62a], W.-M. Yao[17a], Y. C. Yap[48], H. Ye[14c], H. Ye[55], J. Ye[44], S. Ye[29], X. Ye[62a], Y. Yeh[96], I. Yeletskikh[38], B. K. Yeo[17a], M. R. Yexley[96], P. Yin[41], K. Yorita[168], S. Younas[27b], C. J. S. Young[54], C. Young[143], Y. Yu[62a], M. Yuan[106], R. Yuan[62b,k], L. Yue[96], M. Zaazoua[62a], B. Zabinski[87], E. Zaid[52], T. Zakareishvili[149b], N. Zakharchuk[34], S. Zambito[56], J. A. Zamora Saa[137b,137d], J. Zang[153], D. Zanzi[54], O. Zaplatilek[132], C. Zeitnitz[171], H. Zeng[14a], J. C. Zeng[162], D. T. Zenger Jr[26], O. Zenin[37], T. Ženiš[28a], S. Zenz[94], S. Zerradi[35a], D. Zerwas[66], M. Zhai[14a,14e], B. Zhang[14c], D. F. Zhang[139], J. Zhang[62b], J. Zhang[6], K. Zhang[14a,14e], L. Zhang[14c], P. Zhang[14a,14e], R. Zhang[170], S. Zhang[106], T. Zhang[153], X. Zhang[62c], X. Zhang[62b], Y. Zhang[5,62c], Y. Zhang[96], Z. Zhang[17a],

Z. Zhang[66], H. Zhao[138], P. Zhao[51], T. Zhao[62b], Y. Zhao[136], Z. Zhao[62a], A. Zhemchugov[38], K. Zheng[162], X. Zheng[62a], Z. Zheng[143], D. Zhong[162], B. Zhou[106], H. Zhou[7], N. Zhou[62c], Y. Zhou[7], C. G. Zhu[62b], J. Zhu[106], Y. Zhu[62c], Y. Zhu[62a], X. Zhuang[14a], K. Zhukov[37], V. Zhulanov[37], N. I. Zimine[38], J. Zinsser[63b], M. Ziolkowski[141], L. Živković[15], A. Zoccoli[23a,23b], K. Zoch[56], T. G. Zorbas[139], O. Zormpa[46], W. Zou[41], L. Zwalinski[36]

[1] Department of Physics, University of Adelaide, Adelaide, Australia
[2] Department of Physics, University of Alberta, Edmonton, AB, Canada
[3] [(a)]Department of Physics, Ankara University, Ankara, Türkiye; [(b)]Division of Physics, TOBB University of Economics and Technology, Ankara, Türkiye
[4] LAPP, Université Savoie Mont Blanc, CNRS/IN2P3, Annecy, France
[5] APC, Université Paris Cité, CNRS/IN2P3, Paris, France
[6] High Energy Physics Division, Argonne National Laboratory, Argonne, IL, USA
[7] Department of Physics, University of Arizona, Tucson, AZ, USA
[8] Department of Physics, University of Texas at Arlington, Arlington, TX, USA
[9] Physics Department, National and Kapodistrian University of Athens, Athens, Greece
[10] Physics Department, National Technical University of Athens, Zografou, Greece
[11] Department of Physics, University of Texas at Austin, Austin, TX, USA
[12] Institute of Physics, Azerbaijan Academy of Sciences, Baku, Azerbaijan
[13] Institut de Física d'Altes Energies (IFAE), Barcelona Institute of Science and Technology, Barcelona, Spain
[14] [(a)]Institute of High Energy Physics, Chinese Academy of Sciences, Beijing, China; [(b)]Physics Department, Tsinghua University, Beijing, China; [(c)]Department of Physics, Nanjing University, Nanjing, China; [(d)]School of Science, Shenzhen Campus of Sun Yat-sen University, Shenzhen, China; [(e)]University of Chinese Academy of Science (UCAS), Beijing, China
[15] Institute of Physics, University of Belgrade, Belgrade, Serbia
[16] Department for Physics and Technology, University of Bergen, Bergen, Norway
[17] [(a)]Physics Division, Lawrence Berkeley National Laboratory, Berkeley, CA, USA; [(b)]University of California, Berkeley, CA, USA
[18] Institut für Physik, Humboldt Universität zu Berlin, Berlin, Germany
[19] Albert Einstein Center for Fundamental Physics and Laboratory for High Energy Physics, University of Bern, Bern, Switzerland
[20] School of Physics and Astronomy, University of Birmingham, Birmingham, UK
[21] [(a)]Department of Physics, Bogazici University, Istanbul, Türkiye; [(b)]Department of Physics Engineering, Gaziantep University, Gaziantep, Türkiye; [(c)]Department of Physics, Istanbul University, Istanbul, Türkiye
[22] [(a)]Facultad de Ciencias y Centro de Investigaciónes, Universidad Antonio Nariño, Bogotá, Colombia; [(b)]Departamento de Física, Universidad Nacional de Colombia, Bogotá, Colombia
[23] [(a)]Dipartimento di Fisica e Astronomia A. Righi, Università di Bologna, Bologna, Italy; [(b)]INFN Sezione di Bologna, Bologna, Italy
[24] Physikalisches Institut, Universität Bonn, Bonn, Germany
[25] Department of Physics, Boston University, Boston, MA, USA
[26] Department of Physics, Brandeis University, Waltham, MA, USA
[27] [(a)]Transilvania University of Brasov, Brasov, Romania; [(b)]Horia Hulubei National Institute of Physics and Nuclear Engineering, Bucharest, Romania; [(c)]Department of Physics, Alexandru Ioan Cuza University of Iasi, Iasi, Romania; [(d)]National Institute for Research and Development of Isotopic and Molecular Technologies, Physics Department, Cluj-Napoca, Romania; [(e)]National University of Science and Technology Politechnica, Bucharest, Romania; [(f)]West University in Timisoara, Timisoara, Romania; [(g)]Faculty of Physics, University of Bucharest, Bucharest, Romania
[28] [(a)]Faculty of Mathematics, Physics and Informatics, Comenius University, Bratislava, Slovak Republic; [(b)]Department of Subnuclear Physics, Institute of Experimental Physics of the Slovak Academy of Sciences, Kosice, Slovak Republic
[29] Physics Department, Brookhaven National Laboratory, Upton, NY, USA
[30] Universidad de Buenos Aires, Facultad de Ciencias Exactas y Naturales, Departamento de Física, y CONICET, Instituto de Física de Buenos Aires (IFIBA), Buenos Aires, Argentina
[31] California State University, CA, USA

[32] Cavendish Laboratory, University of Cambridge, Cambridge, UK
[33] [(a)]Department of Physics, University of Cape Town, Cape Town, South Africa; [(b)]iThemba Labs, Western Cape, South Africa; [(c)]Department of Mechanical Engineering Science, University of Johannesburg, Johannesburg, South Africa; [(d)]National Institute of Physics, University of the Philippines Diliman (Philippines), Quezon City, Philippines; [(e)]Department of Physics, University of South Africa, Pretoria, South Africa; [(f)]University of Zululand, KwaDlangezwa, South Africa; [(g)]School of Physics, University of the Witwatersrand, Johannesburg, South Africa
[34] Department of Physics, Carleton University, Ottawa, ON, Canada
[35] [(a)]Faculté des Sciences Ain Chock, Réseau Universitaire de Physique des Hautes Energies-Université Hassan II, Casablanca, Morocco; [(b)]Faculté des Sciences, Université Ibn-Tofail, Kénitra, Morocco; [(c)]Faculté des Sciences Semlalia, LPHEA-Marrakech, Université Cadi Ayyad, Marrakech, Morocco; [(d)]LPMR, Faculté des Sciences, Université Mohamed Premier, Oujda, Morocco; [(e)]Faculté des sciences, Université Mohammed V, Rabat, Morocco; [(f)]Institute of Applied Physics, Mohammed VI Polytechnic University, Ben Guerir, Morocco
[36] CERN, Geneva, Switzerland
[37] Affiliated with an Institute Covered by a Cooperation Agreement with CERN, Geneva, Switzerland
[38] Affiliated with an International Laboratory Covered by a Cooperation Agreement with CERN, Geneva, Switzerland
[39] Enrico Fermi Institute, University of Chicago, Chicago, IL, USA
[40] LPC, Université Clermont Auvergne, CNRS/IN2P3, Clermont-Ferrand, France
[41] Nevis Laboratory, Columbia University, Irvington, NY, USA
[42] Niels Bohr Institute, University of Copenhagen, Copenhagen, Denmark
[43] [(a)]Dipartimento di Fisica, Università della Calabria, Rende, Italy; [(b)]INFN Gruppo Collegato di Cosenza, Laboratori Nazionali di Frascati, Frascati, Italy
[44] Physics Department, Southern Methodist University, Dallas, TX, USA
[45] Physics Department, University of Texas at Dallas, Richardson, TX, USA
[46] National Centre for Scientific Research "Demokritos", Agia Paraskevi, Greece
[47] [(a)]Department of Physics, Stockholm University, Stockholm, Sweden; [(b)]Oskar Klein Centre, Stockholm, Sweden
[48] Deutsches Elektronen-Synchrotron DESY, Hamburg and Zeuthen, Germany
[49] Fakultät Physik , Technische Universität Dortmund, Dortmund, Germany
[50] Institut für Kern- und Teilchenphysik, Technische Universität Dresden, Dresden, Germany
[51] Department of Physics, Duke University, Durham, NC, USA
[52] SUPA-School of Physics and Astronomy, University of Edinburgh, Edinburgh, UK
[53] INFN e Laboratori Nazionali di Frascati, Frascati, Italy
[54] Physikalisches Institut, Albert-Ludwigs-Universität Freiburg, Freiburg, Germany
[55] II. Physikalisches Institut, Georg-August-Universität Göttingen, Göttingen, Germany
[56] Département de Physique Nucléaire et Corpusculaire, Université de Genève, Geneva, Switzerland
[57] [(a)]Dipartimento di Fisica, Università di Genova, Genoa, Italy; [(b)]INFN Sezione di Genova, Genoa, Italy
[58] II. Physikalisches Institut, Justus-Liebig-Universität Giessen, Giessen, Germany
[59] SUPA-School of Physics and Astronomy, University of Glasgow, Glasgow, UK
[60] LPSC, Université Grenoble Alpes, CNRS/IN2P3, Grenoble INP, Grenoble, France
[61] Laboratory for Particle Physics and Cosmology, Harvard University, Cambridge, MA, USA
[62] [(a)]Department of Modern Physics and State Key Laboratory of Particle Detection and Electronics, University of Science and Technology of China, Hefei, China; [(b)]Institute of Frontier and Interdisciplinary Science and Key Laboratory of Particle Physics and Particle Irradiation (MOE), Shandong University, Qingdao, China; [(c)]School of Physics and Astronomy, Shanghai Jiao Tong University, Key Laboratory for Particle Astrophysics and Cosmology (MOE), SKLPPC, Shanghai, China; [(d)]Tsung-Dao Lee Institute, Shanghai, China
[63] [(a)]Kirchhoff-Institut für Physik, Ruprecht-Karls-Universität Heidelberg, Heidelberg, Germany; [(b)]Physikalisches Institut, Ruprecht-Karls-Universität Heidelberg, Heidelberg, Germany
[64] [(a)]Department of Physics, Chinese University of Hong Kong, Shatin, N.T., Hong Kong, China; [(b)]Department of Physics, University of Hong Kong, Hong Kong, China; [(c)]Department of Physics and Institute for Advanced Study, Hong Kong University of Science and Technology, Clear Water Bay, Kowloon, Hong Kong, China
[65] Department of Physics, National Tsing Hua University, Hsinchu, Taiwan
[66] IJCLab, Université Paris-Saclay, CNRS/IN2P3, 91405 Orsay, France
[67] Centro Nacional de Microelectrónica (IMB-CNM-CSIC), Barcelona, Spain
[68] Department of Physics, Indiana University, Bloomington, IN, USA

[69] [(a)]INFN Gruppo Collegato di Udine, Sezione di Trieste, Udine, Italy; [(b)]ICTP, Trieste, Italy; [(c)]Dipartimento Politecnico di Ingegneria e Architettura, Università di Udine, Udine, Italy
[70] [(a)]INFN Sezione di Lecce, Lecce, Italy; [(b)]Dipartimento di Matematica e Fisica, Università del Salento, Lecce, Italy
[71] [(a)]INFN Sezione di Milano, Milan, Italy; [(b)]Dipartimento di Fisica, Università di Milano, Milan, Italy
[72] [(a)]INFN Sezione di Napoli, Naples, Italy; [(b)]Dipartimento di Fisica, Università di Napoli, Naples, Italy
[73] [(a)]INFN Sezione di Pavia, Pavia, Italy; [(b)]Dipartimento di Fisica, Università di Pavia, Pavia, Italy
[74] [(a)]INFN Sezione di Pisa, Pisa, Italy; [(b)]Dipartimento di Fisica E. Fermi, Università di Pisa, Pisa, Italy
[75] [(a)]INFN Sezione di Roma, Rome, Italy; [(b)]Dipartimento di Fisica, Sapienza Università di Roma, Rome, Italy
[76] [(a)]INFN Sezione di Roma Tor Vergata, Rome, Italy; [(b)]Dipartimento di Fisica, Università di Roma Tor Vergata, Rome, Italy
[77] [(a)]INFN Sezione di Roma Tre, Rome, Italy; [(b)]Dipartimento di Matematica e Fisica, Università Roma Tre, Rome, Italy
[78] [(a)]INFN-TIFPA, Povo, Italy; [(b)]Università degli Studi di Trento, Trento, Italy
[79] Department of Astro and Particle Physics, Universität Innsbruck, Innsbruck, Austria
[80] University of Iowa, Iowa City, IA, USA
[81] Department of Physics and Astronomy, Iowa State University, Ames, IA, USA
[82] Istinye University, Sariyer, Istanbul, Türkiye
[83] [(a)]Departamento de Engenharia Elétrica, Universidade Federal de Juiz de Fora (UFJF), Juiz de Fora, Brazil; [(b)]Universidade Federal do Rio De Janeiro COPPE/EE/IF, Rio de Janeiro, Brazil; [(c)]Instituto de Física, Universidade de São Paulo, São Paulo, Brazil; [(d)]Rio de Janeiro State University, Rio de Janeiro, Brazil
[84] KEK, High Energy Accelerator Research Organization, Tsukuba, Japan
[85] Graduate School of Science, Kobe University, Kobe, Japan
[86] [(a)]AGH University of Krakow, Faculty of Physics and Applied Computer Science, Kraków, Poland; [(b)]Marian Smoluchowski Institute of Physics, Jagiellonian University, Kraków, Poland
[87] Institute of Nuclear Physics Polish Academy of Sciences, Kraków, Poland
[88] Faculty of Science, Kyoto University, Kyoto, Japan
[89] Research Center for Advanced Particle Physics and Department of Physics, Kyushu University, Fukuoka , Japan
[90] Instituto de Física La Plata, Universidad Nacional de La Plata and CONICET, La Plata, Argentina
[91] Physics Department, Lancaster University, Lancaster, UK
[92] Oliver Lodge Laboratory, University of Liverpool, Liverpool, UK
[93] Department of Experimental Particle Physics, Jožef Stefan Institute and Department of Physics, University of Ljubljana, Ljubljana, Slovenia
[94] School of Physics and Astronomy, Queen Mary University of London, London, UK
[95] Department of Physics, Royal Holloway University of London, Egham, UK
[96] Department of Physics and Astronomy, University College London, London, UK
[97] Louisiana Tech University, Ruston, LA, USA
[98] Fysiska institutionen, Lunds universitet, Lund, Sweden
[99] Departamento de Física Teorica C-15 and CIAFF, Universidad Autónoma de Madrid, Madrid, Spain
[100] Institut für Physik, Universität Mainz, Mainz, Germany
[101] School of Physics and Astronomy, University of Manchester, Manchester, UK
[102] CPPM, Aix-Marseille Université, CNRS/IN2P3, Marseille, France
[103] Department of Physics, University of Massachusetts, Amherst, MA, USA
[104] Department of Physics, McGill University, Montreal, QC, Canada
[105] School of Physics, University of Melbourne, Victoria, Australia
[106] Department of Physics, University of Michigan, Ann Arbor, MI, USA
[107] Department of Physics and Astronomy, Michigan State University, East Lansing, MI, USA
[108] Group of Particle Physics, University of Montreal, Montreal, QC, Canada
[109] Fakultät für Physik, Ludwig-Maximilians-Universität München, Munich, Germany
[110] Max-Planck-Institut für Physik (Werner-Heisenberg-Institut), Munich, Germany
[111] Graduate School of Science and Kobayashi-Maskawa Institute, Nagoya University, Nagoya, Japan
[112] Department of Physics and Astronomy, University of New Mexico, Albuquerque, NM, USA
[113] Institute for Mathematics, Astrophysics and Particle Physics, Radboud University/Nikhef, Nijmegen, Netherlands
[114] Nikhef National Institute for Subatomic Physics and University of Amsterdam, Amsterdam, Netherlands
[115] Department of Physics, Northern Illinois University, DeKalb, IL, USA

[116] [(a)]New York University Abu Dhabi, Abu Dhabi, United Arab Emirates; [(b)]University of Sharjah, Sharjah, United Arab Emirates
[117] Department of Physics, New York University, New York, NY, USA
[118] Ochanomizu University, Otsuka, Bunkyo-ku, Tokyo, Japan
[119] Ohio State University, Columbus, OH, USA
[120] Homer L. Dodge Department of Physics and Astronomy, University of Oklahoma, Norman, OK, USA
[121] Department of Physics, Oklahoma State University, Stillwater, OK, USA
[122] Palacký University, Joint Laboratory of Optics, Olomouc, Czech Republic
[123] Institute for Fundamental Science, University of Oregon, Eugene, OR, USA
[124] Graduate School of Science, Osaka University, Osaka, Japan
[125] Department of Physics, University of Oslo, Oslo, Norway
[126] Department of Physics, Oxford University, Oxford, UK
[127] LPNHE, Sorbonne Université, Université Paris Cité, CNRS/IN2P3, Paris, France
[128] Department of Physics, University of Pennsylvania, Philadelphia, PA, USA
[129] Department of Physics and Astronomy, University of Pittsburgh, Pittsburgh, PA, USA
[130] [(a)]Laboratório de Instrumentação e Física Experimental de Partículas - LIP, Lisbon, Portugal; [(b)]Departamento de Física, Faculdade de Ciências, Universidade de Lisboa, Lisbon, Portugal; [(c)]Departamento de Física, Universidade de Coimbra, Coimbra, Portugal; [(d)]Centro de Física Nuclear da Universidade de Lisboa, Lisbon, Portugal; [(e)]Departamento de Física, Universidade do Minho, Braga, Portugal; [(f)]Departamento de Física Teórica y del Cosmos, Universidad de Granada, Granada, Spain; [(g)]Departamento de Física, Instituto Superior Técnico, Universidade de Lisboa, Lisbon, Portugal
[131] Institute of Physics of the Czech Academy of Sciences, Prague, Czech Republic
[132] Czech Technical University in Prague, Prague, Czech Republic
[133] Charles University, Faculty of Mathematics and Physics, Prague, Czech Republic
[134] Particle Physics Department, Rutherford Appleton Laboratory, Didcot, UK
[135] IRFU, CEA, Université Paris-Saclay, Gif-sur-Yvette, France
[136] Santa Cruz Institute for Particle Physics, University of California Santa Cruz, Santa Cruz, CA, USA
[137] [(a)]Departamento de Física, Pontificia Universidad Católica de Chile, Santiago, Chile; [(b)]Millennium Institute for Subatomic physics at high energy frontier (SAPHIR), Santiago, Chile; [(c)]Instituto de Investigación Multidisciplinario en Ciencia y Tecnología, y Departamento de Física, Universidad de La Serena, La Serena, Chile; [(d)]Department of Physics, Universidad Andres Bello, Santiago, Chile; [(e)]Instituto de Alta Investigación, Universidad de Tarapacá, Arica, Chile; [(f)]Departamento de Física, Universidad Técnica Federico Santa María, Valparaíso, Chile
[138] Department of Physics, University of Washington, Seattle, WA, USA
[139] Department of Physics and Astronomy, University of Sheffield, Sheffield, UK
[140] Department of Physics, Shinshu University, Nagano, Japan
[141] Department Physik, Universität Siegen, Siegen, Germany
[142] Department of Physics, Simon Fraser University, Burnaby, BC, Canada
[143] SLAC National Accelerator Laboratory, Stanford, CA, USA
[144] Department of Physics, Royal Institute of Technology, Stockholm, Sweden
[145] Departments of Physics and Astronomy, Stony Brook University, Stony Brook, NY, USA
[146] Department of Physics and Astronomy, University of Sussex, Brighton, UK
[147] School of Physics, University of Sydney, Sydney, Australia
[148] Institute of Physics, Academia Sinica, Taipei, Taiwan
[149] [(a)]E. Andronikashvili Institute of Physics, Iv. Javakhishvili Tbilisi State University, Tbilisi, Georgia; [(b)]High Energy Physics Institute, Tbilisi State University, Tbilisi, Georgia; [(c)]University of Georgia, Tbilisi, Georgia
[150] Department of Physics, Technion, Israel Institute of Technology, Haifa, Israel
[151] Raymond and Beverly Sackler School of Physics and Astronomy, Tel Aviv University, Tel Aviv, Israel
[152] Department of Physics, Aristotle University of Thessaloniki, Thessaloniki, Greece
[153] International Center for Elementary Particle Physics and Department of Physics, University of Tokyo, Tokyo, Japan
[154] Department of Physics, Tokyo Institute of Technology, Tokyo, Japan
[155] Department of Physics, University of Toronto, Toronto, ON, Canada
[156] [(a)]TRIUMF, Vancouver, BC, Canada; [(b)]Department of Physics and Astronomy, York University, Toronto, ON, Canada
[157] Division of Physics and Tomonaga Center for the History of the Universe, Faculty of Pure and Applied Sciences, University of Tsukuba, Tsukuba, Japan

[158] Department of Physics and Astronomy, Tufts University, Medford, MA, USA
[159] United Arab Emirates University, Al Ain, United Arab Emirates
[160] Department of Physics and Astronomy, University of California Irvine, Irvine, CA, USA
[161] Department of Physics and Astronomy, University of Uppsala, Uppsala, Sweden
[162] Department of Physics, University of Illinois, Urbana, IL, USA
[163] Instituto de Física Corpuscular (IFIC), Centro Mixto Universidad de Valencia-CSIC, Valencia, Spain
[164] Department of Physics, University of British Columbia, Vancouver, BC, Canada
[165] Department of Physics and Astronomy, University of Victoria, Victoria, BC, Canada
[166] Fakultät für Physik und Astronomie, Julius-Maximilians-Universität Würzburg, Würzburg, Germany
[167] Department of Physics, University of Warwick, Coventry, UK
[168] Waseda University, Tokyo, Japan
[169] Department of Particle Physics and Astrophysics, Weizmann Institute of Science, Rehovot, Israel
[170] Department of Physics, University of Wisconsin, Madison, WI, USA
[171] Fakultät für Mathematik und Naturwissenschaften, Fachgruppe Physik, Bergische Universität Wuppertal, Wuppertal, Germany
[172] Department of Physics, Yale University, New Haven, CT, USA

[a] Also Affiliated with an Institute Covered by a Cooperation Agreement with CERN, Geneva, Switzerland
[b] Also at An-Najah National University, Nablus, Palestine
[c] Also at Borough of Manhattan Community College, City University of New York, New York, NY, USA
[d] Also at Center for High Energy Physics, Peking University, Beijing, China
[e] Also at Center for Interdisciplinary Research and Innovation (CIRI-AUTH), Thessaloniki, Greece
[f] Also at Centro Studi e Ricerche Enrico Fermi, Rome, Italy
[g] Also at CERN, Geneva, Switzerland
[h] Also at Département de Physique Nucléaire et Corpusculaire, Université de Genève, Geneva, Switzerland
[i] Also at Departament de Fisica de la Universitat Autonoma de Barcelona, Barcelona, Spain
[j] Also at Department of Financial and Management Engineering, University of the Aegean, Chios, Greece
[k] Also at Department of Physics and Astronomy, Michigan State University, East Lansing, MI, USA
[l] Also at Department of Physics, Ben Gurion University of the Negev, Beer Sheva, Israel
[m] Also at Department of Physics, California State University, Sacramento, USA
[n] Also at Department of Physics, King's College London, London, UK
[o] Also at Department of Physics, Stanford University, Stanford, CA, USA
[p] Also at Department of Physics, University of Fribourg, Fribourg, Switzerland
[q] Also at Department of Physics, University of Thessaly, Volos, Greece
[r] Also at Department of Physics, Westmont College, Santa Barbara, USA
[s] Also at Hellenic Open University, Patras, Greece
[t] Also at Institucio Catalana de Recerca i Estudis Avancats, ICREA, Barcelona, Spain
[u] Also at Institut für Experimentalphysik, Universität Hamburg, Hamburg, Germany
[v] Also at Institute for Nuclear Research and Nuclear Energy (INRNE) of the Bulgarian Academy of Sciences, Sofia, Bulgaria
[w] Also at Institute of Applied Physics, Mohammed VI Polytechnic University, Ben Guerir, Morocco
[x] Also at Institute of Particle Physics (IPP), Canada
[y] Also at Institute of Physics and Technology, Mongolian Academy of Sciences, Ulaanbaatar, Mongolia
[z] Also at Institute of Physics, Azerbaijan Academy of Sciences, Baku, Azerbaijan
[aa] Also at Institute of Theoretical Physics, Ilia State University, Tbilisi, Georgia
[ab] Also at L2IT, Université de Toulouse, CNRS/IN2P3, UPS, Toulouse, France
[ac] Also at Lawrence Livermore National Laboratory, Livermore, USA
[ad] Also at National Institute of Physics, University of the Philippines Diliman (Philippines), Quezon City, Philippines
[ae] Also at Technical University of Munich, Munich, Germany
[af] Also at The Collaborative Innovation Center of Quantum Matter (CICQM), Beijing, China
[ag] Also at TRIUMF, Vancouver, BC, Canada
[ah] Also at Università di Napoli Parthenope, Naples, Italy
[ai] Also at University of Colorado Boulder, Department of Physics, Colorado, USA

[aj] Also at Washington College, Chestertown, MD, USA
[ak] Also at Yeditepe University, Physics Department, Istanbul, Türkiye
* Deceased